EFFECT OF MASS ECCENTRICITY ON VIBRATION OF A STOCKBRIDGE DAMPER

By

Md. Sharful Insan

1018102086

Submitted in partial fulfillment of the requirement for the degree of

Master of Science in Mechanical Engineering

Under the Supervision of

Dr. Muhammad Ashiqur Rahman

Professor

Department of Mechanical Engineering

Bangladesh University of Engineering & Technology

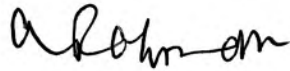Department of Mechanical Engineering

Bangladesh University of Engineering and Technology

Dhaka-1000, Bangladesh

July 2022

i

The thesis titled **"EFFECT OF MASS ECCENTRICITY ON VIBRATION OF A STOCKBRIDGE DAMPER"** submitted by Md. Sharful Insan, Student ID:1018102086 Session: October 2018, has been accepted as satisfactory in partial fulfillment of the requirement for the degree of MASTER OF SCIENCE IN MECHANICAL ENGINEERING on 26 July 2022.

BOARD OF EXAMINERS

....
Dr. Muhammad Ashiqur Rahman
Professor and Head
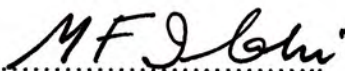Department of Mechanical Engineering
BUET, Dhaka-1000

Chairman &
Ex-Officio

....
Dr. Md. Afsar   Ali
Professor
Department of Mechanical Engineering
BUET, Dhaka-1000

Member

....
Dr. Md. Abdus Salam Akanda
Professor
Department of Mechanical Engineering
BUET, Dhaka-1000

Member

....
Dr. Muhammad Fazli Ilahi
Professor and Vice Chancellor
Ahsanullah University of Science and Technology
Dhaka-1208

Member
(External)

CANDIDATE'S DECLARATION

It is hereby declared that this thesis or any part of it has not been submitted elsewhere for the award of any degree or diploma.

Sharful Insan.

Md. Sharful Insan

LIST OF CONTENTS

LIST OF SYMBOLS & ABBREVIATIONS

h	=	Torsional influence coefficient ($\frac{1}{Nm}$)
J_i	=	Mass moment of inertia about elastic axis (kgm^2)
J_{cg}	=	Mass moment of inertia about center of gravity (kgm^2)
d	=	Diameter of the messenger cable (m)
E	=	Modulus of elasticity (GPa)
V	=	Shear force (N)
e	=	Eccentricity of the damper (mm)
G	=	Center of gravity
T	=	Torque (Nm)
I	=	Moment of inertia (m^4)
i	=	Radial direction
j	=	Tangential direction
EI	=	Flexural rigidity of elastic axis (Nm^2)
M	=	Bending moment (Nm)
m	=	Damper mass (kg)
y	=	Linear displacement (m)
Φ	=	Torsional rotation of elastic axis
ω	=	Natural frequency (rad/s)
θ	=	Angular displacement (rad)
G	=	Shear modulus (GPa)
t	=	Time (s)
c	=	Distance of center of gravity from the elastic axis (m)
l	=	Length of the stock bridge damper (m)
DOF	=	Degree of freedom
2DOFS	=	Two degrees of freedom system
3DOFS	=	Three degrees of freedom system
4DOFS	=	Four degrees of freedom system

LIST OF FIGURES

lumped masses are at unequal distance for 3DOFS].

LIST OF TABLES

ACKNOWLEDGEMENT

ABSTRACT

Natural frequency is a system's most important dynamic attribute. Resonance occurs when a time-varying force is applied to a system with a frequency that is equal to the system's natural frequency. This will result in the system's maximum amplitude, which could lead to system failure. A stockbridge damper is typically used worldwide as well as Bangladesh for damping vibration of overhead transmission lines. This work aims to investigate the change in vibration characteristics when the mass eccentricity of a stockbridge damper triggers a torsional mode of vibration in addition to the existing bending mode. We considered typical data of a stockbridge damper used in Bangladesh and modeled this stockbridge damper as a double cantilever beam having long and short sides. Each side was divided into two DOFS, three DOFS, and four DOFS. The natural frequencies are calculated on both sides by keeping the lumped masses at equal and unequal distances.

This study is based on two methods– The Myklestad's method used for uncoupled bending analysis and coupled flexure-torsion vibration method used for bending-twisting analysis. In this respect, a computer program is developed. This developed computational program has a graphical representation that shows stockbridge damper's characteristics in terms of the displacement (y) versus natural frequency (ω) curves.

First, it is analyzed how mass eccentricity affects vibration. It is found that the natural frequency of coupled flexure-torsion vibration is greater than that for the uncoupled bending vibration. Natural frequency is increased when mass eccentricity is gradually increased for 2DOFS. The natural frequency is further increased for 3DOFS and 4DOFS. Briefly it can be concluded that if the value of mass eccentricity increases, the natural frequency will also increase, and vice versa for both sides of the stockbridge damper.

Second, the impact of lumped mass distance on vibration is analyzed. Lumped mass distance has shown a great impact on the natural frequency of the stockbridge damper. The natural frequency was calculated first keeping lumped masses at equal distances and keeping the same lumped masses at unequal distances. For the long side of 2DOFS, ω_1 for mode shape 1 is increased by 20.1% and ω_2 for mode shape 2 is decreased by 45.3% at unequal distance compared to equal distance. Where ω_1 and ω_2

represent the first and second natural frequencies of the system respectively. However, on the short side, natural frequency is increased in both ω_1 and ω_2 by 30.2% and 63.4%, respectively. On the long side of the stockbridge damper and unequal distances of lumped masses for 3DOFS, the natural frequency ω_1 is increased for mode shape 1 by 15%, ω_2 for mode shape 2 by 22.2%, while ω_3 is decreased for mode shape 3 by 39% compare to the case when lumped masses were kept at equal distance. But on the short side of unequal distance, the natural frequencies are increased by 43.7%, 83.4%, and 81.1% respectively. Now for long side unequal distance of 4DOFS, the natural frequency ω_1 for mode shape 1 is increased by 8.5%, ω_2 for mode shape 2 by 17.7%, but ω_3 is decreased for mode shape 3 by 17.8% and ω_4 for mode shape 4 by 26.5%, where ω_3 and ω_4 represent the third and fourth natural frequency of the system respectively. However, in short side, the natural frequency ω_1 for mode shape 1 is increased by 9.2%, ω_2 for mode shape 2 is increased by 22.6%, and ω_3 for mode shape 3 is increased by 25.6% but ω_4 is changed randomly.

Third, the effect of DOF on vibration is analyzed. The natural frequency is changed as DOF increases. Between 2 and 3 DOFS, the natural frequency is increased in 3DOFS by 50.3% for mode shape 1(ω_1) and by 44.9% for mode shape 2 (ω_2) on the long side equal distance and also increased 48.2 % and 45.6 % for long side unequal distance. On the short side and an equal distances, the natural frequencies in mode shapes 1(ω_1) and 2(ω_2) are increased by 51.2% and 15.1%, respectively. Regarding the unequal distance, the natural frequencies in mode shapes 1(ω_1) and shape 2(ω_2) have likewise increased by 50% and 73.6%, respectively.

In comparison to 3 DOFS with 4 DOFS, the natural frequency is increased in 4DOFS by 22.4% for mode shape 1(ω_1), 27% for mode shape 2(ω_2), and 17.1% for mode shape 3(ω_3) in long side equal distance and 17.2%, 25.3% and 26.9% for long side unequal distance. In short side and equal distance, natural frequency in mode shape 1(ω_1), mode shape 2(ω_2) and mode shape 3(ω_3) is decreased by 54.4%, 28.8% and 75.9% respectively and also decreased 69%, 52.9% and 76.1% for unequal distance respectively. Thus we can conclude that mass eccentricity, the separation between lumped masses, and DOF have a significant influence on vibration in both coupled flexure torsion vibration and uncoupled bending vibration of stockbridge damper.

The loss of energy from the oscillatory system results in the decay of amplitude of vibration. Generally, in forced vibration with damping, energy dissipation (W_d) depends on many factors such as temperature, frequency or amplitude. We considered the simplest case of energy dissipation with viscous damping. The energy dissipated per cycle becomes, $W_d = \pi c \omega X^2$. Where, c= damping co-efficient, ω = natural frequency, X = amplitude of vibration. The preceding equation at resonance becomes, $W_d = 2\zeta \pi k X^2$ where, ζ= damping ratio, k= spring constant. In present analysis ζ is very small and therefore was not considered in mathematical modelling.

CHAPTER 1

INTRODUCTION

1.1 The influence of the stockbridge damper on aeolian vibration of conductors

Stockbridge dampers are used to suppress aeolian vibrations on overhead transmission lines. Overhead power transmission lines get exposed to wind motions that cause them to vibrate. Aeolian vibrations are the most common kind of vibrations observed in transmission lines and are caused by vortex shedding due to the flow of natural wind. Aeolian vibrations can cause fatigue and eventual failure of the transmission lines. In order to deal with these negative effects of aeolian vibrations, stockbridge damper is the most conveniently and commonly used damper. Stockbridge damper is used to reduce the intensity of vibrations on power lines in order to extend their life. Stockbridge damper system can control the aeolian vibrations in a transmission line by dissipating excitation energy through the self-excitation of the damper system. A stockbridge type damper transforms vibration energy it absorbs into thermal energy and acoustic energy. This energy is dissipated, reducing the steady-state amplitude of aeolian vibration of a conductor damper system. There have been a number of designs of dampers or damping mechanisms to reduce the severity of aeolian vibration. The severity of this vibration depends on a number of factors, including the velocity and direction of the wind, the tension in the conductor, and the total number of damping system. The stockbridge damper targets oscillations due to aeolian vibration; it is less effective outside the amplitude and frequency range. Stockbridge damper has a great influence to reduce aeolian vibration of conductors to increase their lifespan. It is commonly accepted that the stockbridge dampers cause a reduction in the amplitude of aeolian vibration because of their dissipative power. During its operation, the damper's messenger cable vibrates and bending stress is developed. The change of resonance frequency as well as the related bending stress of the messenger cable can be used to make the life assessment of the stockbridge damper.

1.2 Motivation for this study

Overhead transmission lines (current carrying conductors) and their hardware fittings fail mainly due to unavoidable aeolian vibration. Therefore, stockbridge dampers are primarily used to suppress or reduce vibrations of those transmission lines. A few recent studies (numerical as well as experimental) on this damper are listed in [1-8]. The vibration behavior, primarily the normal modes and the resonant frequencies, characterize the effectiveness of the stockbridge damper [1-3]. In [4] the numerical simulations and parametric studies showed a correlation between the increase of natural frequencies and the change in the geometry of the counterweight. The natural frequencies and the subsequent mode shapes of this damper, based on both analytical and finite element models are presented in [4]. Design sensitivity analysis of the resonant frequency of a Stockbridge damper was done in [5]. It considered several design parameters, including length of the messenger wire, inertia of the counterweight, and gyration radius of the counter-weight [5]. During its operation, the damper's messenger cable vibrates and bending is developed. Therefore, the results of the vibration damper feature can provide a basis for the optimum design of the stockbridge damper [6]. The efficiency of vibration damping is analyzed in the frequency domain corresponding to aeolian frequencies[7]. Two-mass dampers were analyzed and their dynamic characteristics were presented and described by the power function in the frequency domain [7]. Hysteric damping property of the stockbridge damper was investigated in [8]. In previous studies [1-8] it was assumed that mass center of the damper is perfectly on the centroid axis and thus vibration of the stockbridge damper system only in bending mode was considered.

But due to unavoidable imperfections, mass center is not likely to be exactly on the centroidal axis. Therefore, vibration behavior of stockbridge dampers, taking into account the effect of mass eccentricity, should be rigorously explored. In this context, this thesis aims to investigate the effect of mass eccentricity on vibration of the stockbridge damper.

1.3 (a) Objectives with specific aims

Aim of this work is to investigate the change in vibration characteristics when mass eccentricity of a stockbridge damper triggers torsional mode of vibration in addition to existing bending mode.

The specific aims of this study are:

(i)   To study the general physical and geometrical properties of the stockbridge dampers typically used in Bangladesh for damping vibration of overhead transmission lines (current carrying conductors).

(ii)   To analyze the vibration characteristics of the stockbridge damper system in bending mode.

(iii)   To analyze the coupled bending and torsional vibration effect of the stockbridge damper due to change in its center of gravity from the centroidal axis.

(iv)   To study the effect of different essential parameters (geometric and physical properties of the same damper) on vibration of the same damper.

(b) Possible outcome

Stockbridge dampers are primarily used to suppress or reduce vibrations of transmission lines. Therefore, this thesis would help to predict the change in vibration behavior of overhead transmission lines in Bangladesh due to coupled flexure torsional vibration of the stockbridge damper.

1.4 Outline of Methodology

A classical vibration analysis procedure, known as Myklestad's method [9], will be used to progressively compute the deflection, slope, bending moment, twisting moment and shear force from one section to the next one of the vibrating damper. Briefly, this is accomplished assuming the natural frequency and using equilibrium equations. The boundary conditions must also be satisfied. Thus the results will be obtained numerically in terms of the natural frequencies (ω) versus displacement (y) curve. For this purpose, a computer code will be developed in Matlab and in Engineering Equation Solver (EES) software. Next, reliability of the code will be checked. This will be accomplished by comparing the results generated by the code with the solutions for typical problems available in the literature [9].

Major steps will be as follows:

i.   To carefully study a typical stockbridge damper used in Bangladesh. This is to determine all the required physical and geometrical properties to be used in vibration analysis.

ii.   To numerically determine the natural frequencies and mode shapes of a stockbridge damper by Myklestad's method. This step will cover only uncoupled flexural vibration.

iii. To select reasonable value of mass eccentricity of the damper from [10]. This mass eccentricity will invariably induce vibration in twisting mode in addition to the bending mode analyzed in the previous step. Changed natural frequencies and normal modes of vibration of stockbridge damper will be determined again.

iv.   Change in vibration behavior due to coupled flexure-torsion vibration at different modes (especially, at higher modes) will be analyzed.

Any change in damping capacity of the stockbridge damper (due to different values of mass eccentricity); will be determined in terms of resonant frequencies.

1.5 Thesis overview

This work is divided into five main chapters. This present chapter introduces the importance of stockbridge damper and shows the work objectives, possible outcome and outline of methodology. Chapter 2 and chapter 3 contain the literature review of previous works and all the mathematical formulations respectively.

Chapter 4 presents the majority of the results obtained, as well as the effect of mass eccentricity analysis on vibration of the stockbridge damper.

Finally, chapter 5 presents the conclusions of this work as well as the proposed future works.

2.1 Study of previous works

A large number of studies are reported in the literature dealing with the effect of dynamic behavior of stockbridge damper, out of which only a few are discussed. Overhead transmission lines (current carrying conductors) and their hardware fittings fail mainly due to unavoidable aeolian vibration. Therefore, stockbridge dampers are primarily used to suppress or reduce vibrations of those transmission lines. A few recent studies (numerical as well as experimental) on this damper are listed in references. The vibration behavior, primarily the normal modes and the resonant frequencies, characterized the effectiveness of the stockbridge damper.

Barbieri et al. [1] gave a mathematical model and practical review of dynamic behavior of stockbridge damper. This work is to validate a nonlinear mathematical model (finite element method) for dynamic simulation of stockbridge dampers of electric transmission line cables. To obtain the mathematical model, a nonlinear cantilever beam with a tip mass was used. The mathematical model incorporates a nonlinear stiffness matrix of the element due to the nonlinear curvature effect of the beam.

Barbieri et al. [2] did experimental and numerical investigation of nonlinear dynamical behavior of a wire-rope isolator and an asymmetric stockbridge damper. The wire-rope isolator system was excited using an electromechanical shaker with constant values of acceleration, and the stockbridge damper was excited using a cam machine with different profiles. In this work, the physical parameters used in a Bouc-Wen model were adjusted using PSO method through the comparison between numerical and experimental results for two different systems: wire-rope isolator and stockbridge damper. The vibration behavior, primarily the normal modes and the resonant frequencies, characterized the effectiveness of the stockbridge damper.

Vaja et al. [4] presented an analytical model of a novel aeolian vibration damper with an increased number of resonant frequencies. The analytical model is used to deduce the resonant frequencies of the damper. A 3D finite element model has been developed to validate the analytical model. The natural frequencies and the subsequent mode shapes of both analytical and finite element models are presented. An experiment is conducted to

validate the proposed models. The numerical simulations and parametric studies conducted previously showed a correlation between the increase of natural frequencies and the change in the geometry of the counterweight.

Kim [5] carried on the design sensitivity analysis of the resonant frequency of a stockbridge damper. It considered several design parameters, including length of the messenger wire, inertia of the counterweight, and gyration radius of the counter-weight. The design guidelines for a stockbridge damper were derived from the sensitivity analysis results.

Kalombo et al. [6] have determined the bending stress of stockbridge damper messenger cable. During its operation, the damper's messenger cable vibrates and bending is developed. Therefore, the results of the vibration damper feature can provide a basis for the optimum design of the shock absorbers. The analyzed model represents a component of a non-destructive procedure that can be used to predict the remaining life of stockbridge damper as well as evaluating their condition.

Golebiowska and Dutkiewicz [7] have shown the experimental analysis of efficiency of mass dampers. The efficiency of vibration damping is analyzed in the frequency domain corresponding to aeolian frequencies. Two-mass dampers were analyzed and their dynamic characteristics were presented and described by the power function in the frequency domain.

Foti and Martinelli [8] have shown the hysteretic behavior of stockbridge dampers. Aim of this work was to develop a simple, but accurate, mechanical model of a stockbridge damper to use in the assessment of such structures vibrations. The model is based on a beam like description of the messenger cable and on a nonlinear formulation of the cross sections cyclic bending behavior. Hysteric damping property of the stockbridge damper was investigated.

Kalombo et al. [14] have developed a mathematical model describing the bending stress of the stockbridge damper's messenger cable near the clamped end. During damper's operation, the damper's messenger cable vibrates and bending stress is developed.

Sakawa and Luo [21] developed a mathematical model and controlled the coupled bending and torsional vibration of flexible beams. An evolution equation which governs

coupled bending and torsional vibrations of flexible beams with a tip body is derived based on lagrangian dynamic.

Gokdag and Kopmaz [22] have studied the coupled flexural–torsional free and forced vibrations of a beam with tip and/or in span attachments. First, a mathematical model is established, which consists of a beam with several tip attachments, i.e., a tip mass of non-negligible dimensions, a linear spring grounding the tip mass, and a torsional spring connected at the end of the beam. The modal functions of this model and the orthogonality condition among them are derived. For the purpose of verification the properties of the tip attachments are changed, and the numerical results are obtained.

Havard [23] reviewed the fundamentals of conductor vibration control, stockbridge damper properties, the practices of damper application, the types of damage experienced, use of vibration recorders for critical spans, the impact of in-span masses such as aircraft warning markers, and some approaches to inspection protocols.

Tigli [24] have shown an optimum design of dynamic vibration absorbers (DVAs) installed on linear damped systems that are subjected to random loads is studied and closed-form design formulas are provided. Another important finding of the paper is that for specific applications where all of the response parameters are desired to be minimized simultaneously, DVAs designed per velocity criteria provide the best overall performance with the least complexity in the design equations.

Wang [25] have described the three forms of conductor vibrations and the control technologies from utilities' practical point of view. As an example, a design consideration is discussed. This paper also captured the challenges of vibration control on high temperature low sag conductors, based on experiences in North America.

In previous studies it was assumed that mass center of the damper is perfectly on the centroid axis and thus vibration of the stockbridge damper system only in bending mode was considered. But due to unavoidable imperfections, mass center is not likely to be exactly on the centroid axis. Therefore, vibration behavior of stockbridge dampers taking into account the effect of mass eccentricity should be rigorously explored. This was the prime objective of this research work.

2.2 Brief descriptions of aeolian vibration damping devices

In order to deal with the negative effects of aeolian vibrations, a variety of impact and tuned dampers are designed. Among them the most commonly used ones are torsional dampers, Elgra dampers, spiral dampers, spring-piston dampers, pneumatic dampers and stockbridge dampers [11-13]. Torsional dampers, Elgra dampers and spiral dampers are classified as the impact dampers that use collision energy to dissipate the vibration energy. Torsional dampers simply increase the interstrand friction of the conductor as a result of the torsional motion produced by the offset weights when the conductor vibrates. They are effective on conductors smaller than about 12.5 mm in diameter. Unfortunately, torsional dampers are efficient in a narrow frequency range and have a tendency to freeze up in the winter. Elgra dampers, on the other hand, are effective to give different frequency responses with their variety of plate-type weights. In a vibration activity, these weights move up and down on the spindle to dissipate the energy by the help of Neoprene washers but they are very noisy and cause excessive wear at the connection point of the conductor [11-13].
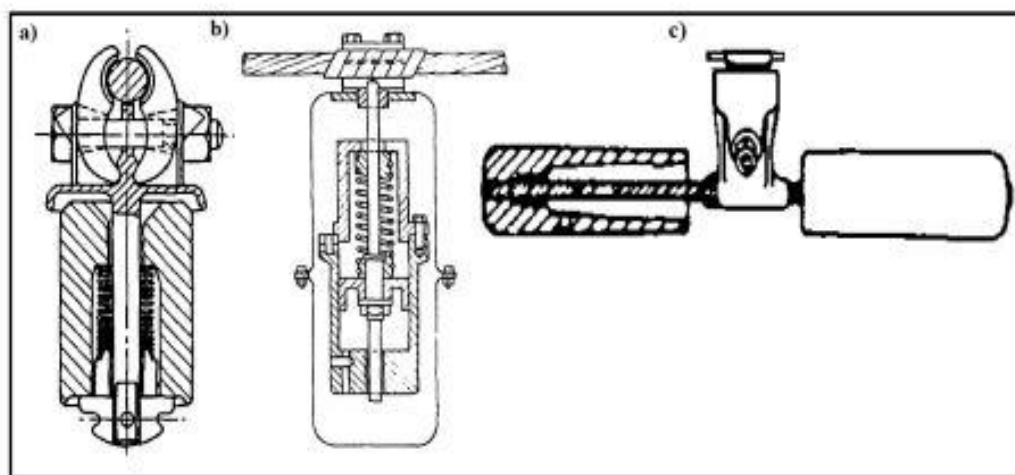
Figure 2.1: Tuned dampers a) spring-piston damper, b) pneumatic damper and stockbridge damper [11-13].

Spiral dampers are geometrically separated from the torsional dampers and the Elgra dampers but they also suppress the vibration by impacting against the conductor. Generally, spiral dampers are effective in the frequency range of 100 Hz to 300 Hz and these frequencies occur on conductors smaller than about 16 mm in diameter. Since the spiral damper suppresses the vibrations within its length, it should be made long enough to cover as many vibration loops as it can [13]. Spring-piston dampers, pneumatic

dampers and stockbridge dampers (Figure 2.1) are classified as the tuned dampers which are effective when their natural frequency coincide with the excitation frequency of the conductor and this working principle is discussed in more detail in the next subsection. Unlike the spring-piston dampers and the pneumatic dampers, the stockbridge dampers can be tuned to be effective over a wide range of frequency and they can dissipate vibrations in any directions. Since the stockbridge dampers are the focus of this study, they are discussed in more detail in subsections 2.2.1 and 2.2.2.

2.2.1 Stockbridge damper

Stockbridge dampers are used to suppress aeolian vibrations on overhead transmission lines caused by the wind. It consists of two masses at the ends of a short length of cable (messenger) clamped to the main cable (conductor) as seen in Figure 2.2. Aeolian vibration is one of the causes of fatigue failure of power line conductors. The most common method used to protect conductors against this type of failure is to dissipate the energy transferred by the wind to the power line by means of suitable dynamic dampers. The most commonly used basic damper has been designed for the first time by G H Stockbridge in 1924 [14]. It is called stockbridge damper and consists of two masses rigidly attached to the ends of a double strand wire cable called messenger cable. The messenger cable is rigidly assembled to the power line by means of clamps. Figure 2.2 shows the different parts of a stockbridge damper.
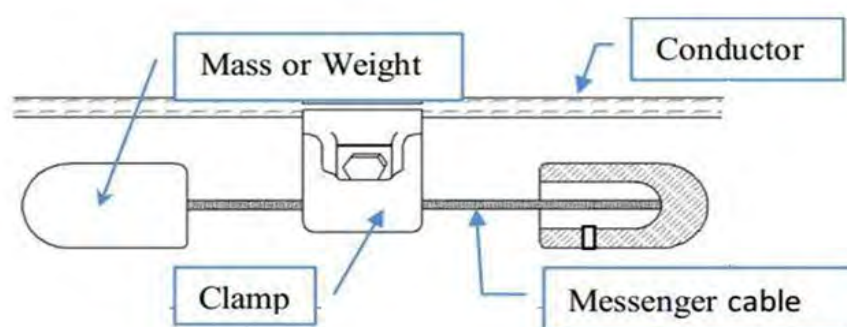
Figure 2.2: Parts of a stockbridge damper [14].

In this design, concrete blocks were placed symmetrically on the messenger cable as seen in Figure 2.3.
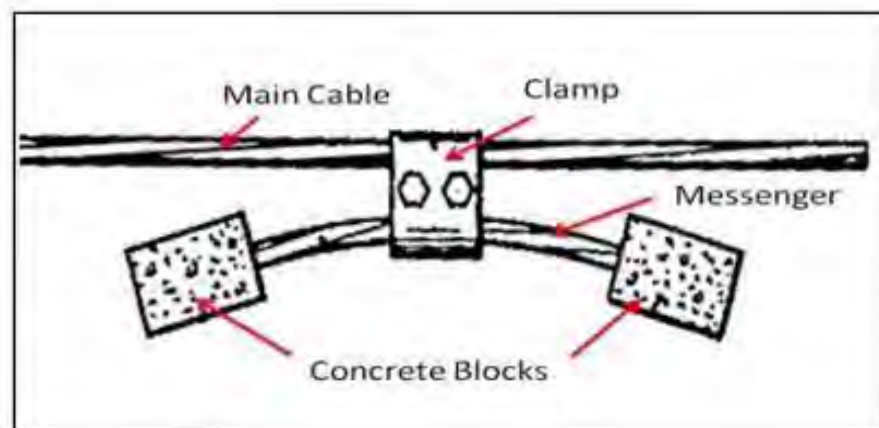
Figure 2.3: Original concrete block design of stockbridge damper [15].

2.2.2 Working principle of stockbridge damper

When the damper is placed on a vibrating conductor, vibrations pass down through the clamp and reach to the weights. Movement of the weights will produce bending of the messenger cable, which causes the individual wire strands in figure 2.4 to rub together and dissipate energy. This action constitutes the damping effect of the stockbridge damper.
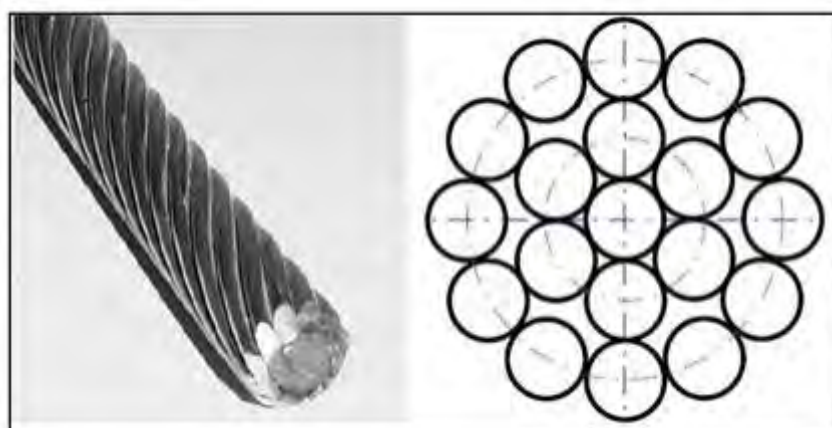
Figure 2.4: The messenger cable (left) and the individual wire strands (right) [17].

In the early designs, the messenger cable consists of 7 individual wire strands but once the importance of the messenger cable is realized, it has been started to construct modern designs with 19 individual wire strands on their messenger cable [16]. Appropriate choice of mass blocks, messenger cable length and stiffness of the damper

increases the mechanical impedance of the cable which in turn decreases oscillations of the main cable substantially.

In a symmetrical stockbridge damper, each of weight has two identical degrees of freedom (y, θ), which correspond to first and second modes of the damper, in the vertical plane. As illustrated in figure 2.5, the outer ends of the damper weights have the maximum displacement in the 1st mode and the inner ends of the damper weights have the maximum displacement in the 2nd mode [16]. On the other hand, asymmetric placement of the weights on the messenger cable and the usage of two different weights on the stockbridge damper provide the broadest effective frequency range in more advance designs. In general, the asymmetric stockbridge damper consists of two unequal masses attached to the end of two unequal lengths of wire strands, which are known as messenger cables.
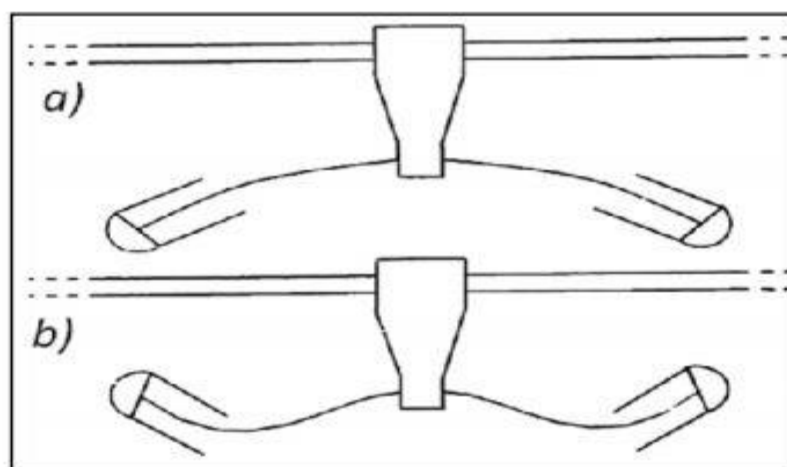
Figure 2.5: Representations for a) the first mode, b) the second mode of a symmetrical stockbridge damper [18].

The ends of a power line span, where it is clamped to the transmission towers, are at most risk. Generally, there are two dampers per span which are at anti-nodes where the amplitude of the standing wave is a maximum. More than two dampers can be also installed if necessary on longer spans.

2.2.3 Bending parameters in stockbridge damper

Stockbridge damper is attached on the power line, therefore it moves with it through the wind. During its operation, the damper's messenger cable vibrates and bending stress is developed [14].
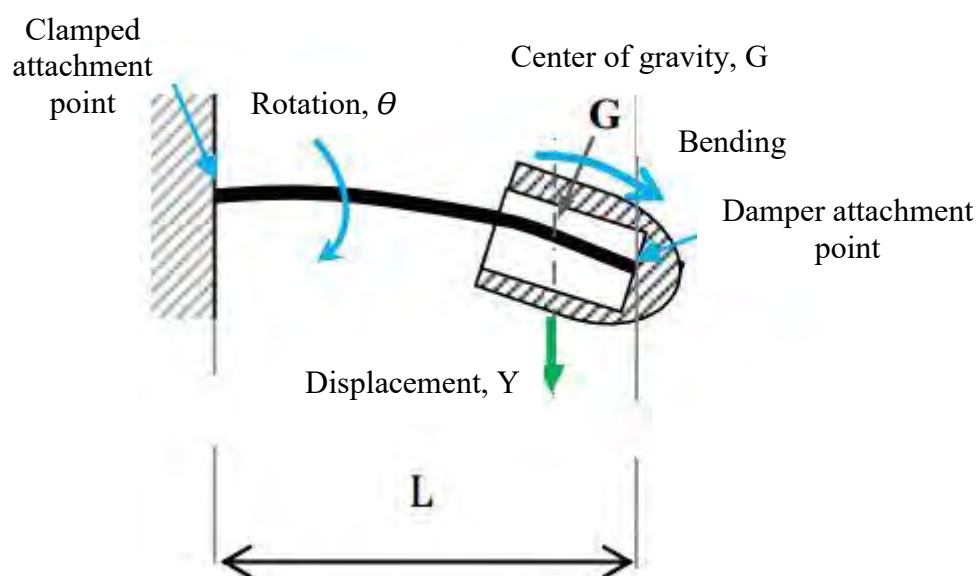
Figure 2.6: Moment and force acting on the damper's messenger cable [14].

During the vibration of stockbridge damper, the movement of damper's weight is characterized by two degrees of freedom: the alternative motion of translation, y and the rotation, θ. Bending moment is also developed at the clamp attachment point of the cable.

Different types of conductors are used in high voltage (132 kV, 230 kV and 400 kV) overhead transmission lines in Bangladesh. Aeolian vibration of those transmission lines under typical weather condition of Bangladesh should be well understood to ensure safe and prolonged service of conductors. To suppress these aeolian vibrations on overhead transmission lines stockbridge dampers are used in Bangladesh.

2.2.4 Specifications and material properties of stockbridge damper

Damper mass	Messenger cable	Messenger cable	Damper mass
(Small)	(Short side)	(Long side)	(Big)
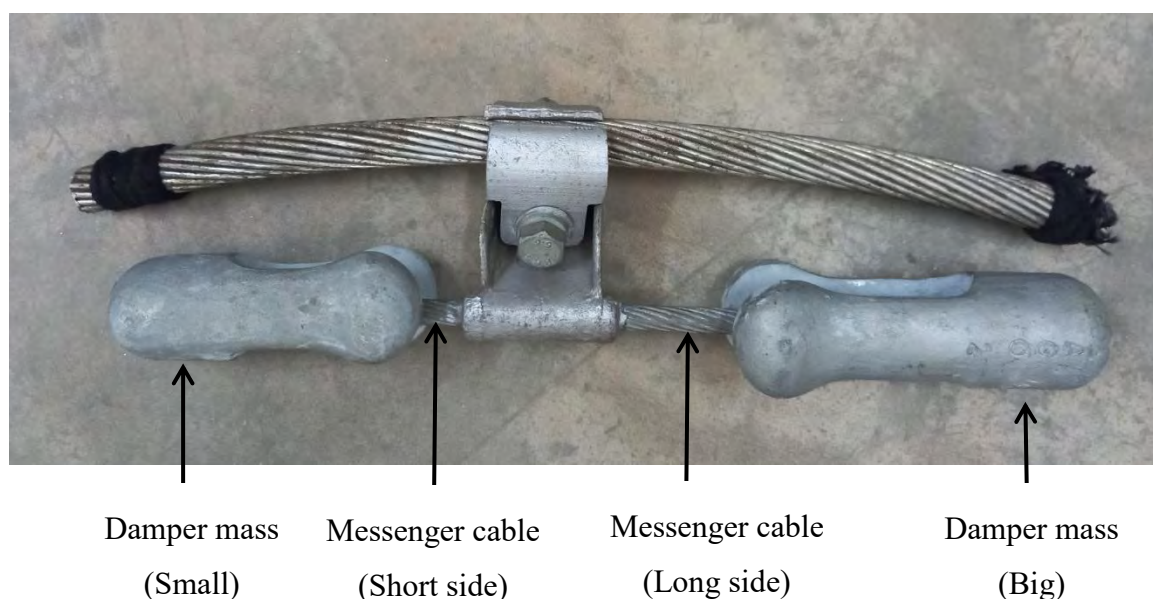
Figure 2.7: Asymmetric stockbridge damper.

Description	Symbol/ Unit	Value
Length of messenger cable (Long side)	L [mm]	270
Length of messenger cable (Short side)	L [mm]	230
Total mass of the damper	m [kg]	4.5
Damper mass in long side	m [kg]	2.1
Messenger cable mass in long side	m [kg]	0.3
Damper mass in short side	m [kg]	1.9
Messenger cable mass in short side	m [kg]	0.2

Shear Modulus(Tensile steel)	G [Pa]	79.3×10^9
Diameter of messenger cable	D [mm]	10
Modulus of Elasticity (Tensile steel)	E [Pa]	200×10^9
Materials flexural rigidity	EI [Nm^2]	98.2

3.1 General

In many vibrational systems, like a stockbridge damper we can consider the mass to be lumped on a cantilever beam. Myklestad [9] devised a simple procedure for the calculation of the natural frequencies of such a system. Myklestad's method was used to calculate the vibration of a cantilever beam, where only bending effect was examined. Many of these procedures were developed in the early years and may be considered as classical methods. Primarily, Myklestad's method is used for uncoupled flexure vibration. However, natural modes of vibration of stockbridge dampers are likely to be coupled flexure-torsion vibration, which for higher modes differs considerably from those of uncoupled modes.

Assumptions:

(1) Stockbridge damper is modelled as a double cantilever beam.
(2) Lumped masses are assumed on elastic axis of the cantilever beams.
(3) Vibration of the stockbridge damper is considered in single, vertical plane.
(4) The clamp attached point is considered as the fixed end for both sides of the stockbridge damper.

3.2 Myklestad's method for vibration in bending mode

When a beam is replaced by lumped masses connected by massless beam sections, a method developed by Myklestad, N. O. can be used to progressively compute the deflection, slope, moment and shear from one section to the next. This method can be applied to any lumped mass system, linear spring-mass systems, beams modeled by discrete masses and beam springs etc.

Uncoupled flexural vibration:

Figure 3.1 shows a typical section of an idealized beam with lumped masses at different stations i, i+1 etc. By taking the free-body section in the manner indicated, it will be possible to write equations for the shear (V) and moment (M) at i+1 entirely in

terms of quantities at i. These can then be substituted into the geometric equations for θ and y.
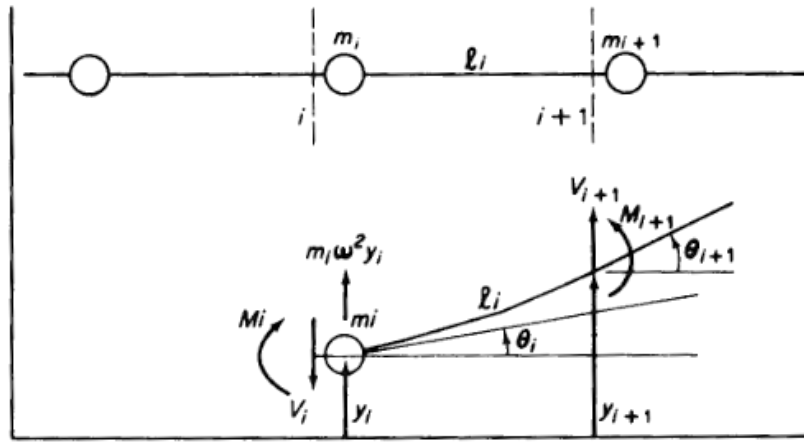
Figure 3.1 Typical section of an idealized beam [9].

From equilibrium considerations, we have

$$V_{i+1} = V_i - m_i\omega^2 y_i \qquad\qquad (3.2.1)$$

$$M_{i+1} = M_i - V_{i+1}l_i \qquad\qquad (3.2.2)$$

From geometric considerations, using influence coefficients of uniform beam sections, we have

$$\theta_{i+1} = \theta_i + M_{i+1}\ (l/EI)_i + V_{i+1}\ (l^2/2EI)_i \qquad\qquad (3.2.3)$$

$$y_{i+1} = y_i + \theta_i\ l_i + M_{i+1}\ (l^2/2EI)_i + V_{i+1}\ (l^3/3EI)_i \qquad\qquad (3.2.4)$$

Where,

$(l/EI)_i$ = Slope at $i+1$ measured from a tangent at i due to a unit moment at $i+1$;

$(l^2/2EI)_i$ = Slope at $i+1$ measured from a tangent at i due to a unit shear at $i+1$= deflection at $i+1$ measured from a tangent at i due to a unit moment at $i+1$;

$(l^3/3EI)_i$ = Deflection at $i+1$ measured from a tangent at i due to a unit shear at $i+1$;

Thus, Equations (3.2.1) through (3.2.4) in the sequence given enable the calculations to proceed from $i\ to\ i+1$.

16

Boundary Conditions:

When an undamped system is vibrating freely at any one of its natural frequencies, no external force, torque, or moment is necessary to maintain the vibration. Also, the amplitude of the mode shape is immaterial to the vibration. Recognizing these facts, Myklestad proposed a method of calculation for the natural frequencies and mode shapes of uncoupled systems by assuming a frequency and starting with unit amplitude at free end of the system and progressively calculating the shear, moment and angular displacement to the other fixed end. The frequencies that result in zero displacement or compatible boundary conditions at the fixed end are the natural frequencies of the system.

Four boundary conditions at each end, two are generally known. For example, a cantilever beam with $i = 1$ at the free end would have $V_1 = M_1 = 0$. As the amplitude is arbitrary, we can choose $y_1 = 1$. Having done so, the slope θ_1 is fixed to a value that is yet to be determined. Because of the linear character of the problem, the four quantities at the fixed end station (n) will be in the form,

$$V_n = a_1 + b_1\theta_1 \qquad\qquad (3.2.5)$$

$$M_n = a_2 + b_2\theta_1 \qquad\qquad (3.2.6)$$

$$\theta_n = a_3 + b_3\theta_1 \qquad\qquad (3.2.7)$$

$$y_n = a_4 + b_4\theta_1 \qquad\qquad (3.2.8)$$

Where a_i, b_i are constants and θ_1 is unknown. Thus, the frequencies that satisfy the boundary condition, $\theta_n = y_n = 0$ for the cantilever beam will establish θ_1 and the natural frequencies of the beam i.e.

$$\theta_1 = -a_3/b_3 \qquad\qquad (3.2.9)$$

$$y_n = a_4 - (a_3/b_3)\,b_4 = 0 \qquad (3.2.10)$$

Hence by plotting y_n vs ω, the natural frequencies of the beam can be found [9].

Solution Procedures (Y vs ω Curves):

We know, at fixed end of a cantilever beam the value of linear and angular displacement ($\theta_n = y_n = 0$) will be zero. Now from the y_n vs ω plotting graph, zero crossing line corresponds to the values of ω are the natural frequencies of the system.

The computation is started at free end. Since each of the quantities V, M, θ and y will be in the form a + b, they are arranged into two sections, each of which can be computed separately. The calculation for one section is started with $V_1 = M_1 = \theta_1 = 0$ and $y_1 = 1$.The another section, which are proportional to θ, are started with the initial values of $V_1 = 0$, $M_1 = 0$, $\theta_1 = 1\theta$, and $y_1 = 0$. To start the computation we note that the moment and shear at station l are zero. We can choose the deflection at station l to be 1.0, in which case the slope at this point becomes an unknownθ. We therefore carry out two sections of calculations for each quantity starting with $\theta_1 = 0$, $y_1 = 1$ and $\theta_1 = \theta$, $y_1 = 0$. The unknown slope $\theta_1 = \theta$ is found by forcing θ_n at the fixed end to be zero, after which the deflection y_n can be calculated and plotted against ω. The natural frequencies of the system are those for which $y_n = 0$.

3.3 Coupled flexure-torsion vibration

Natural modes of vibration of stockbridge damper and other beam structures are often coupled flexure-torsion vibration, which for higher modes differs considerably from those of uncoupled modes. To treat such problems, we must model the beam which is shown in figures 3.3.1 and 3.3.2 .The elastic axis of the beam about which the torsional rotation takes place is assumed to be initially straight. It is able to twist. The principal axes of bending for all cross sections are parallel in the undeformed state. Masses are lumped at each station with its center of gravity at distance c_i from the elastic axis and J_i is the mass moment of inertia of the section about the elastic axis, i.e.

$$J_i = J_{cg} + m_i c_i^2 \qquad\qquad (3.3.1)$$

Figure 3.3.1 and 3.3.2 shows the i th section, from which the following equations can be written:

$$V_{i+1} = V_i - m_i \omega^2 (y_i + c_i \Phi i) \qquad\qquad (3.3.2)$$

$$M_{i+1} = M_i - V_{i+1} l_i \qquad\qquad (3.3.3)$$

$$T_{i+1} = T_i + J_i\omega^2\phi_i + m_i c_i \omega^2 y_i \tag{3.3.4}$$

$$\theta_{i+1} = \theta_i + M_{i+1}\left(\frac{l}{EI}\right)_i + V_{i+1}\left(\frac{l^2}{2EI}\right)_i \tag{3.3.5}$$

$$y_{i+1} = y_i + \theta_i\, l_i + M_{i+1}\left(\frac{l^2}{2EI}\right)_i + V_{i+1}\left(\frac{l^3}{3EI}\right)_i \tag{3.3.6}$$

$$\phi_{i+1} = \phi_i + T_{i+1}h_i \tag{3.3.7}$$

Where, T = the torque,

h = the torsional influence coefficient = (l/GI_p),

ϕ = the torsional rotation of elastic axis.
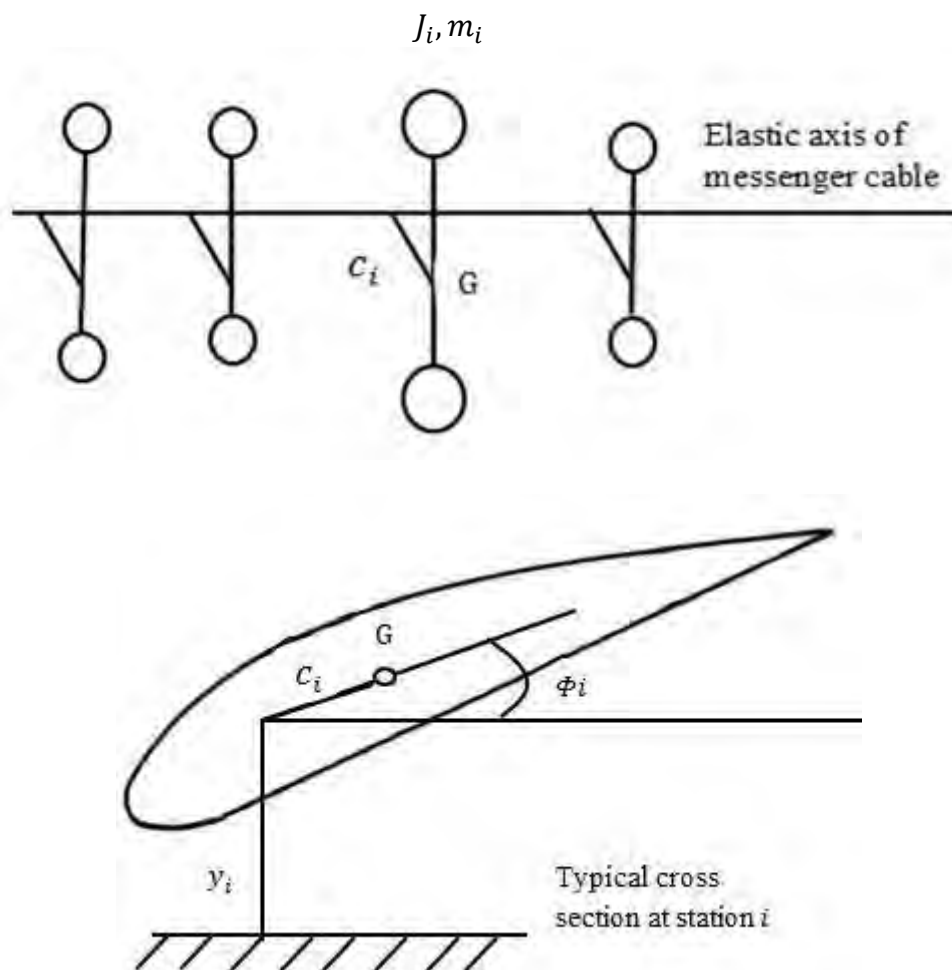
Figure 3.3.1: Lumped mass system (Isometric view).
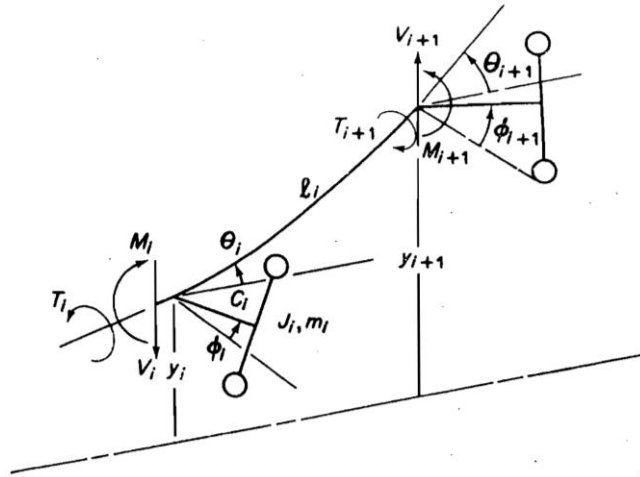
Figure 3.3.2: i th section of couple flexure-torsion vibration [9].

Boundary Conditions:

For free-ended beams, we have the following boundary conditions at tip to start the computation, $V_1 = M_1 = T_1 = 0$ and $\theta_1 = \theta$, $y_1 = 1$, $\phi_1 = \phi$ and at the fixed end, $y = 0$, $\theta = 0$ and $\phi = 0$. Here, the quantities at any station are linearly related to θ_1 and ϕ_1. Natural frequencies are established by the satisfaction of the boundary conditions at the other end. Often, for symmetric beams such as the airplane wing, only one-half the beam needs to be considered. The satisfaction of the boundary conditions for the symmetric and anti-symmetric modes enables sufficient equations for the solution.

Solution Procedures (Y vs ω Curves):

By using these boundary conditions, we solved the above coupled flexure-torsion vibration equations (3.3.1-3.3.7) and found the natural frequency of the system. The computation is started at free end where the displacement is assumed unit amount ($y_1 = 1$). We advanced our calculations from free end to the fixed end of the stockbridge damper modelled as a cantilever beam. We started our calculations with a single value of ω then found a single value of displacement (y_n). Following the similar steps we found the different values of y_n for various values of ω. These calculation procedures are performed by developing numerical codes which are available in appendix D. Hence by plotting y_n vs. ω the natural frequencies of the cantilever beam was found. We know, at fixed end of the cantilever beam, the value of linear and angular displacement ($\theta_n = y_n = 0$) will be zero. Now from the y_n vs ω plotting graph, zero crossing line corresponds to the values of ω are the natural frequencies of the system.

Natural modes of vibration of stockbridge damper and other beam structures are likely to be coupled flexure-torsion vibration which for higher modes differs considerably from those of uncoupled modes. In coupled flexure- torsion vibration analysis, there is assumed mass eccentricity (c_i) between the elastic axis of the messenger cable and center of gravity of the stockbridge damper as explained in chapter 3. The values of mass eccentricities (c_i) is taken from [10] according to ISO limit. The loss of energy from the oscillatory system results in the decay of amplitude of vibration.

Generally, in forced vibration with damping, energy dissipation (W_d) depends on many factors such as temperature, frequency or amplitude. We considered the simplest case of energy dissipation with viscous damping. The energy dissipated per cycle becomes, $W_d = \pi c \omega X^2$. Where, c= damping co-efficient, ω = natural frequency, X = amplitude of vibration. The preceding equation at resonance becomes, $W_d = 2\zeta\pi k X^2$ where, ζ= damping ratio, k= spring constant. In present analysis ζ is very small and therefore was not considered in mathematical modelling.

4.1 Validation of the computational procedure of uncoupled bending vibration analysis for 3 DOFS

The reliability of the numerical code has been accomplished by comparing the results generated by the code with the solutions for typical problems available in the literature [9]. The massless beam sections are assumed to be identical so that the influence coefficients for each section are equal (Figure 4.1.1). The validation of the computational procedure is done according to the problems of [9]. Results, in terms of zero crossing of displacement (y) versus natural frequency (ω) curves are generated by the procedure explained in chapter 3.
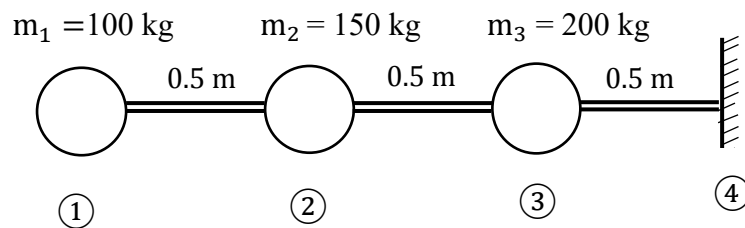
Figure 4.1.1: Lumped parameter system [9].

We start by calculating the natural frequency of a 3DOFS in uncoupled bending mode, which means there is no mass eccentricity (c_1=0 mm, c_2=0 mm and c_3=0 mm) in this lumped mass system. The result of the natural frequency in this case is shown in Figure 4.1.2.
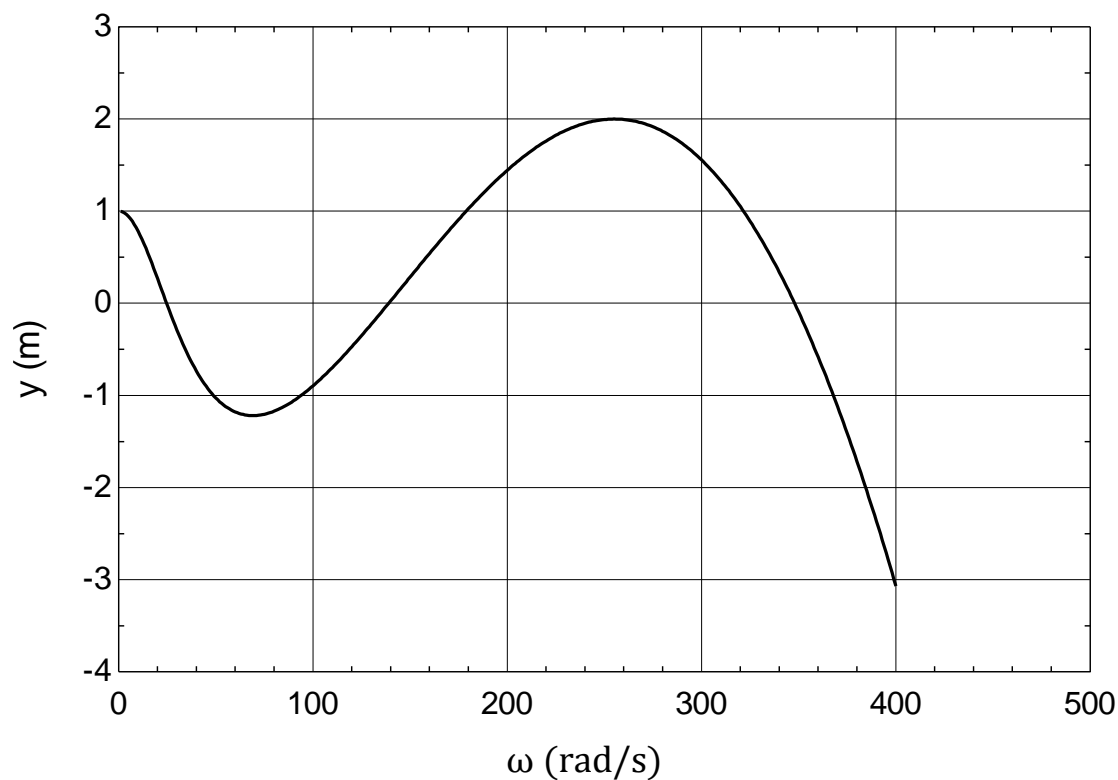
Figure 4.1.2 Displacement vs. Natural frequency in uncoupled bending vibration [Example problem in [9]].

Natural frequency (rad/s) calculated by present procedure and corresponding results in[9]:

$$\omega_1 = 24.5 \quad \text{[solution in [9] between 20 to 30}$$

$$\omega_2 = 138.9 \text{ [solution in [9] 138.98]}$$

$$\omega_3 = 347.5 \text{ [solution in [9] between 340 to 350]}$$

Where ω_1, ω_2 and ω_3 represent the first, second and third natural frequencies of the system respectively. As shown these computational results have matched with good accuracy with the results given in solutions of [9].

After ensuring the code's reliability, we shall investigate the stockbridge damper vibration effect both in uncoupled bending as well as coupled bending-twisting vibration in different modes.

4.2 Stockbridge damper natural frequency analysis both in uncoupled bending and coupled bending-twisting vibration mode

The messenger cable on one side of the stockbridge damper is longer and the corresponding damper mass is greater than on the other side. The long and short sides of the stockbridge damper are separated into 2DOFS, 3DOFS, and 4DOFS respectively. The lumped masses are considered in equal and unequal distances for all DOFS. Next the effects of different parameters on vibration for these 2DOFS, 3DOFS & 4DOFS are described below.

CASE 1: STOCKBRIDGE DAMPER ACTING AS A 2 DOFS (LONG SIDE)

4.3: Lumped masses are at equal distance (Long side)

The stockbridge damper is modeled as a cantilever beam in this case, with the damper's mass divided into two parts. These two parts are thought to be equally spaced apart. Figure 4.3 displays the parameter-evaluated stockbridge damper as a two degree of freedom system.
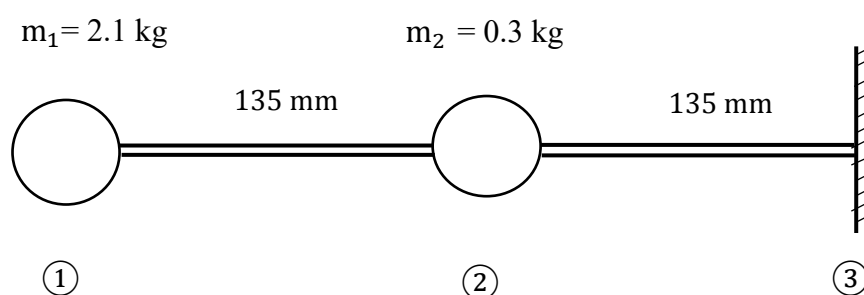
Figure 4.3: Lumped parameter system in stockbridge damper [Long side and lumped masses are at equal distance for 2DOFS].

Uncoupled bending vibration ($c_i = 0$) (Long Side)

We start by calculating the natural frequency of this 2 DOFS in the uncoupled bending mode, which means there is no mass eccentricity ($c_1=0$ mm, $c_2=0$ mm) in this lumped mass system. The result of the natural frequency, in this case is shown in Figure 4.3.1.

Figure 4.3.1: Displacement vs. Natural frequency in uncoupled bending vibration for 2 DOFS.

Natural frequency (rad/s):

$$\omega_1 = 168$$

$$\omega_2 = 679$$

Coupled bending-twisting vibration ($c_i \neq 0$) (Long Side)

Here, we start by calculating the natural frequency of this 2DOFS in coupled bending-twisting mode, which means there is acting some mass eccentricity ($c_1=0.1$ mm and $c_2=0.05$ mm) in this lumped mass system. The results of the natural frequency in this case, are shown in Figure 4.3.2.

Figure 4.3.2: Displacement vs. Natural frequency in coupled bending-twisting vibration for 2 DOFS.

Natural frequency (rad/s):

$$\omega_1 = 169$$
$$\omega_2 = 688$$

Uncoupled bending and Coupled bending-twisting vibration comparison (Long Side)

Graph 4.3.3 compares the influence of mass eccentricity on vibration between uncoupled bending and coupled bending-twisting vibration modes, which is generated using graphs 4.3.1 and 4.3.2 respectively.
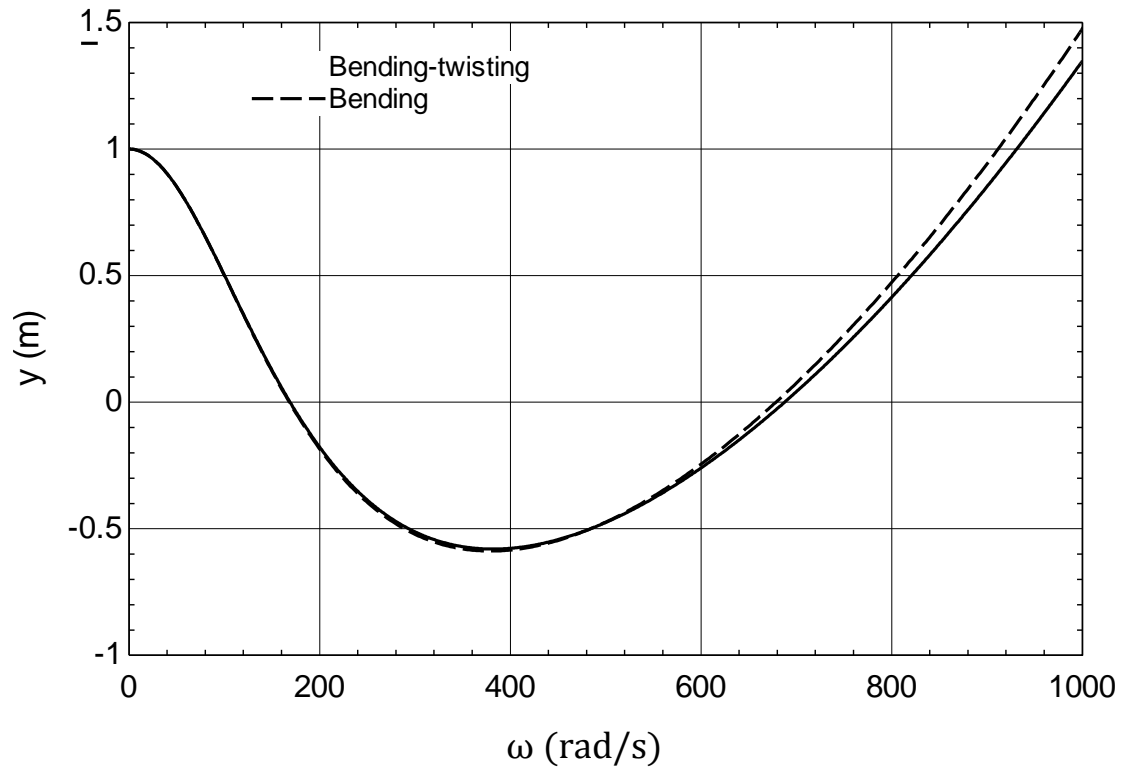
Figure 4.3.3: Displacement vs. Natural frequency in uncoupled bending and coupled bending-twisting vibration for 2 DOFS.

Table 1: Comparison of uncoupled bending & coupled bending-twisting natural frequency for 2 DOFS (Long side and lumped masses are at equal distance)

The natural frequency has increased both in ω_1 for mode shape 1 and ω_2 for mode shape 2 due to the effect of mass eccentricity, as seen in table 1. Where, ω_1 and ω_2 represent the first and second natural frequencies of the system respectively. After comparing the results between uncoupled bending and coupled bending-twisting vibration, now we calculate the natural frequency for different values of mass eccentricity. These are described in the following:

Natural frequency (rad/s)	
Bending vibration (c_1=0 mm, c_2=0 mm)	Bending-twisting vibration (c_1=0.1 mm, c_2=0.05 mm)
$\omega_1 = 168$	$\omega_1 = 169$
$\omega_2 = 679$	$\omega_2 = 688$

Effect of increasing c_i on coupled bending-twisting vibration (Long Side)

The value of mass eccentricity is increased by double from the initial assuming value c_1=0.1 mm, to c_1=0.2 mm and c_2=0.05 mm to c_2=0.1 mm. After increasing c_i the result of natural frequency is also increased for the same 2DOFS. The results are shown in figure 4.3.4.
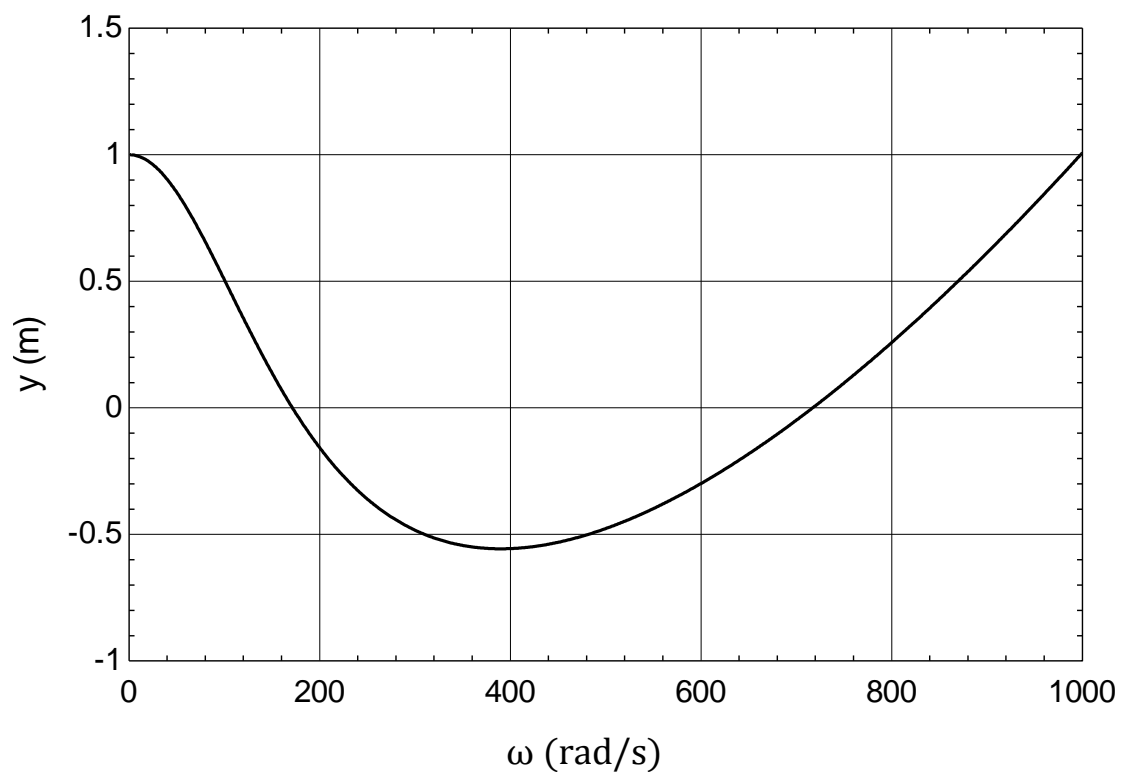
Figure 4.3.4: Displacement vs. Natural frequency in coupled bending-twisting vibration for 2 DOFS.

Natural frequency (rad/s):

$$\omega_1 = 172$$

$$\omega_2 = 718$$

Effect of randomly increased value of c_i on coupled bending-twisting vibration (Long Side)

Now, the value of mass eccentricity of the same 2DOFS is randomly increased from the initial assuming value $c_1=0.1$ mm, to $c_1=0.4$ mm and $c_2=0.05$ mm to $c_2=0.08$ mm. In this case, natural frequency is also increased for both mode shape $1(\omega_1)$ and mode shape 2 (ω_2). The results are shown in figure 4.3.5.
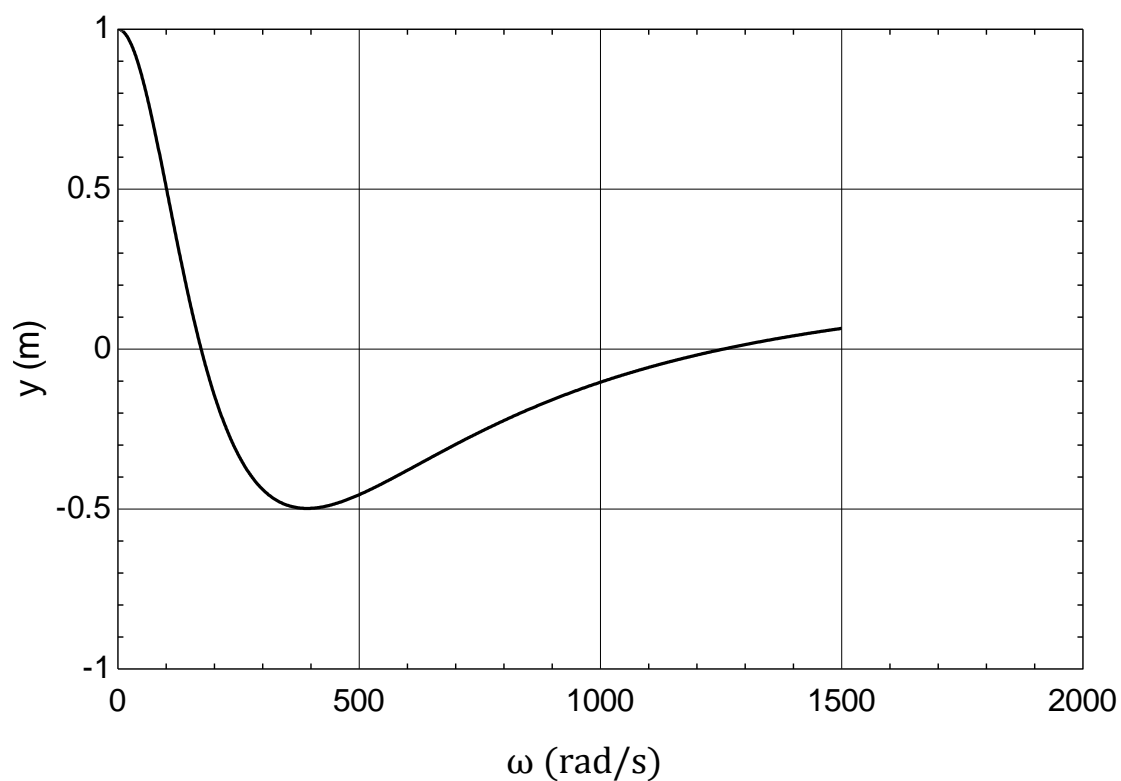
Figure 4.3.5: Displacement vs. Natural frequency in coupled bending-twisting vibration for 2 DOFS.

Natural frequency (rad/s):

$$\omega_1 = 173$$

$$\omega_2 = 1254$$

Effect of decreasing c_i on coupled bending-twisting vibration (Long Side)

Here, the value of mass eccentricity is decreased by half from the initial assuming value, c_1=0.1 mm, to c_1=0.05 mm and c_2=0.05 mm to c_2=0.025 mm. After decreasing, c_i natural frequency is decreased. The effect of decreasing mass eccentricity is shown in figure 4.3.6.
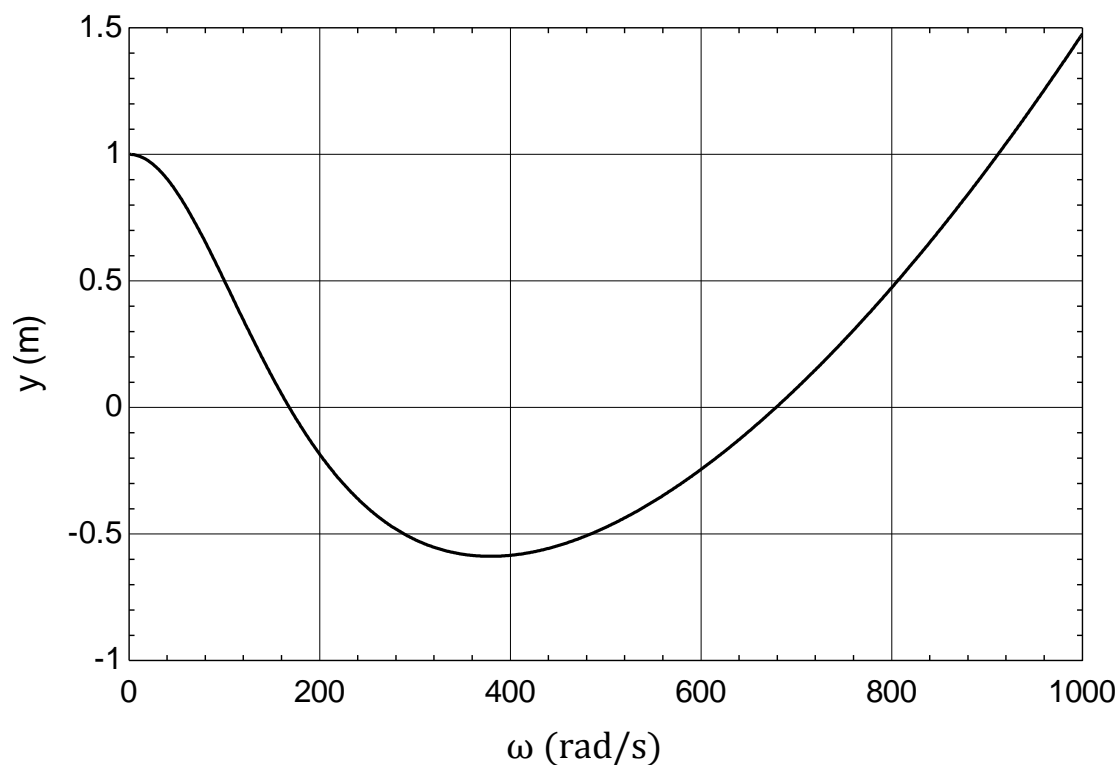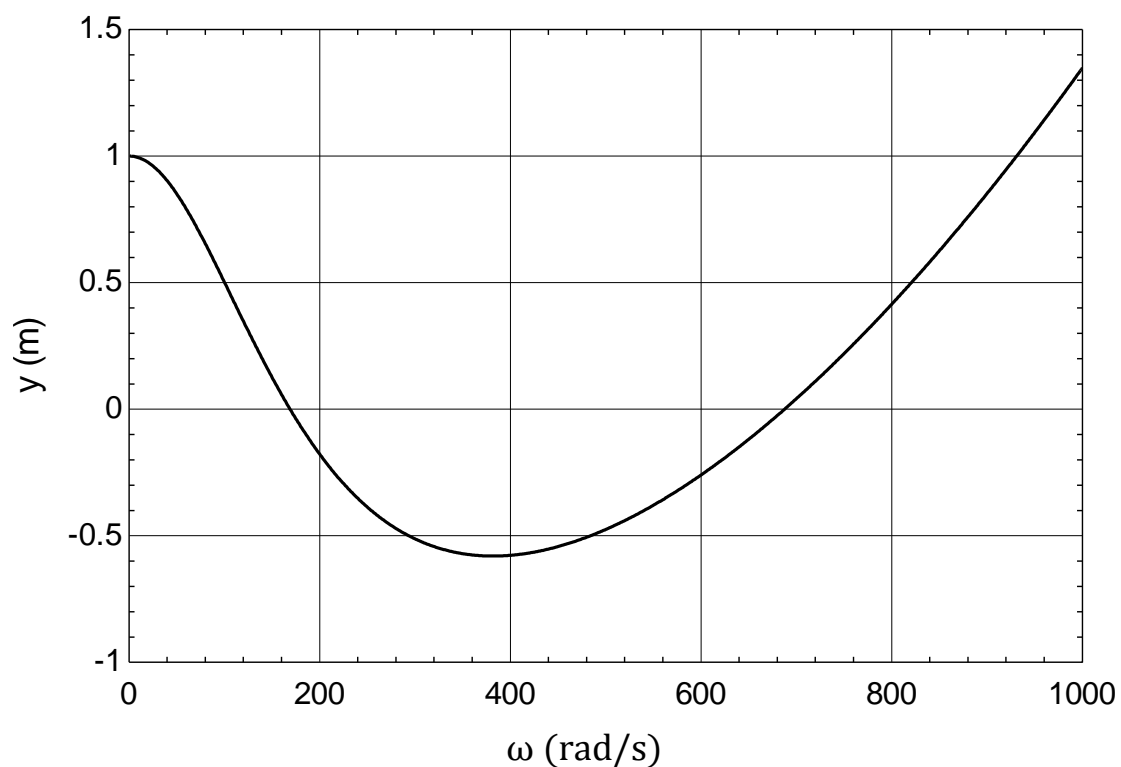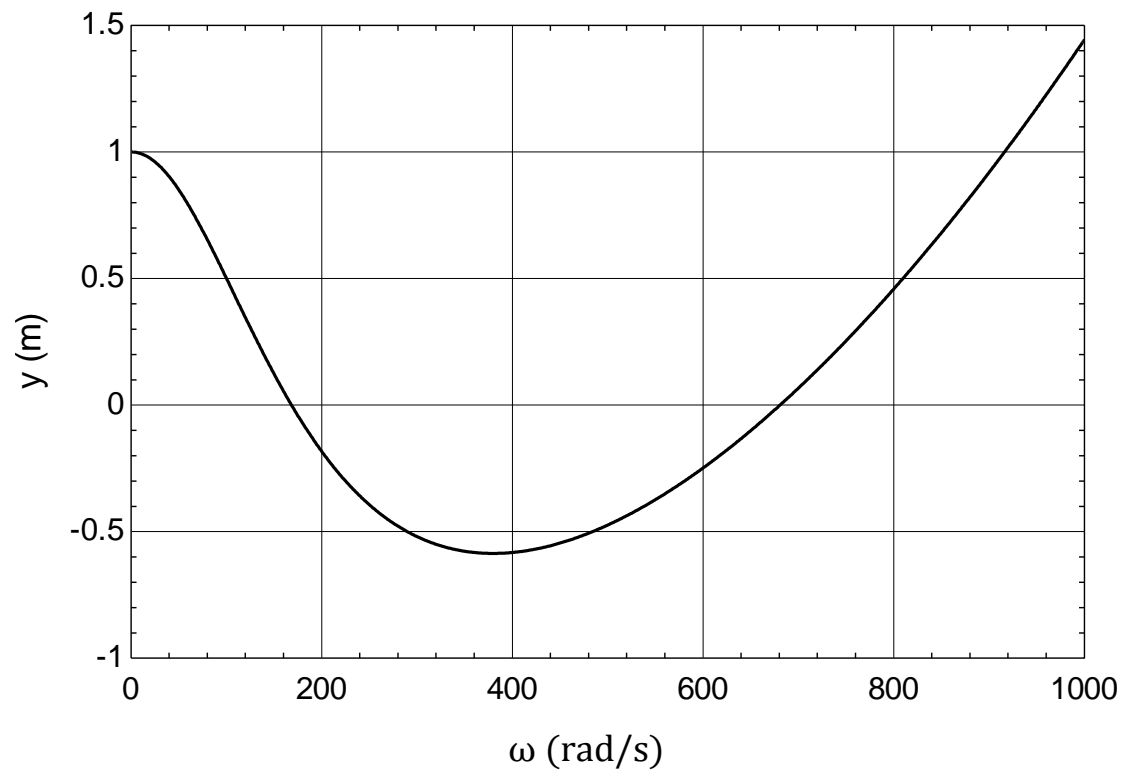

Figure 4.3.6: Displacement vs. Natural frequency in coupled bending-twisting vibration for 2 DOFS.

Natural frequency (rad/s):

$$\omega_1 = 168$$

$$\omega_2 = 681$$

4.4: Lumped masses are at unequal distance (Long side)

In this scenario, the stockbridge damper is modeled as a cantilever beam, with the mass of the damper separated into two portions same as before but the distance between these two lumped masses is presumed to be unequal. The parameter evaluated stockbridge damper as a 2DOFS is shown in figure 4.4.

m$_1$= 2.1 kg   m$_2$ = 0.3 kg

160 mm   110 mm

①   ②   ③

Figure 4.4: Lumped parameter system in stockbridge damper [Long side and lumped masses are at unequal distance for 2DOFS].

We calculated the natural frequency of this 2DOFS both in uncoupled bending ($c_i = 0$) as well as coupled bending-twisting ($c_i \neq 0$) modes for different values of mass eccentricity same as before. The results of the natural frequency are shown in table 2. Table 2 is also shown the comparison of the natural frequency of the long side of the stockbridge damper when lumped masses are kept at an equal and unequal distances.

Table 2: Summary of the natural frequency of uncoupled bending and coupled bending-twisting vibration for 2 DOFS for different values of mass eccentricity (Long side and lumped masses are at equal and unequal distances)

Eccentricity (mm)	Natural frequency at long side (rad/s)	
	Equal distance between lumped mass (mm) $L_1=L_2=135$	Unequal distance between lumped mass (mm) $L_1=160$ & $L_2=110$
$c_1=0$ $c_2=0$	$\omega_1 = 168$ $\omega_2 = 679$	$\omega_1 = 191$ $\omega_2 = 676$
$c_1=0.1$ $c_2=0.05$	$\omega_1 = 169$ $\omega_2 = 688$	$\omega_1 = 192$ $\omega_2 = 686$
$c_1=0.2$ $c_2=0.1$	$\omega_1 = 172$ $\omega_2 = 718$	$\omega_1 = 195$ $\omega_2 = 717$
$c_1=0.4$ $c_2=0.08$	$\omega_1 = 173$ $\omega_2 = 1254$	$\omega_1 = 197$ $\omega_2 = 800$
$c_1=0.05$ $c_2=0.025$	$\omega_1 = 168$ $\omega_2 = 681$	$\omega_1 = 191$ $\omega_2 = 678$

Table 2 shows that the natural frequency has increased by increasing the value of mass eccentricity and vice versa both in the equal and unequal distance of the lumped masses. The natural frequency has increased in bending-twisting vibration mode ($c_i \neq 0$) both in mode shape 1 (ω_1) and mode shape 2 (ω_2) compare to the uncoupled bending mode ($c_i = 0$). These results in table 2 are calculated only for the long side of the stockbridge damper.

CASE 2: STOCKBRIDGE DAMPER ACTING AS A 2 DOFS (SHORT SIDE)

4.5: Lumped masses are at equal distance (Short side)

In case 2, the same procedure followed on the short side to calculate the natural frequency of this 2 DOFS. The masses of the damper are separated into two portions. The distances between these two portions are presumed to be equal. The parameter evaluated by the stockbridge damper as a 2DOFS is shown in figure 4.5.

m_1= 1.9 kg m_2= 0.2 kg

115 mm   115 mm

①   ②   ③
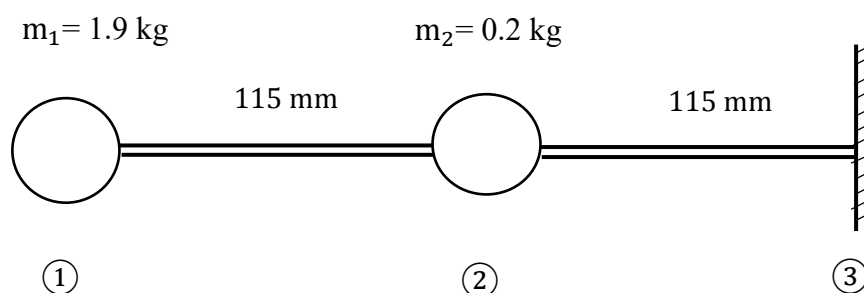
Figure 4.5: Lumped parameter system in stockbridge damper [Short side and lumped masses are at equal distance for 2DOFS].

Uncoupled bending ($c_i = 0$) and Coupled bending-twisting ($c_i \neq 0$) vibration comparison

On the short side of the stockbridge damper, Graph 4.5.1 compares the effects of mass eccentricity on vibration between uncoupled bending and coupled bending-twisting vibration modes. There is no mass eccentricity in the uncoupled bending mode (c_1=0 mm, c_2=0 mm), but there is acting eccentricity in the coupled bending-twisting mode (c_1=0.1 mm and c_2=0.05 mm). Due to the influence of mass eccentricity, which is depicted in figure 4.5.1 and the natural frequency has increased in the bending-twisting vibration mode.
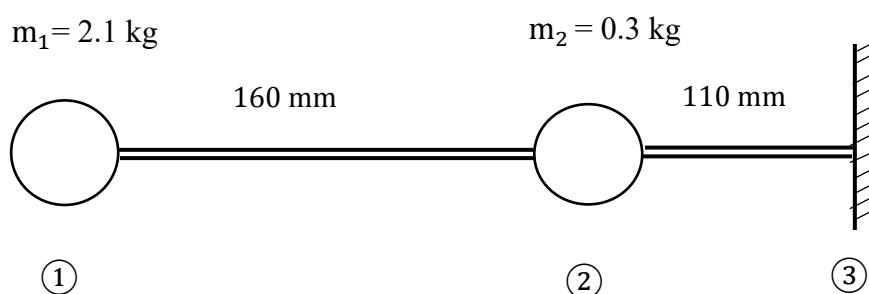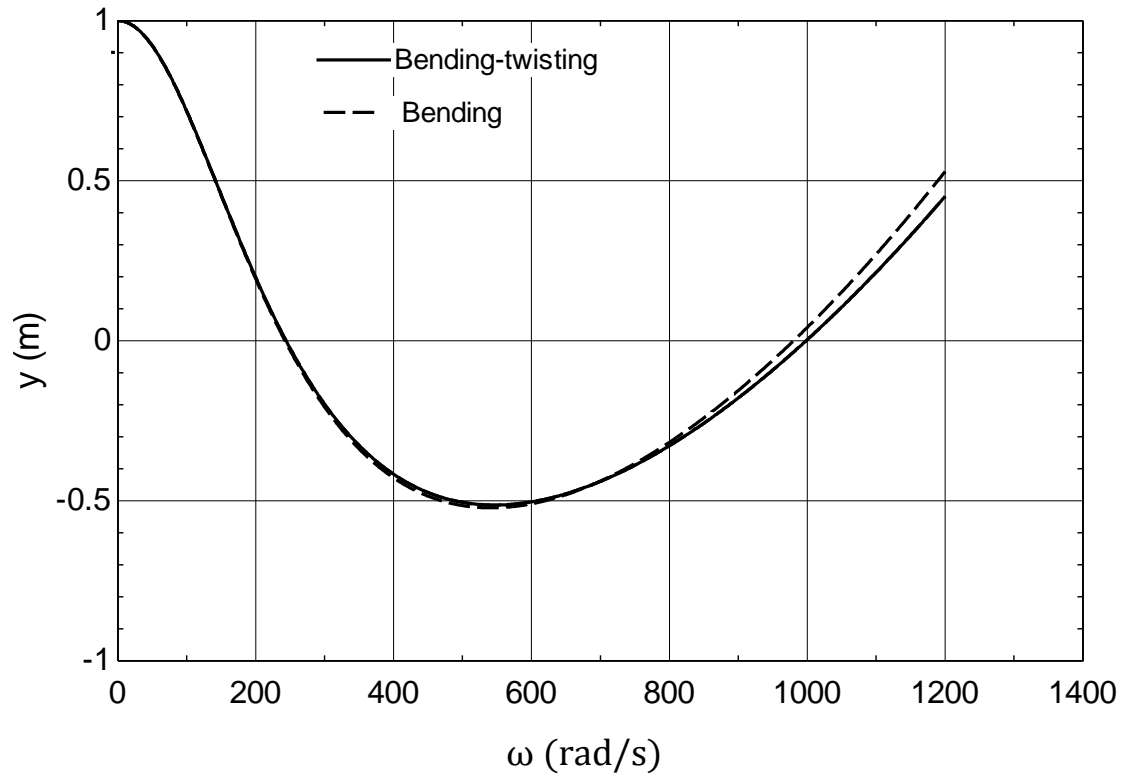
Figure 4.5.1: Displacement vs. Natural frequency in uncoupled bending and coupled bending-twisting vibration for 2 DOFS.

Table 3: Uncoupled bending & Coupled bending-twisting Natural Frequency Comparison for 2 DOFS (Short side and lumped masses are at equal distance)

Natural frequency (rad/s)	
Bending vibration (c_1=0 mm, c_2=0 mm)	Bending-twisting vibration (c_1=0.1 mm, c_2=0.05 mm)
$\omega_1 = 242$	$\omega_1 = 243$
$\omega_2 = 979$	$\omega_2 = 997$

Table 3 shows the results of the natural frequency which is generated from figure 4.5.1. The natural frequency has increased in bending-twisting vibration mode both in ω_1 for mode shape 1 and ω_2 for mode shape 2 compared to the uncoupled bending mode. But this change is not too large. Similarly we calculate the natural frequency in short side for different values of mass eccentricity same as before.

Effect of increasing c_i on coupled bending-twisting vibration (Short Side)

The mass eccentricity is increased by double from the initially assumed value of c_1=0.1 mm, to c_1=0.2 mm and c_2=0.05 mm to c_2=0.1 mm similar to the long side. The natural frequency corresponding to this mass eccentricity has increased which is shown in figure 4.5.4.

Figure 4.5.2: Displacement vs. Natural frequency in coupled bending-twisting vibration for 2 DOFS.

Natural frequency (rad/s):

$$\omega_1 = 248$$
$$\omega_2 = 1060$$

Effect of randomly increased value of c_i on coupled bending-twisting vibration (Short Side)

The natural frequency of the same problem is calculated by randomly increasing the mass eccentricity from c_1 =0.1 mm to c_1=0.4 mm and c_2 =0.05 mm to c_2 =0.08 mm. The effect of increasing c_i in natural frequency is shown in Figure 4.5.3.
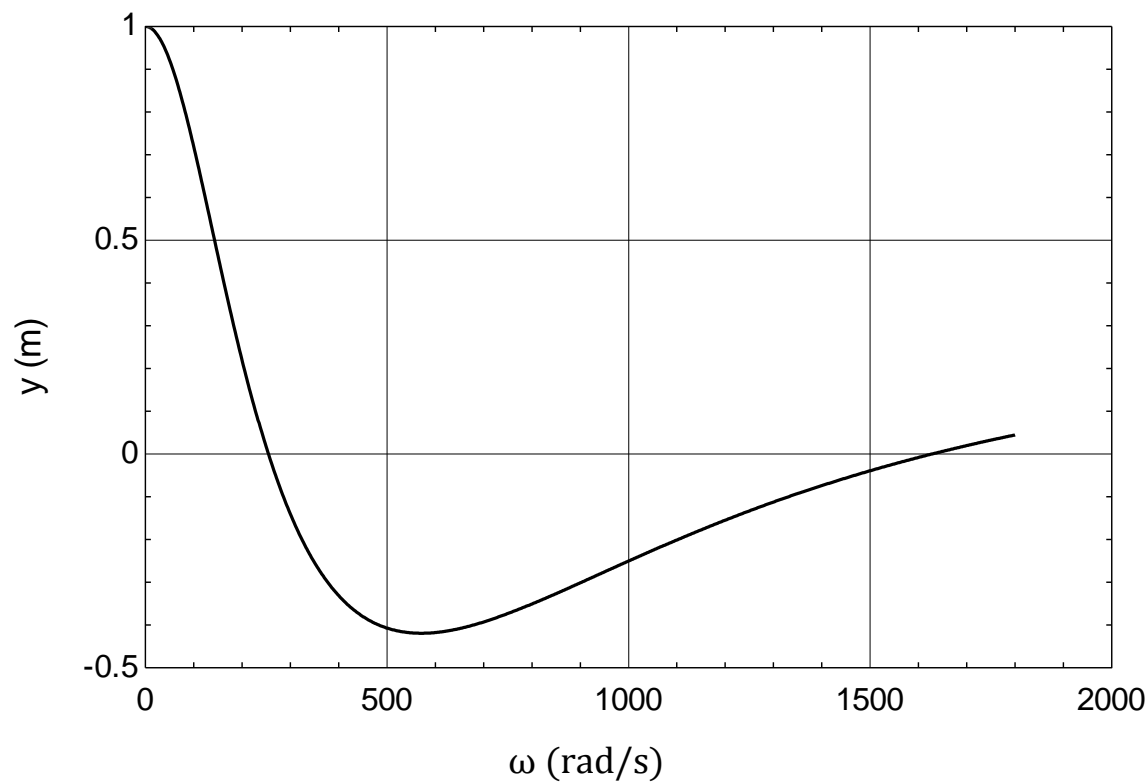
Figure 4.5.3: Displacement vs. Natural frequency in coupled bending-twisting vibration for 2 DOFS.

Natural frequency (rad/s):

$$\omega_1 = 254$$
$$\omega_2 = 1629$$

Effect of decreasing c_i on coupled bending-twisting vibration (Short Side)

After increasing the value of mass eccentricity, now we decreased by half of the initial assuming value of mass eccentricity to find the change of natural frequency of the identical problem. Mass eccentricity has decreased from c_1=0.1 mm, to c_1=0.05 mm and c_2=0.05 mm to c_2=0.025 mm. The corresponding results are shown in figure 4.5.6. The natural frequency obtained from this result has decreased by decreasing mass eccentricity.

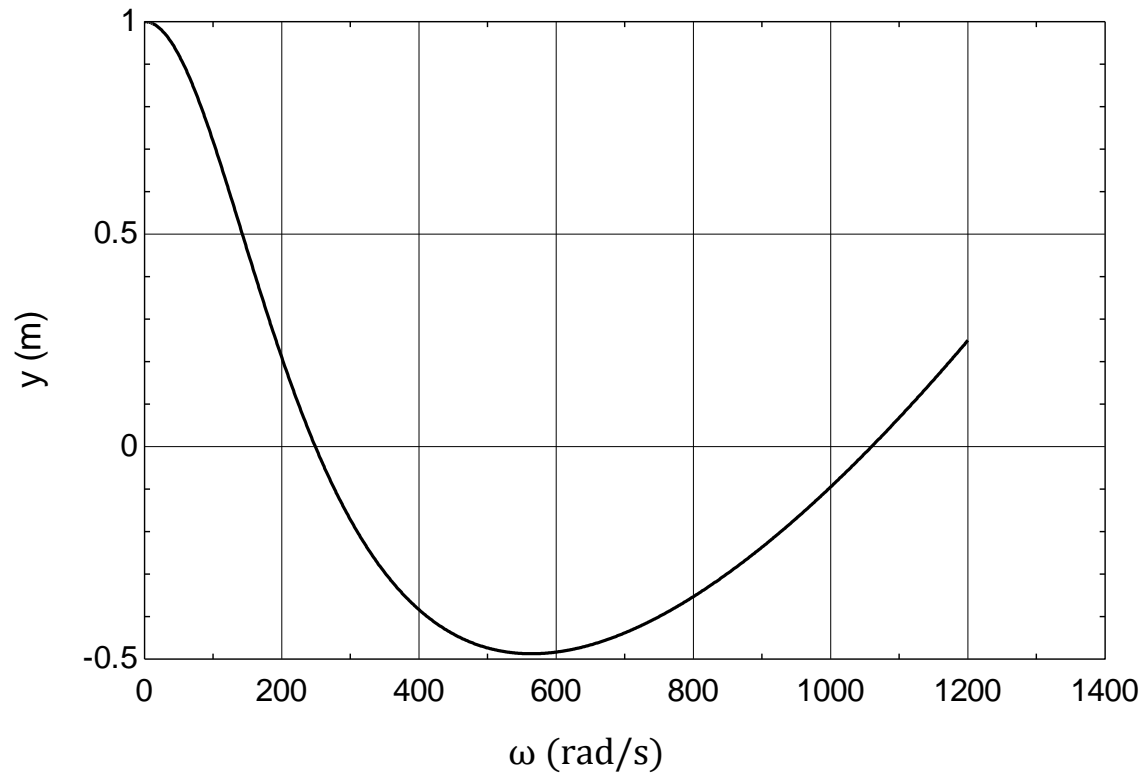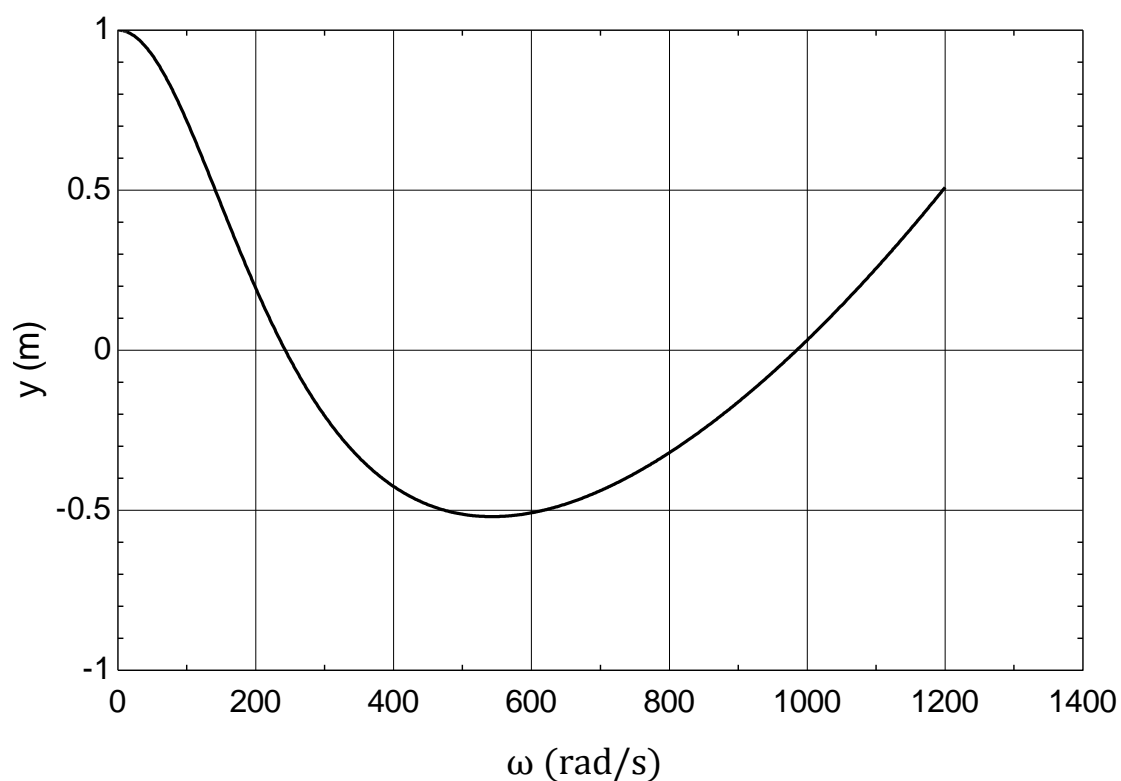Figure 4.5.4: Displacement vs. Natural frequency in coupled bending-twisting vibration for 2 DOFS.

Natural frequency (rad/s):

$$\omega_1 = 242$$
$$\omega_2 = 984$$

4.6: Lumped masses are at unequal distance (Short side)

Figure 4.6 is represented the short side of the stockbridge damper. In the same way as before, the mass of the damper is considered into two portions and the distances between these two portions are presumed to be unequal. The parameter evaluated the stockbridge damper as a 2DOFS.
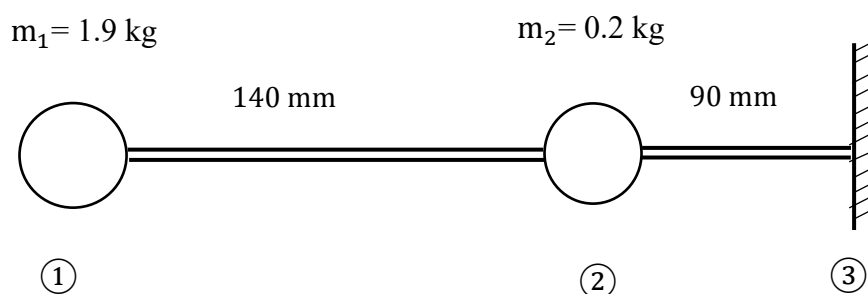
Figure 4.6: Lumped parameter system in stockbridge damper [Short side and lumped masses are at unequal distance for 2DOFS].

.

Similarly, we calculated the natural frequency of this short side (unequal distance between lumped mass) both in uncoupled bending ($c_i = 0$) as well as coupled bending-twisting ($c_i \neq 0$) modes for different values of mass eccentricity same as bofore. The results of the natural frequency are shown in table 4. Table 4 is also shown the comparison of natural frequency of the short side when lumped masses are kept at equal and unequal distances. The graphs corresponding of the results are kept in Appendix-A. Sometimes the density of the materials is not uniform throughout the length. So, when we considered the lumped masses are at unequal distances, which will show the effect of change of natural frequency compare to keeping the lumped masses in equal distances.

Table 4: Summary of natural frequency of uncoupled bending and coupled bending-twisting vibration for 2DOFS for different values of mass eccentricity (Short side and lumped masses are at equal and unequal distances)

Eccentricity (mm)	Natural frequency (rad/s)	
	Equal distance between lumped mass (mm) $L_1=L_2=115$	Unequal distance between lumped mass (mm) $L_1=140$ & $L_2=90$
$c_1=0$ $c_2=0$	$\omega_1 = 242$ $\omega_2 = 979$	$\omega_1 = 315$ $\omega_2 = 1035$
$c_1=0.1$ $c_2=0.05$	$\omega_1 = 243$ $\omega_2 = 997$	$\omega_1 = 318$ $\omega_2 = 1063$
$c_1=0.2$ $c_2=0.1$	$\omega_1 = 248$ $\omega_2 = 1060$	$\omega_1 = 325$ $\omega_2 = 1168$
$c_1=0.4$ $c_2=0.08$	$\omega_1 = 254$ $\omega_2 = 1629$	$\omega_1 = 348$ $\omega_2 = 1238$
$c_1=0.05$ $c_2=0.025$	$\omega_1 = 242$ $\omega_2 = 984$	$\omega_1 = 316$ $\omega_2 = 1043$

Table 4 shows the results obtained from short side of the stockbridge damper. The natural frequency has also increased by increasing the value of mass eccentricity and vice versa in both distances. The natural frequency has also increased here in bending-twisting vibration mode ($c_i \neq 0$) both in mode shape 1 (ω_1) and mode shape 2 (ω_2) compare to the uncoupled bending mode ($c_i = 0$).

The natural frequency is increased when lumped masses are at unequal distance compare to equal distance. But it is not in likewise increased. When mass eccentricity has randomly increased for the values of $c_1=0.4$ & $c_2=0.08$, the natural frequency has decreased in mode shape 2.

Table 5: Summary of natural frequency of uncoupled bending and coupled bending-twisting vibration for 2 DOFS for different values of mass eccentricity (Long side and short side where lumped masses are at equal and unequal distance)

Eccentricity (mm)	Natural frequency (rad/s)			
	Long side (mm)		Short side (mm)	
	$L_1=L_2=135$	$L_1=160$ & $L_2=110$	$L_1=L_2=115$	$L_1=140$ & $L_2=90$
$c_1=0$ $c_2=0$	$\omega_1 = 168$ $\omega_2 = 679$	$\omega_1 = 191$ $\omega_2 = 676$	$\omega_1 = 242$ $\omega_2 = 979$	$\omega_1 = 315$ $\omega_2 = 1035$
$c_1=0.1$ $c_2=0.05$	$\omega_1 = 169$ $\omega_2 = 688$	$\omega_1 = 192$ $\omega_2 = 686$	$\omega_1 = 243$ $\omega_2 = 997$	$\omega_1 = 318$ $\omega_2 = 1063$
$c_1=0.2$ $c_2=0.1$	$\omega_1 = 172$ $\omega_2 = 718$	$\omega_1 = 195$ $\omega_2 = 717$	$\omega_1 = 248$ $\omega_2 = 1060$	$\omega_1 = 325$ $\omega_2 = 1168$
$c_1=0.4$ $c_2=0.08$	$\omega_1 = 173$ $\omega_2 = 1254$	$\omega_1 = 203$ $\omega_2 = 800$	$\omega_1 = 254$ $\omega_2 = 1629$	$\omega_1 = 348$ $\omega_2 = 1238$
$c_1=0.05$ $c_2=0.025$	$\omega_1 = 168$ $\omega_2 = 681$	$\omega_1 = 191$ $\omega_2 = 678$	$\omega_1 = 242$ $\omega_2 = 984$	$\omega_1 = 316$ $\omega_2 = 1043$

Table 5 shows the whole results which are obtained on both sides of the stockbridge damper in 2 DOFS. The discussion against these obtained results of natural frequency is described below:

Effect of mass eccentricity on natural frequency:

Mass eccentricity has a great impact on natural frequency in the 2DOFS of the stockbridge damper shown in table 5. The natural frequency of uncoupled bending ($c_i = 0$) vibration mode is lower than the coupled bending-twisting ($c_i \neq 0$) vibration mode i.e. the natural frequency is increased in coupled bending-twisting mode due to mass eccentricity. When we gradually increased the value of mass eccentricity, natural frequency is also increased both in ω_1 for mode shape 1 and ω_2 for mode shape 2 and vice versa. The difference in natural frequency is not too large compared to the immediate value of mass eccentricity. This impact is shown in table 5 on both sides of the stockbridge damper.

Effect of lumped mass distance on natural frequency:

On the both sides, natural frequency is calculated by keeping the lumped masses are at an equal and unequal distance. We know that sometimes the density of the materials is not uniform throughout the entire length. To represent this ununiformed case, we considered lumped masses are at an equal and unequal distance. On the long side, when lumped masses are at an unequal distance the natural frequency is increased in mode shape $1(\omega_1)$ but the natural frequency is decreased in mode shape $2(\omega_2)$ compare to the equal distance. On long side ω_1 is increased by 20.1% and ω_2 is decreased by 45.3% for entire values of mass eccentricity. But on the short side, natural frequency is increased both in mode shape $1(\omega_1)$ 30.2 % and mode shape 2 (ω_2) 63.4 % in unequal distance compare to the equal distance.

CASE 3: STOCKBRIDGE DAMPER ACTING AS A 3 DOFS (LONG SIDE)

In this case, we will find the effect of mass eccentricity by increasing the DOF while keeping the stockbridge damper's overall mass and length constant. On both sides, we treated the stockbridge damper as a 3 DOFS. When DOF is increased lumped masses are distributed in many positions over the entire length.

4.7. Lumped masses are at equal distance (Long side)

In this scenario, the stockbridge damper is modeled as a cantilever beam, with the mass of the damper separated into three portions. The distance between these three portions is presumed to be equal. The parameter evaluated the stockbridge damper as a 3DOFS on the long side which is shown in Figure 4.7.
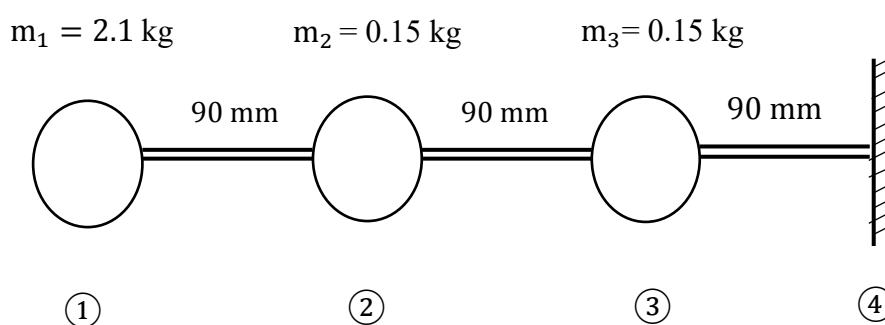

Figure 4.7: Lumped parameter system ın stockbridge damper [Long side and lumped masses are at equal distance for 3DOFS].

Uncoupled bending vibration ($c_i = 0$) (Long Side)

Assuming that there is no mass eccentricity (c_1=0 mm, c_2=0 mm and c_3=0 mm), we first determine the natural frequency of these three DOFS in uncoupled bending mode. Figure 4.7.1 displays the outcomes of the natural frequency in this instance.

Figure 4.7.1: Displacement vs. Natural frequency in uncoupled bending vibration for 3 DOFS.

Natural frequency (rad/s):

$$\omega_1 = 245$$

$$\omega_2 = 803$$

$$\omega_3 = 3324$$

Coupled bending-twisting vibration ($c_i \neq 0$) (Long Side)

In this coupled bending-twisting vibration mode, there is acting some mass eccentricity.The values of mass eccentricity in station 1, station 2 and station 3 are c_1=0.1 mm, c_2=0.05 mm and c_3=0.01 mm respectively. After considering mass eccentricity, the results of the natural frequency in this case are shown in figure 4.7.2.
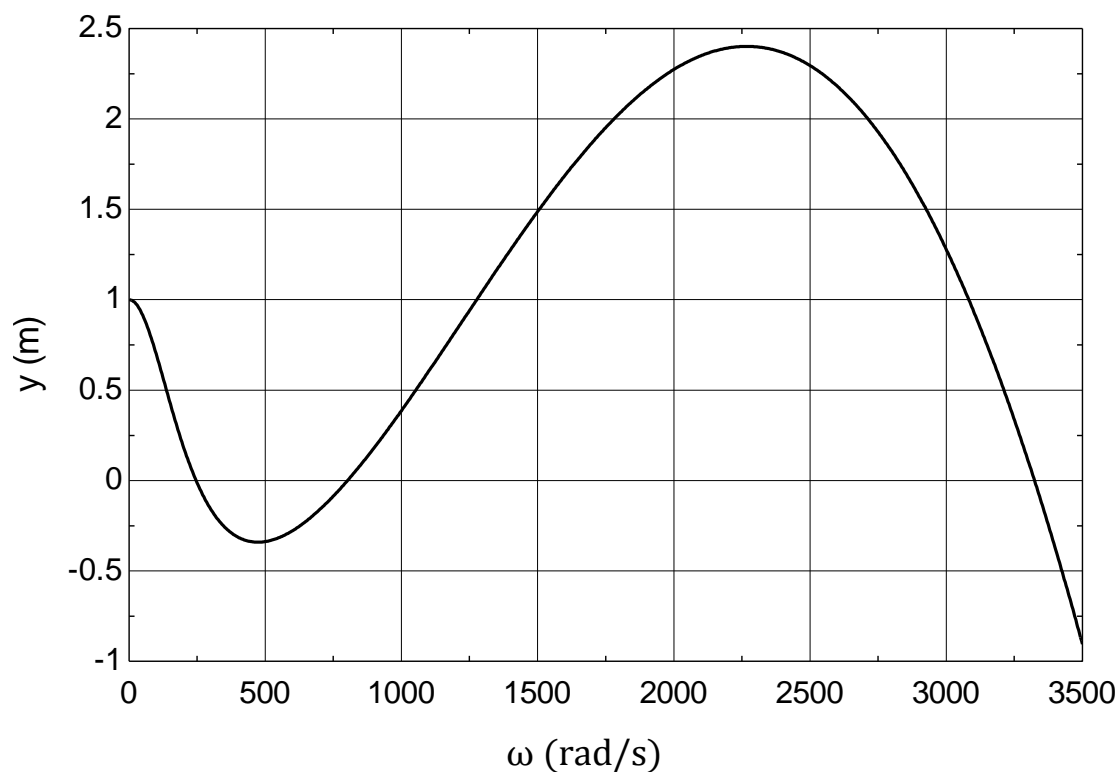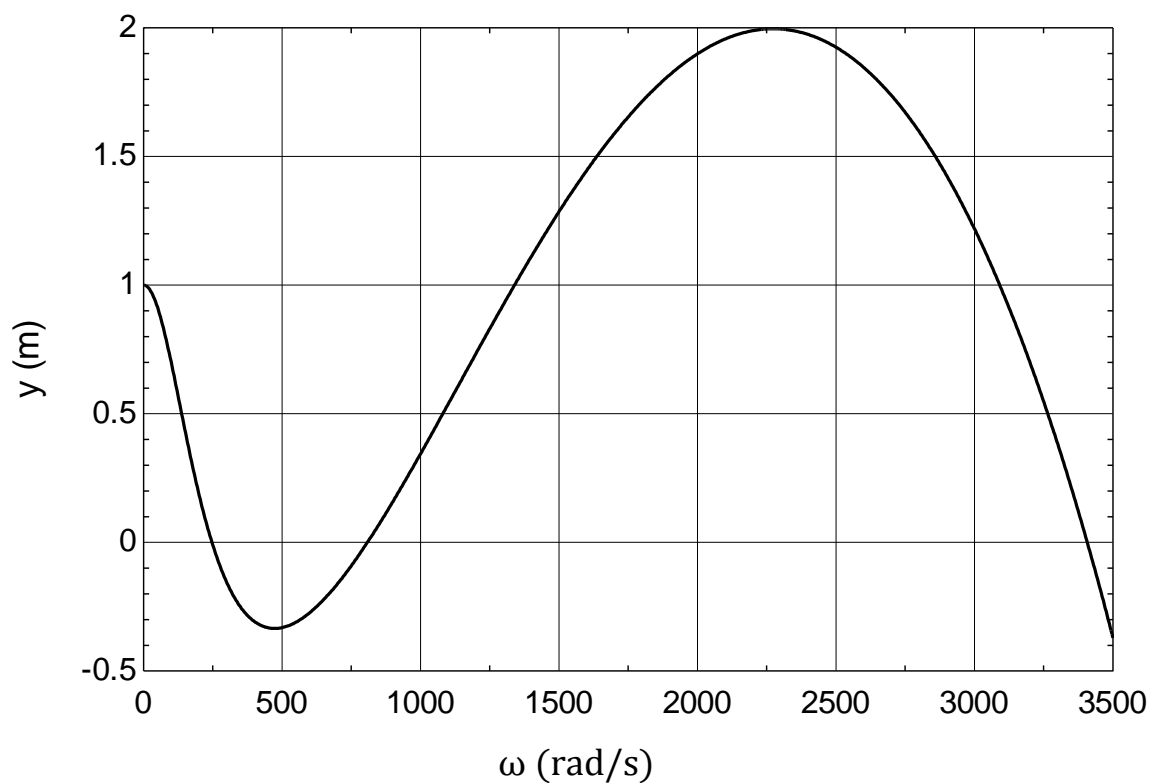
Figure 4.7.2: Displacement vs. Natural frequency in coupled bending vibration for 3 DOFS

Natural frequency (rad/s):

$$\omega_1 = 246$$
$$\omega_2 = 808$$
$$\omega_3 = 3407$$

Uncoupled bending and Coupled bending-twisting vibration comparison

The graph 4.7.3 compares the influence of mass eccentricity on vibration between uncoupled bending and coupled bending-twisting vibration modes, which were generated using graphs 4.7.1 and 4.7.2 respectively. This graph 4.7.3 shows the mass eccentricity effect on natural frequency between uncoupled bending and coupled bending-twisting vibration.
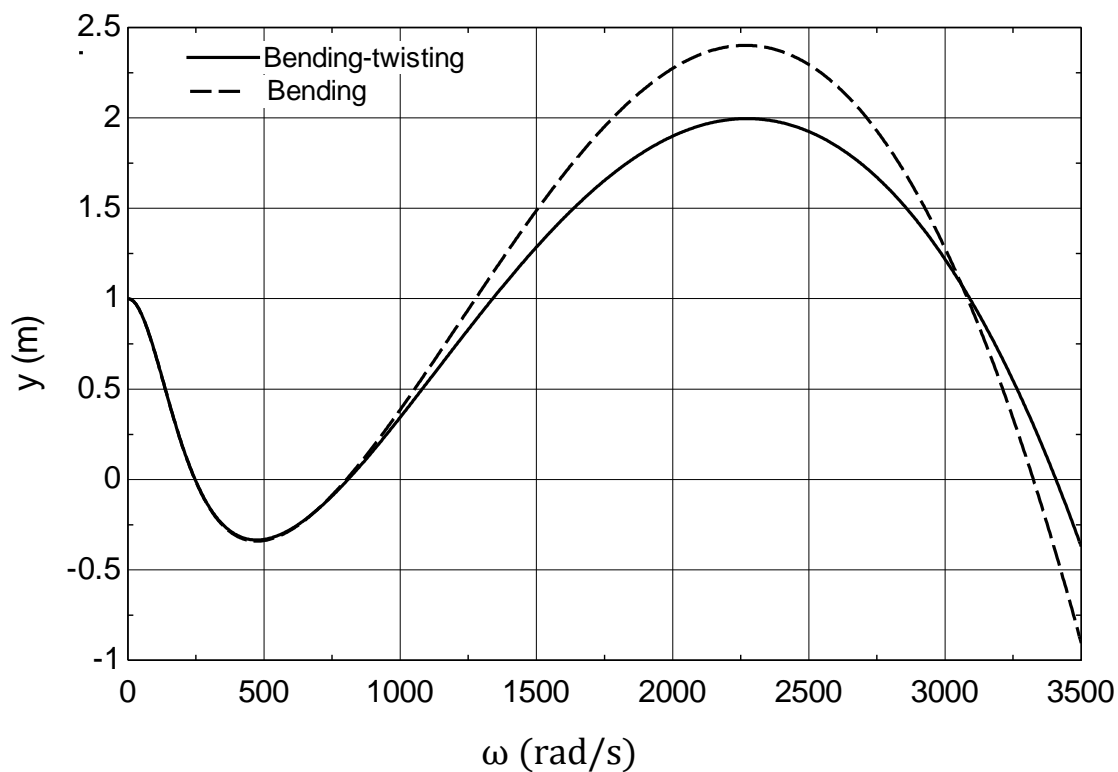
Figure 4.7.3: Displacement vs. Natural frequency in uncoupled bending and coupled bending-twisting vibration for 3 DOFS.

Table 6: Uncoupled bending & coupled bending-twisting natural frequency comparison for 3 DOFS (Long side and lumped masses are at equal distance)

Natural frequency (rad/s)	
Bending vibration ($c_1=0$, $c_2=0$, $c_3=0$)	Bending-twisting vibration ($c_1=0.1$ mm, $c_2=0.05$ mm, $c_3=0.01$ mm)
$\omega_1 = 245$	$\omega_1 = 246$
$\omega_2 = 803$	$\omega_2 = 808$
$\omega_3 = 3324$	$\omega_3 = 3407$

The natural frequency has increased both in mode shape 1 (ω_1); mode shape 2 (ω_2) and mode shape 3 (ω_3) due to the effect of mass eccentricity, as seen in table 6. Similarly, for coupled bending-twisting vibration, the mass eccentricity effect will be calculated for the following steps:

Effect of increasing c_i on coupled bending-twisting vibration (Long Side)

The value of mass eccentricity is increased by double from the initial assuming value. The natural frequency of the identical problem is calculated by increasing the mass eccentricity from $c_1=0.1$ mm, to $c_1=0.2$ mm; $c_2=0.05$ mm to $c_2=0.1$ mm and $c_3=0.01$ mm to $c_3=0.02$ mm. The results are shown in figure 4.7.4.

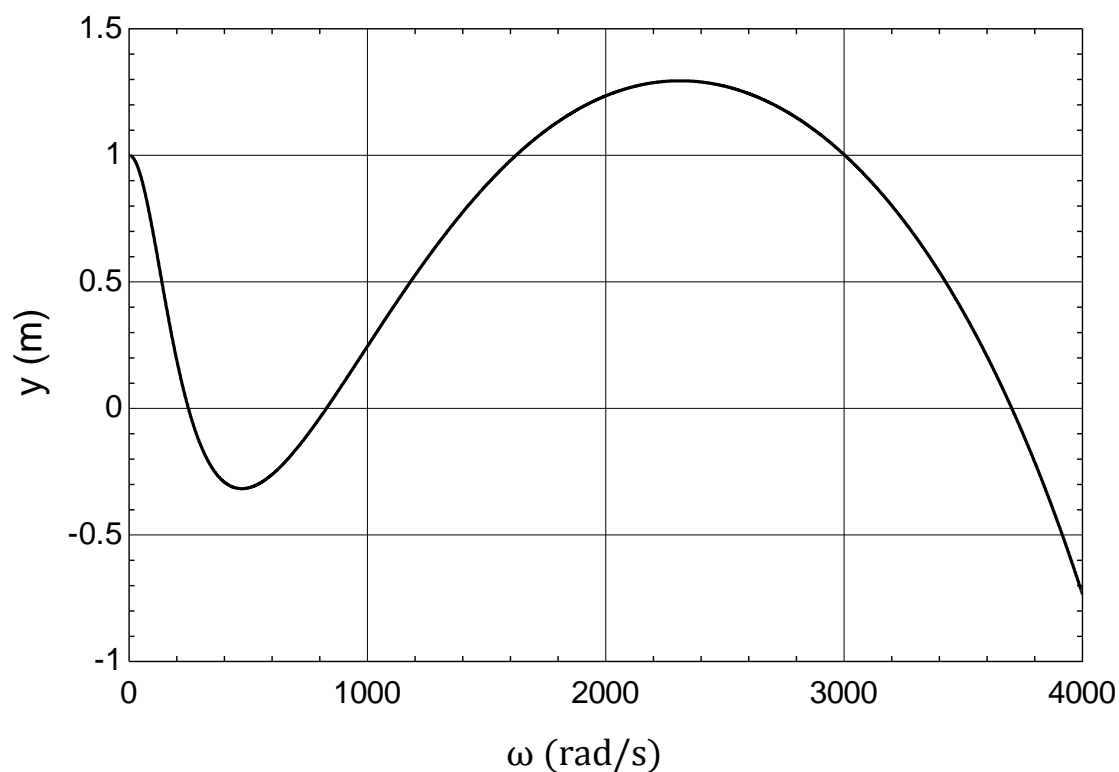Figure 4.7.4: Displacement vs. Natural frequency in coupled bending vibration for 3 DOFS.

Natural frequency (rad/s):

$$\omega_1 = 248$$
$$\omega_2 = 828$$
$$\omega_3 = 3703$$

Effect of randomly increased value of c_i on coupled bending-twisting vibration (Long Side)

The natural frequency of the identical problem is calculated by increasing randomly of the mass eccentricity from c_1=0.2 mm, to c_1=0.4 mm; c_2=0.1 mm to c_2=0.08 mm. and c_3=0.02 mm to c_3=0.016 mm. After changing the values of mass eccentricity in every station, it affected the natural frequency of this 3 DOFS. The obtained results are shown in figure 4.7.5.

Figure 4.7.5: Displacement vs. Natural frequency in coupled bending vibration for 3 DOFS.

Natural frequency (rad/s):

$$\omega_1 = 254$$

$$\omega_2 = 949$$

$$\omega_3 = 5048$$

Effect of decreasing c_i on coupled bending-twisting vibration (Long Side)

Here, the value of mass eccentricity is decreased by half from the initial assuming value. Now the natural frequency of the identical problem is calculated for c_1=0.05 mm; c_2=0.025 mm and c_3=0.005 mm. The effect of decreasing the value of mass eccentricity is shown in figure 4.7.6.
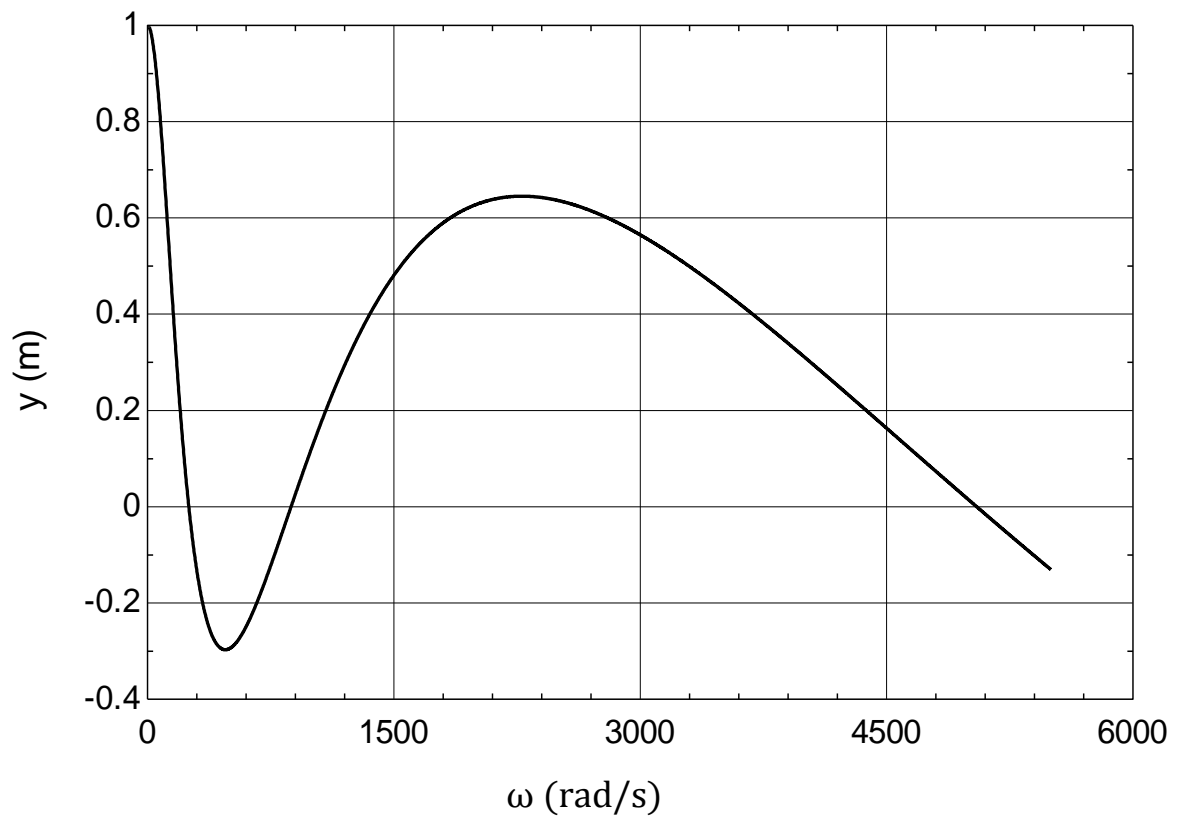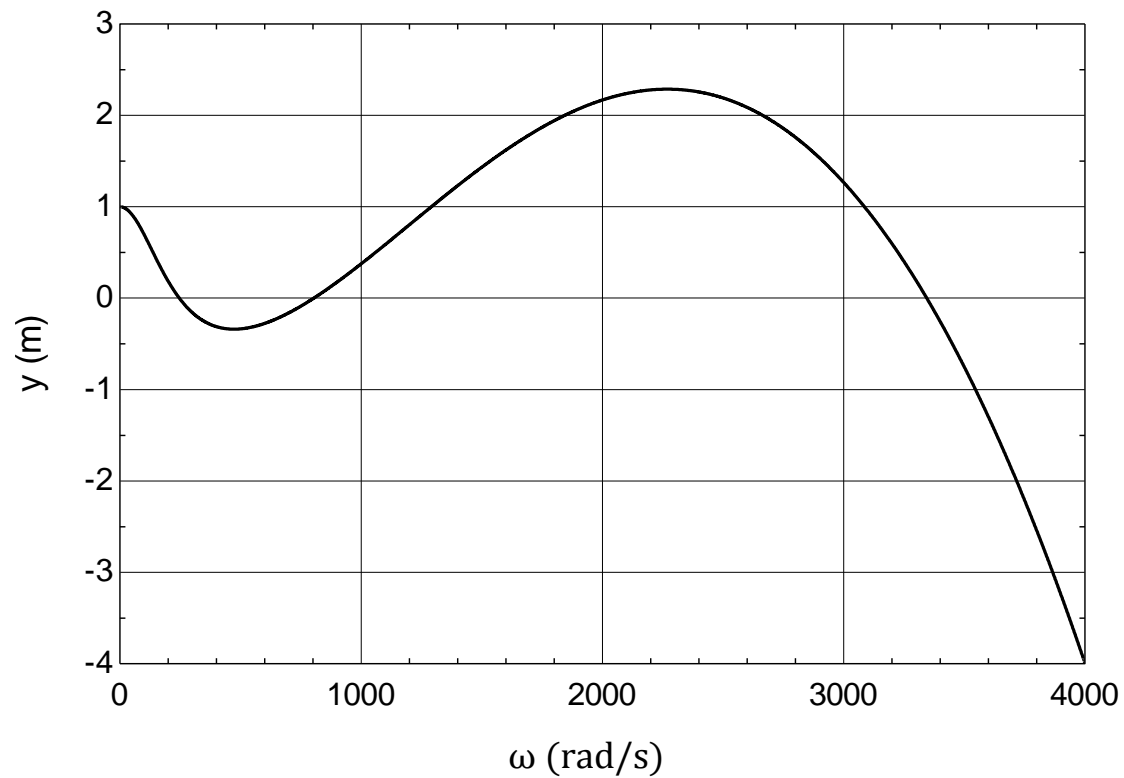

Figure 4.7.6: Displacement vs. Natural frequency in coupled bending vibration for 3 DOFS.

Natural frequency (rad/s):

$$\omega_1 = 246$$
$$\omega_2 = 803$$
$$\omega_3 = 3344$$

Similarly, the effect of mass eccentricity is calculated by keeping the lumped masses at an unequal distance. We also calculated the natural frequency on the short side of this 3DOFS following the same procedure. All of these results are shown in table 7 and corresponding graphs are kept in Appendix-B.

Table 7: Summary of natural frequency of uncoupled bending and coupled bending-twisting vibration for 3 DOFS for different values of mass eccentricity (Long side and Short side where lumped masses are at equal and unequal distances)

Eccentricity (mm)	Natural frequency (rad/s)			
	Long side (mm)		Short side (mm)	
	$L_1=L_2=L_3=90$	$L_1=110, L_2=90$ & $L_3=70$	$L_1=L_2=L_3=76.7$	$L_1=100, L_2=75$ & $L_3=55$
$c_1=0$ $c_2=0$ $c_3=0$	$\omega_1 = 245$ $\omega_2 = 803$ $\omega_3 = 3324$	$\omega_1 = 274$ $\omega_2 = 928$ $\omega_3 = 3062$	$\omega_1 = 336$ $\omega_2 = 1129$ $\omega_3 = 5129$	$\omega_1 = 472$ $\omega_2 = 1808$ $\omega_3 = 6335$
$c_1=0.1$ $c_2=0.05$ $c_3=0.01$	$\omega_1 = 246$ $\omega_2 = 808$ $\omega_3 = 3407$	$\omega_1 = 275$ $\omega_2 = 932$ $\omega_3 = 3125$	$\omega_1 = 368$ $\omega_2 = 1141$ $\omega_3 = 5310$	$\omega_1 = 476$ $\omega_2 = 1820$ $\omega_3 = 6395$
$c_1=0.2$ $c_2=0.1$ $c_3=0.02$	$\omega_1 = 248$ $\omega_2 = 828$ $\omega_3 = 3703$	$\omega_1 = 278$ $\omega_2 = 948$ $\omega_3 = 3341$	$\omega_1 = 371$ $\omega_2 = 1182$ $\omega_3 = 6005$	$\omega_1 = 485$ $\omega_2 = 1855$ $\omega_3 = 6602$
$c_1=0.4$ $c_2=0.08$ $c_3=0.016$	$\omega_1 = 254$ $\omega_2 = 949$ $\omega_3 = 5048$	$\omega_1 = 283$ $\omega_2 = 987$ $\omega_3 = 3685$	$\omega_1 = 374$ $\omega_2 = 1253$ $\omega_3 = 8901$	$\omega_1 = 526$ $\omega_2 = 2078$ $\omega_3 = 9369$
$c_1=0.05$ $c_2=0.025$ $c_3=0.005$	$\omega_1 = 246$ $\omega_2 = 803$ $\omega_3 = 3344$	$\omega_1 = 274$ $\omega_2 = 929$ $\omega_3 = 3077$	$\omega_1 = 366$ $\omega_2 = 1133$ $\omega_3 = 5173$	$\omega_1 = 474$ $\omega_2 = 1811$ $\omega_3 = 6355$

Table 7 shows the complete results of 3DOFS. The discussion against these obtained results is described below:

Effect of mass eccentricity on natural frequency:

The natural frequency of uncoupled bending ($c_i = 0$) vibration mode is lower than the coupled bending-twisting ($c_i \neq 0$) vibration mode i.e. natural frequency is increased in coupled bending-twisting mode due to mass eccentricity. This mass eccentricity effect is similar to 2DOFS. When we gradually increased the value of mass eccentricity, the natural frequency is also increased both in mode shape $1(\omega_1)$ and mode shape $2(\omega_2)$, and mode shape $3(\omega_3)$ and vice versa. The difference in natural frequency is not too large compared to the immediate values of mass eccentricity. This impact is shown in table 7 on both sides of the stockbridge damper.

Effect of lumped mass distance on natural frequency:

 On both sides, the natural frequency is calculated by keeping the lumped masses at an equal and unequal distance. On the long side, when lumped masses are at an unequal distance the natural frequency is increased in mode shape $1(\omega_1)$ by 15% and mode shape $2(\omega_2)$ by 22.2% but the natural frequency is decreased in mode shape $3(\omega_3)$ by 39% compared to the equal distance for entire values of mass eccentricity. But in short side, natural frequency is increased both in mode shape $1(\omega_1)$ 43.7%, mode shape $2(\omega_2)$ 83.4% and mode shape $3(\omega_3)$ 81.1% in unequal distance compare to the equal distance.

So, with a change in lumped mass distances, the natural frequency will be increased in some mode shapes and will be decreased in some mode shapes.

Effect of DOF on natural frequency:

When DOF is increased, lumped masses are distributed in more positions. But the total mass remains to be constant. The natural frequency is increased by increasing DOF compared to 3DOFS with 2DOFS. The natural frequency is changed both in mode shape $1(\omega_1)$ and mode shape $2(\omega_2)$ for both sides which is shown in table 7. On the long side and equal distance of lumped masses, the natural frequency is increased by 50.3% for mode shape $1(\omega_1)$ and 44.9% for mode shape 2 (ω_2). In long side and unequal distance, natural frequency is increased 48.2% for mode shape $1(\omega_1)$ and 45.6% for mode shape 2 (ω_2).

A similar impact is shown on another side of the stockbridge damper. On short side and equal distance, the natural frequency in mode shape $1(\omega_1)$ and mode shape $2(\omega_2)$ is increased by 51.2% and 15.1% respectively. Now for the unequal distance, natural frequency in mode shape $1(\omega_1)$ and mode shape $2(\omega_2)$ is also increased by 50% and 73.6% respectively.

CASE 4: STOCKBRIDGE DAMPER ACTING AS A 4 DOFS (LONG SIDE)

4.8. Lumped masses are at equal distance (Long side)

In this scenario, the stockbridge damper is modeled as a cantilever beam, with the mass of the damper separated into four portions. The total length of the messenger cable is divided into four portions. The distance between these four portions is presumed to be equal. The parameter evaluated stockbridge damper as a four-degree of freedom system is shown in Figure 4.8.
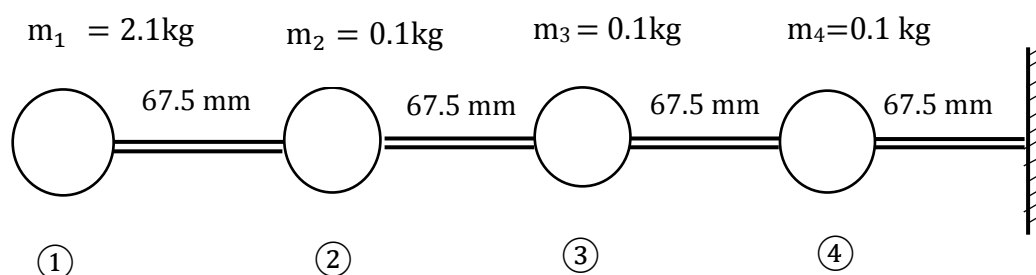
$m_1 = 2.1\text{kg}$ $m_2 = 0.1\text{kg}$ $m_3 = 0.1\text{kg}$ $m_4 = 0.1\text{ kg}$

67.5 mm   67.5 mm   67.5 mm   67.5 mm

① ② ③ ④

Figure 4.8: Lumped parameter system in stockbridge damper [Long side and lumped masses are at equal distance for 4 DOFS].

Uncoupled bending and Coupled bending-twisting vibration comparison

Graph 4.8.1 compares the influence of mass eccentricity in vibration between uncoupled bending and coupled bending-twisting vibration modes. In uncoupled bending, there is no mass eccentricity ($c_1=0$ mm, $c_2=0$ mm, $c_3=0$ mm and $c_4=0$ mm). But in twisting made, there is acting some eccentricity ($c_1=0.1$ mm, $c_2=0.05$ mm, $c_3=0.01$mm, $c_4=0.001$mm).
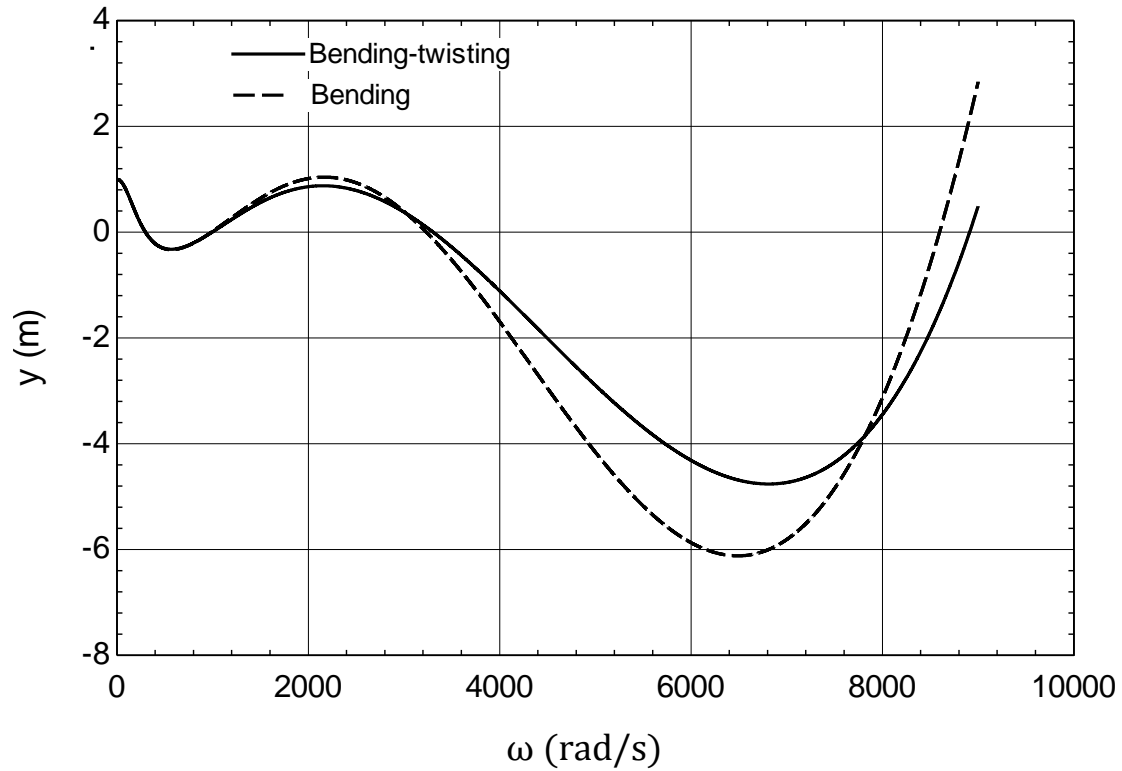
Figure 4.8.1: Displacement vs. Natural frequency in uncoupled bending and coupled
bending-twisting vibration for 4 DOFS.

Table 8: Uncoupled bending & coupled bending-twisting natural frequency comparison for 4 DOFS ((Long side and lumped masses are at equal distance)

Natural frequency (rad/s)	
Bending vibration (c_1=0 mm, c_2=0 mm, c_3=0 mm, c_4=0 mm)	Bending-twisting vibration (c_1=0.1 mm, c_2=0.05 mm, c_3=0.01mm, c_4=0.001mm)
$\omega_1 = 296$	$\omega_1 = 297$
$\omega_2 = 987$	$\omega_2 = 994$
$\omega_3 = 3232$	$\omega_3 = 3303$
$\omega_4 = 8596$	$\omega_4 = 8910$

The natural frequency has increased both in mode shape 1 (ω_1); mode shape 2 (ω_2), mode shape 3 (ω_3), and mode shape 4 (ω_4) due to the effect of mass eccentricity, as seen in table 8.

Effect of increasing c_i on coupled bending-twisting vibration (Long Side)

The natural frequency of this 4 DOFS is calculated by increased the mass eccentricity from $c_1=0.1$ mm, to $c_1=0.2$ mm; $c_2=0.05$ mm to $c_2=0.1$ mm; $c_3=0.01$ mm to $c_3=0.02$ mm and $c_4=0.001$ mm to $c_4=0.002$ mm. All the values of mass eccentricity are increased by double from the initial assumed values. The result is shown in figure 4.8.2.
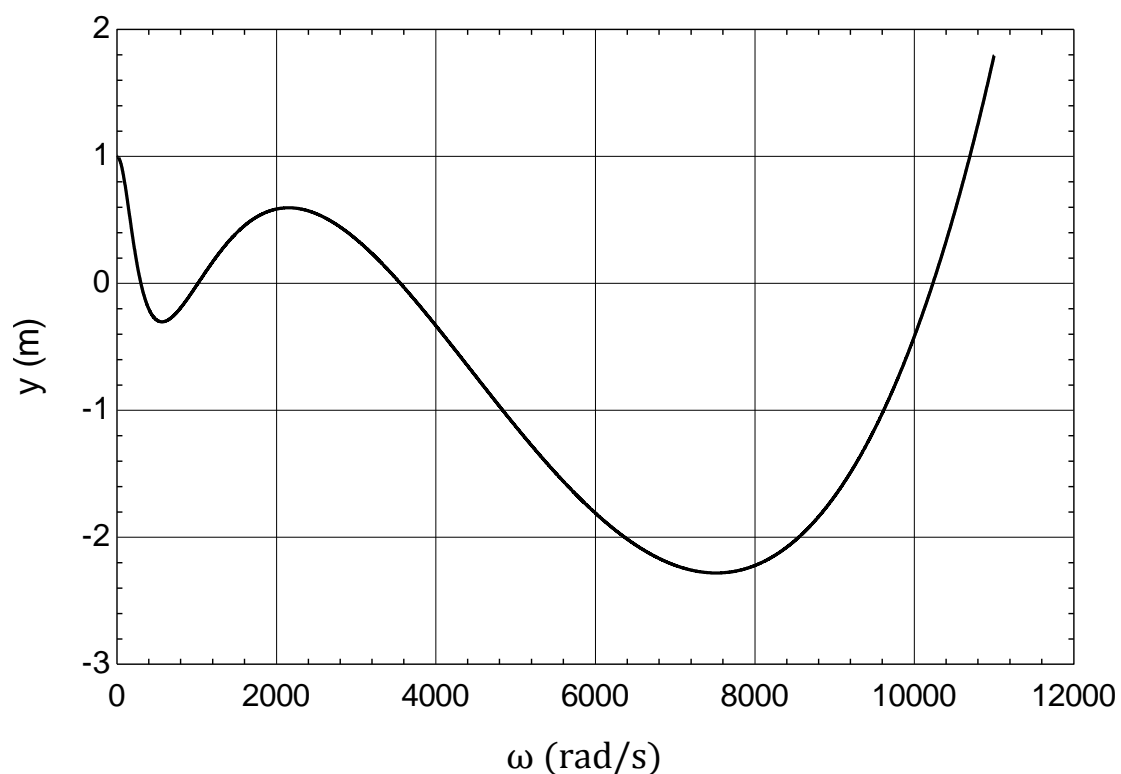
Figure 4.8.2: Displacement vs. Natural frequency in coupled bending vibration for 4 DOFS.

Natural frequency (rad/s):

$$\omega_1 = 299$$

$$\omega_2 = 1014$$

$$\omega_3 = 3553$$

$$\omega_4 = 10231$$

Effect of randomly increased value of c_i on coupled bending-twisting vibration (Long Side)

The natural frequency of the same problem is calculated by increasing randomly the mass eccentricity from $c_1=0.1$ mm, to $c_1=0.4$ mm; $c_2=0.05$ mm to $c_2=0.08$ mm; $c_3=0.01$ mm to $c_3=0.016$ mm and $c_4=0.001$ mm to $c_4=0.002$ mm. The result is shown in figure 4.8.3.
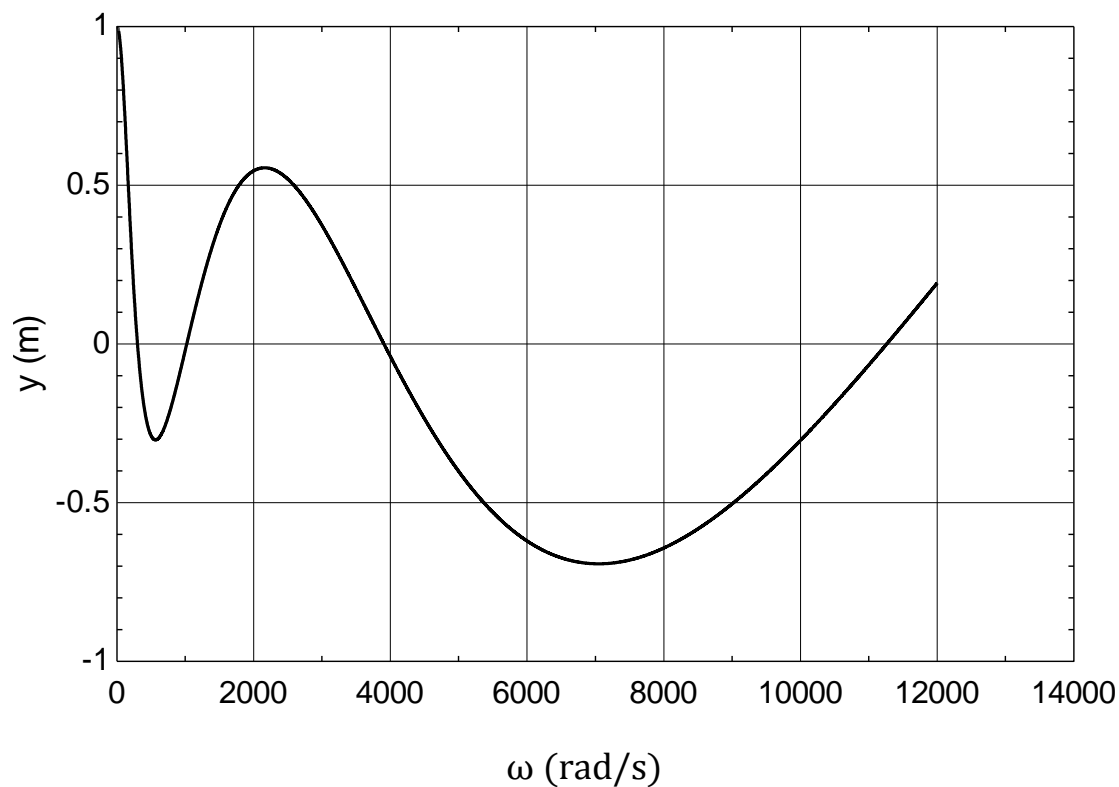

Figure 4.8.3: Displacement vs. Natural frequency in coupled bending vibration for 4 DOFS

Natural frequency (rad/s):

$$\omega_1 = 301$$
$$\omega_2 = 1020$$
$$\omega_3 = 3915$$
$$\omega_4 = 11261$$

Effect of decreasing c_i on coupled bending-twisting vibration (Long Side)

After increasing in two steps, here we decreased the value of mass eccentricity by fifty percent from the initial assuming values. Now the value of mass eccentricity will be c_1=0.05 mm; c_2=0.025 mm; c_3=0.005 mm and c_4=0.0025 mm. The natural frequency corresponding to this mass eccentricity is shown in figure 4.8.4.
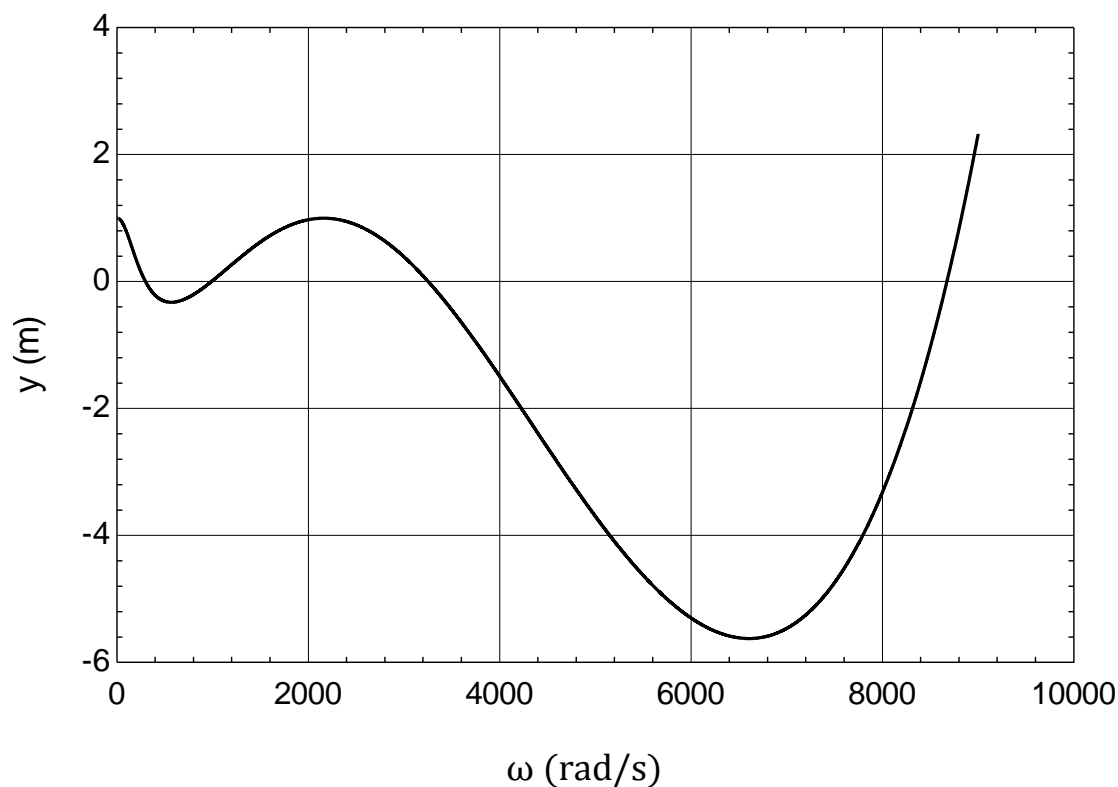

Figure 4.8.4: Displacement vs. Natural frequency in coupled bending vibration for 4 DOFS.

Natural frequency (rad/s):

$$\omega_1 = 296$$
$$\omega_2 = 989$$
$$\omega_3 = 3252$$
$$\omega_4 = 8674$$

Following similar procedures, we calculated the natural frequency on the long side of the damper by keeping the lumped masses at an unequal distance. These results are presented in table 9 and corresponding graphs are kept in Appendix C. We also calculated the

natural frequency on the short side of the stockbridge damper. All of these results are presented in table 9 according to the different values of mass eccentricity.

Table 9: Summary of natural frequency of uncoupled bending and coupled bending-twisting vibration for 4 DOFS for different values of mass eccentricity (Long side and Short side where lumped masses are at equal and unequal distances)

Eccentricity (mm)	Natural frequency (rad/s)			
	Long side (mm)		Short side (mm)	
	$L_1=L_2=L_3=L_4=67.5$	$L_1=77.5,L_2=77.5,$ $L_3=57.5,L_4=57.5$	$L_1=L_2=L_3=L_4=57.5$	$L_1=70,L_2=70,$ $L_3=45,L_4=45$
$c_1=0$ $c_2=0$ $c_3=0$ $c_4=0$	$\omega_1 = 296$ $\omega_2= 987$ $\omega_3= 3232$ $\omega_4= 8596$	$\omega_1 = 315$ $\omega_2= 1120$ $\omega_3= 3205$ $\omega_4= 8223$	$\omega_1 = 153$ $\omega_2= 887$ $\omega_3= 2135$ $\omega_4= 4437$	$\omega_1 = 162$ $\omega_2= 963$ $\omega_3= 2225$ $\omega_4= 4724$
$c_1=0.1$ $c_2=0.05$ $c_3=0.01$ $c_4=0.001$	$\omega_1 = 297$ $\omega_2= 994$ $\omega_3= 3303$ $\omega_4= 8910$	$\omega_1 = 316$ $\omega_2= 1127$ $\omega_3= 3264$ $\omega_4= 8414$	$\omega_1 = 154$ $\omega_2= 905$ $\omega_3= 2189$ $\omega_4= 4640$	$\omega_1 = 163$ $\omega_2= 978$ $\omega_3= 2276$ $\omega_4= 4810$
$c_1=0.2$ $c_2=0.1$ $c_3=0.02$ $c_4=0.002$	$\omega_1 = 299$ $\omega_2= 1014$ $\omega_3= 3553$ $\omega_4= 10231$	$\omega_1 = 318$ $\omega_2= 1147$ $\omega_3= 3464$ $\omega_4= 9156$	$\omega_1 = 156$ $\omega_2= 962$ $\omega_3= 2393$ $\omega_4= 5696$	$\omega_1 = 165$ $\omega_2= 1029$ $\omega_3= 2470$ $\omega_4= 5178$
$c_1=0.4$ $c_2=0.08$ $c_3=0.016$ $c_4=0.002$	$\omega_1 = 301$ $\omega_2= 1020$ $\omega_3= 3915$ $\omega_4= 11261$	$\omega_1 = 321$ $\omega_2= 1164$ $\omega_3= 3905$ $\omega_4= 9850$	$\omega_1 = 158$ $\omega_2= 966$ $\omega_3= 2398$ $\omega_4= 5764$	$\omega_1 = 167$ $\omega_2= 1094$ $\omega_3= 2699$ $\omega_4= 5373$
$c_1=0.05$ $c_2=0.025$ $c_3=0.005$ $c_4=0.0025$	$\omega_1 = 296$ $\omega_2 = 989$ $\omega_3 = 3252$ $\omega_4 = 8674$	$\omega_1 = 315$ $\omega_2 = 1122$ $\omega_3 = 3220$ $\omega_4 = 8272$	$\omega_1 = 153$ $\omega_2 = 892$ $\omega_3 = 2149$ $\omega_4 = 4485$	$\omega_1 = 163$ $\omega_2 = 968$ $\omega_3 = 2236$ $\omega_4 = 4746$

The complete 4DOFS results for the stockbridge damper are displayed in table 9. Below is a description of the argument made about these findings:

Effect of mass eccentricity on natural frequency:

The natural frequency is increased in coupled bending-twisting ($c_i \neq 0$) vibration compare to uncoupled bending ($c_i = 0$) vibration mode due to the effect of mass eccentricity.This mass eccentricity effect is similar to 2DOFS and 3DOFS. When we gradually increased the value of mass eccentricity in both sides of the stockbridge damper, natural frequency is also increased both in ω_1 for mode shape 1, ω_2 for mode shape 2, ω_3 for mode shape 3 and ω_4 mode shape 4 and vice versa. The difference of natural frequency is not too large comparing to the immediate value of mass eccentricity.

Effect of lumped mass distance on natural frequency:

 In both sides of the stockbridge damper, natural frequency is calculated by keeping the lumped masses are at equal and unequal distance. On the long side, when lumped masses are at an unequal distance the natural frequency is increased in mode shape 1(ω_1) by 8.5 % and mode shape 2(ω_2) by 17.7% but the natural frequency is decreased in mode shape 3 (ω_3) by 17.8% and mode shape 4(ω_4) by 26.5% compared to the equal distance of the lumped mass for entire values of mass eccentricity. Now on the short side, the natural frequency is increased both in mode shape 1(ω_1) 9.2%, mode shape 2 (ω_2) 22.6%, and mode shape 3 (ω_3) 25.6 % in unequal distance compare to the equal distance but in mode shape 4(ω_4), this value is randomly changed in unequal distance compare to the equal distance which is shown in table 9.

Effect of DOF on natural frequency:

When we increased DOF i.e. the entire mass of the body spread out in different positions on the elastic axis. Increasing DOF from 3DOFS to 4DOFS, the natural frequency is changed which is shown in table 9. The natural frequency is increased both in mode shape 1(ω_1), mode shape 2(ω_2) and mode shape 3 (ω_3) in long side compare to 3DOFS. In long side and equal distance of lumped masses, natural frequency is increased 22.4% for mode shape 1(ω_1), 27% for mode shape 2(ω_2) and17.1% for mode shape 3(ω_3). In long side and unequal distance, natural frequency is increased 17.2% for mode shape 1(ω_1), 25.3% for mode shape 2 (ω_2) and 26.9% for mode shape 3(ω_3).

But the value of natural frequency is decreased on the short side compared to 3DOFS. In short side and equal distance, natural frequency in mode shape $1(\omega_1)$, mode shape $2(\omega_2)$ and mode shape $3(\omega_3)$ is decreased 54.4%, 28.8% and 75.9% respectively. Now for the short side and unequal distance, natural frequency in mode shape $1(\omega_1)$, mode shape $2(\omega_2)$ and mode shape $3(\omega_3)$ is decreased 69%, 52.9% and 76.1% respectively.

CHAPTER 5

CONCLUSIONS AND RECOMMENDATIONS

5.1 Conclusions

The study of the effect of mass eccentricity on vibration for uncoupled bending and coupled bending-twisting was done numerically. The general physical and geometrical features of a stockbridge damper, which is commonly used in Bangladesh to dampen vibration of overhead transmission lines, were investigated. In bending mode, we investigated the vibration characteristics of that stockbridge damper system. We found 2, 3, and 4 natural frequencies both in uncoupled bending and coupled bending-twisting mode when considering a stockbridge damper as 2DOFS, 3DOFS, and 4DOFS respectively. Then we analyzed the effect of mass eccentricity in every DOFS and found the change of natural frequency between uncoupled bending and coupled bending-twisting vibration mode. We also compared the effect of mass eccentricity on natural frequency by changing the values of mass eccentricity.

Due to the mass eccentricity effect, bending-twisting analysis natural frequency is higher than bending analysis natural frequency in every mode and every DOFS. The values of mass eccentricity are likewise increased, which increases the natural frequency as well and vice versa for both sides of the stockbridge damper. So we can conclude that, in every mode section, bending-twisting analysis natural frequency is higher than bending analysis natural frequency but that change was not too drastic.

The natural frequency has also changed when lumped masses are kept at an equal and unequal distances according to the values of mass eccentricity for both sides of the stockbridge damper. In some cases, the natural frequency is increased for unequal distances compared to equal distances and in some other cases, it is decreased. DOF has similar effect on natural frequency of the stockbridge damper.

As the value of natural frequency is one of a system's most important factors, so the designers must be meticulous in their calculations. Otherwise, it might have an impact on the system's failure, usefulness, and lifespan.

In this thesis the natural frequency of stockbridge damper was calculated using Myklestad and coupled flexure-torsion vibration method but this natural frequency can also be calculated using Dunkerley's equations which are shortly presented in appendix E.

5.2 Recommendations for future work

Given the information obtained from this thesis a number of future works can be proposed:

(1) 3D Modal analysis of this work in Ansys or any specialized software at different planes of stockbridge damper would be an interesting work for bending & bending-twisting analysis to see how stockbridge damper behaves at different positions.

(2) The study of considering the stockbridge damper as a mechanical system with more than four degrees of freedom, due to the flexibility of the messenger cables.

(3) The experimental study of the behavior of the conductor and the stockbridge damper to complement with the numerical data.

(4) The stockbridge damper is made up of a variety of materials. The material employed in this thesis is high tense steel. The effect of mass eccentricity on the stockbridge damper can be compared using different materials.

(5) As indicated in Appendix-E, Dunkerley's method can be used to determine the stockbridge damper's natural frequency, and the findings can be compared to those obtained using the Myklestad and Coupled Flexure-Torsion Vibration methods.

REFERENCES

[1]   Barbieri, N., Marchi, M. E., Mannala, M. J., & Barbieri, R., (2019), "Nonlinear dynamic analysis of a Stockbridge damper", Canadian Journal of Civil Engineering, 46(9), 828-835.

[2]   Barbieri, N., Barbieri, R., & Mannala, M. J., (2016), "Nonlinear dynamic analysis of wire-rope isolator and Stockbridge damper", Nonlinear Dynamics, 86(1), 501-512.

[3]   Barbieri, N., & Barbieri, R., (2012), "Dynamic analysis of Stockbridge damper", Advances in Acoustics and Vibration.

[4]   Vaja, N. K., Barry, O. R., & Tanbour, E. Y., (2018), "On the modeling and analysis of a vibration absorber for overhead powerlines with multiple resonant frequencies", Engineering Structures, 175, 711-720.

[5]   Kim, C. J., (2017), "Design sensitivity analysis of a Stockbridge damper to control resonant frequencies", Journal of Mechanical Science and Technology, 31(9), 4145-4150.

[6]   Kalombo, R. B., Loubser, R., & Moodley, P., (2012, April), "Bending stress of Stockbridge damper messenger cable: experimental data and modelling", In 18th World Conference on Nondestructive Testing.

[7]   Golebiowska, I., & Dutkiewicz, M., (2017), "Experimental analysis of efficiency of mass dampers", In Proceedings of 23th International Conference on Engineering Mechanics (pp. 350-353).

[8]   Foti, F., & Martinelli, L., (2018), "Hysteretic behaviour of Stockbridge dampers: modelling and parameter identification", Mathematical Problems in Engineering.

[9]   Thomson, W. T. & Dahleh, M. D., (1998), "Theory of vibration with applications" (5th Edition), Pearson Education Inc.

[10]   ISO, D., (2003), "Mechanical vibration—Balance quality requirements for rotors in a constant (rigid) state—Part 1: Specification and verification of balance tolerances", ISO 1940-1: 2003.

[11]   Zondi, Z., Kaunda, M., & Ngonda, T., (2021), "Characteristics of the asymmetric Stockbridge damper", In MATEC Web of Conferences (Vol. 347). EDP Sciences.

[12]   Morgan, V. T., (1962), "The detection and damping of overhead-line conductor vibration", Proceedings of the IEE-Part A: Power Engineering, 109(3S), 239-250.

[13]   Dulhunty, P. W., (2015), "Vibration dampers", An evolution in Australia.

[14]   Kalombo, R. B., Loubser, R., & Moodley, P., (2012, April), "Bending stress of stockbridge damper messenger cable: experimental data and modelling", In 18th World Conference on Nondestructive Testing.

[15]   Kasap, H., (2012), "Investigation of Stockbridge dampers for vibration control of overhead transmission lines", Master's thesis, Middle East Technical University.

[16]   Li, L., Kong, D. Y., Long, X. H., & Fanq, Q. H., (2008), "Numerical analysis on aeolian vibration of transmission lines with Stockbridge dampers", Journal of Chongqing University, 7(4), 302-310.

[17]   Sauter, D., (2003), "Modeling the dynamic characteristics of slack wire cables in Stockbridge dampers", Doctoral dissertation, Technische Universität.

[18]   Vecchiarelli, J., (1997), "Aeolian vibration of a conduct or with a FR type damper", Toronto, Canada: University of Toronto.

[19]   Deshpande, A., & Kittur, J., (2017), "Experimental study of effect of eccentricity on vibration of shafts", Rest journal on emerging trends in modelling and manufacturing, 3(3).

[20]   Markiewicz, M., (1995), "Optimum dynamic characteristics of Stockbridge dampers for dead-end spans", Journal of sound and vibration, 188(2), 243-256.

[21]   Sakawa, Y., & Luo, Z. H., (1989), "Modeling and control of coupled bending and torsional vibrations of flexible beams", IEEE transactions on automatic control, 34(9), 970-977.

[22]   Gokdag, H., & Kopmaz, O., (2005), "Coupled bending and torsional vibration of a beam with in-span and tip attachments".

[23]   Havard, D. G., (1999), "Vibration Dampers. Contribution to the CEA workshop on transmission line asset maintenance, session on: Assessment inspection methods, diagnostic tools, testing, condition monitoring, life cycle and aging, remedial measures".

[24]   Tigli, O. F., (2012), "Optimum vibration absorber (tuned mass damper) design for linear damped systems subjected to random loads", Journal of sound and vibration, 331(13), 3035-3049.

[25] Wang, J. J., (2006, October), "Overhead conductor vibrations and control technologies", In 2006 International Conference on Power System Technology (pp. 1-5). IEEE.

Appendix-A:

Stockbridge damper acting as a 2 DOFS

A.1: Lumped masses are at unequal distance (long side)

$m_1 = 2.1$ kg $m_2 = 0.3$ kg

160 mm   110 mm

① ② ③
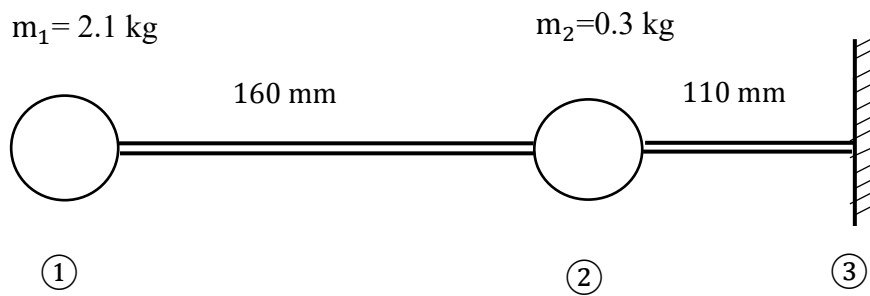
Figure A.1: Lumped parameter system in stockbridge damper [Long side & lumped masses are at unequal distance for 2DOFS].
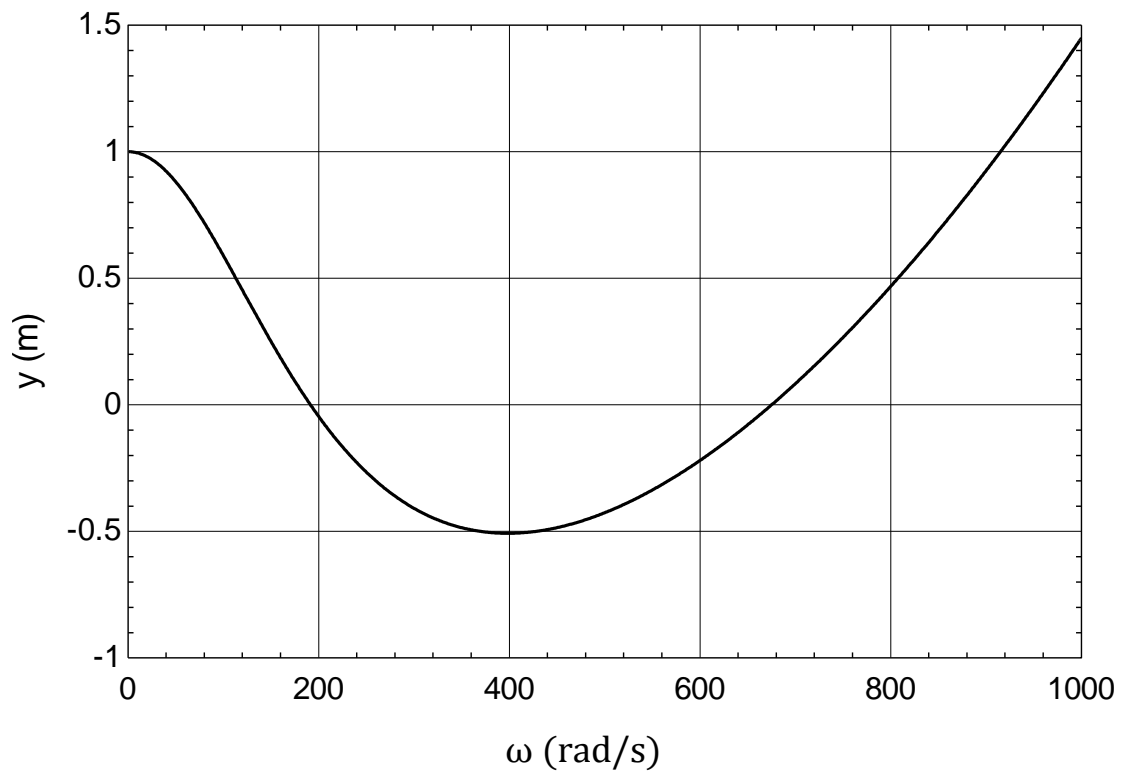
Figure A.1.1: Displacement vs. Natural frequency in uncoupled bending vibration for 2 DOFS [$c_1 = 0$ mm, $c_2 = 0$ mm].

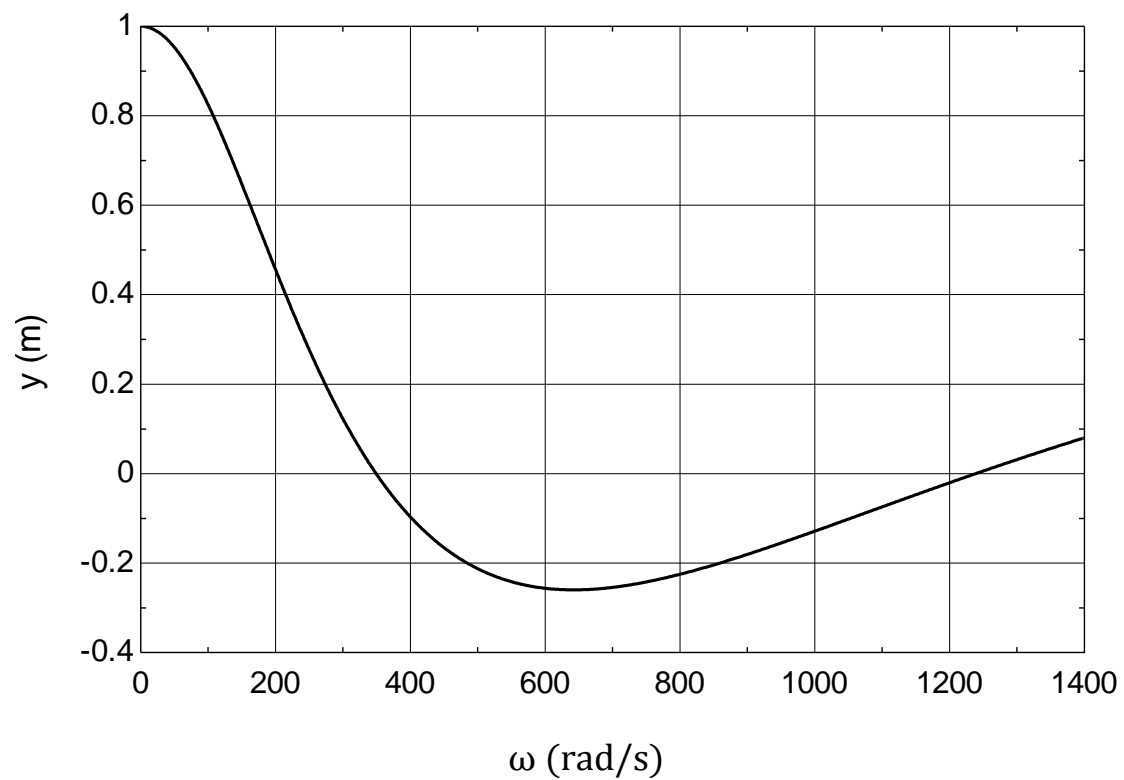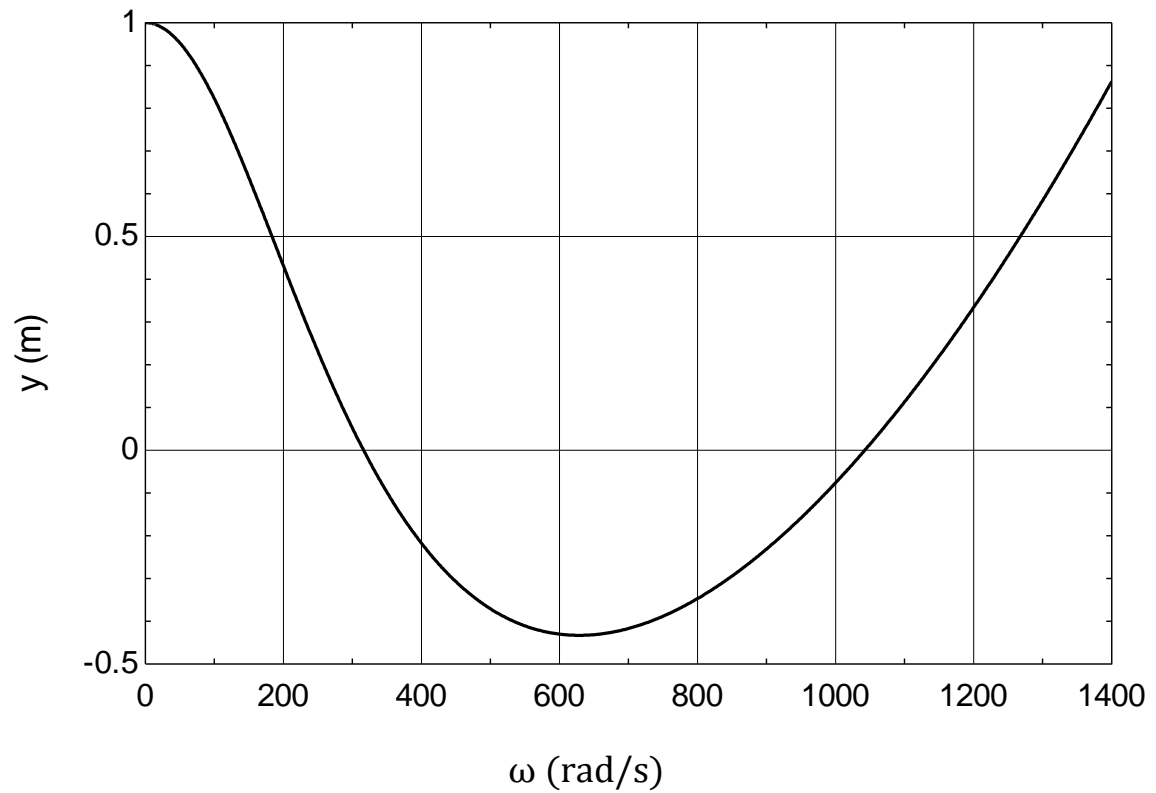Natural frequency (rad/s):

$$\omega_1 = 191$$

$$\omega_2 = 676$$
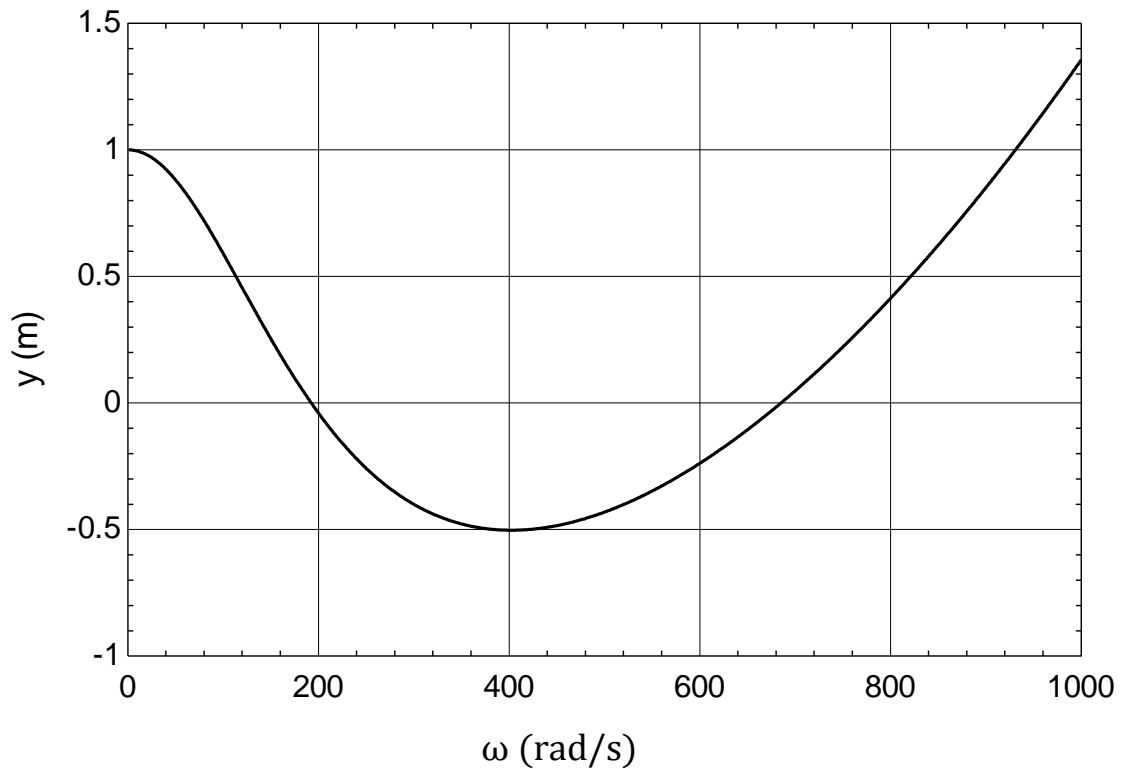
Figure A.1.2: Displacement vs. Natural frequency in coupled bending-twisting vibration for 2 DOFS [c_1=0.1 mm, c_2=0.05 mm].

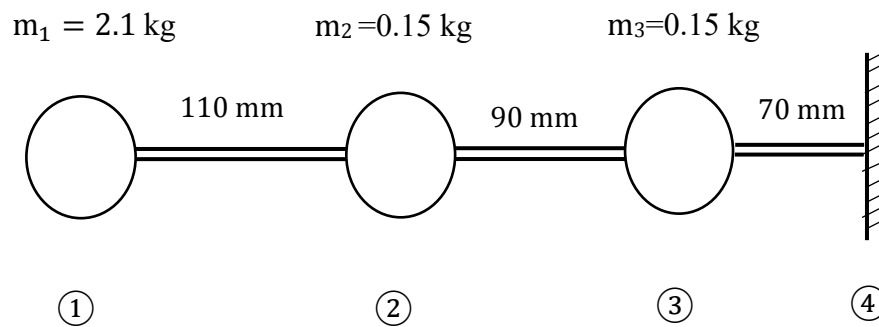Natural frequency (rad/s):

$$\omega_1 = 192$$

$$\omega_2 = 686$$

Graph A.1.3 compares the influence of mass eccentricity on vibration between uncoupled bending and coupled bending-twisting vibration modes, which were generated using graphs A.1.1 and A.1.2 respectively.
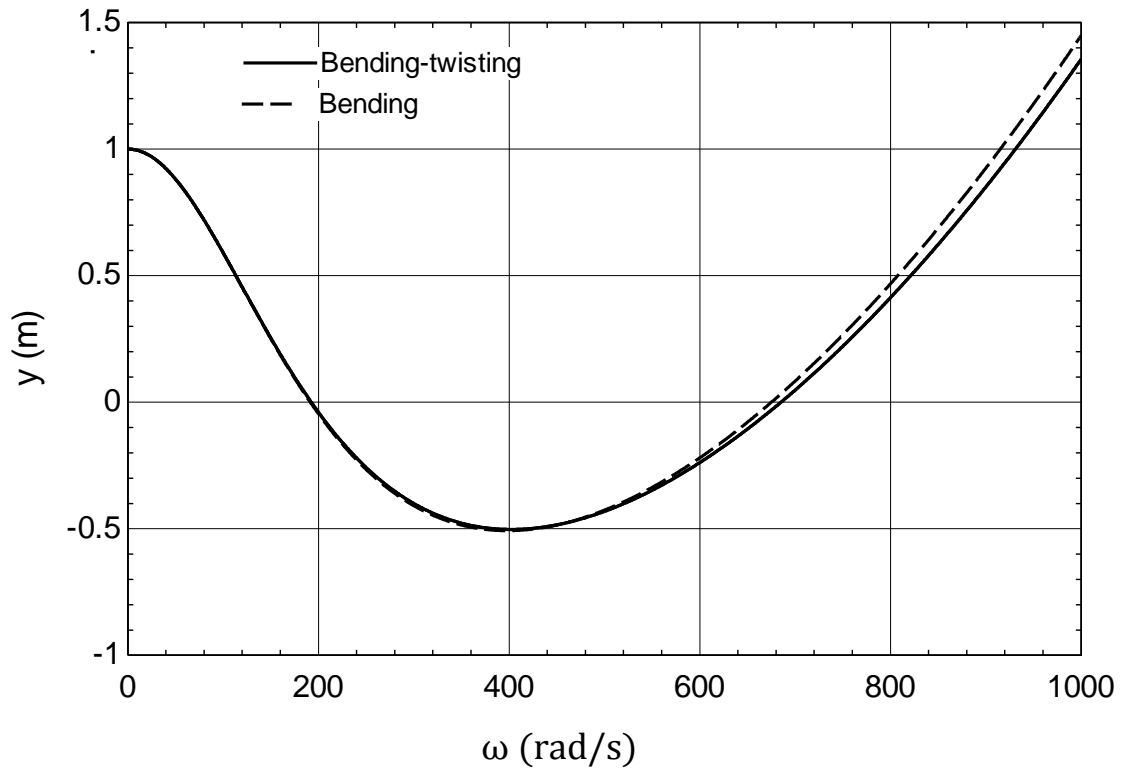
Figure A.1.3: Displacement vs. Natural frequency in uncoupled bending and coupled bending-twisting vibration for 2 DOFS.
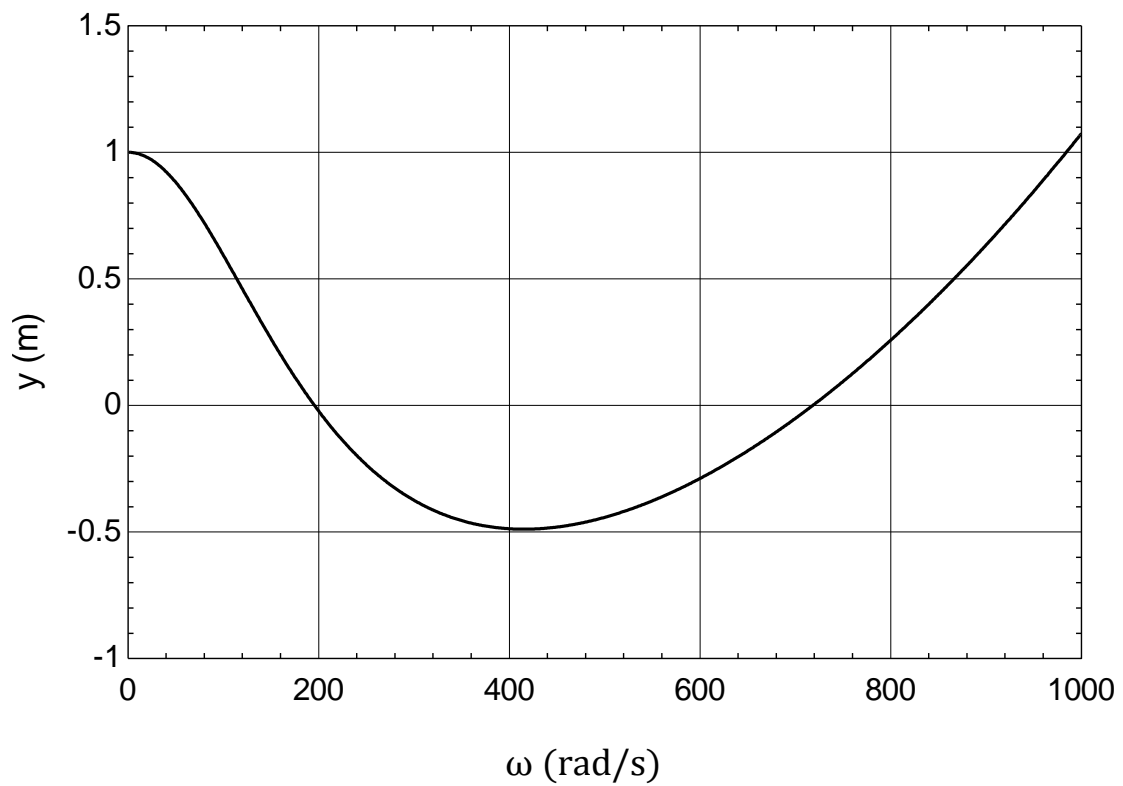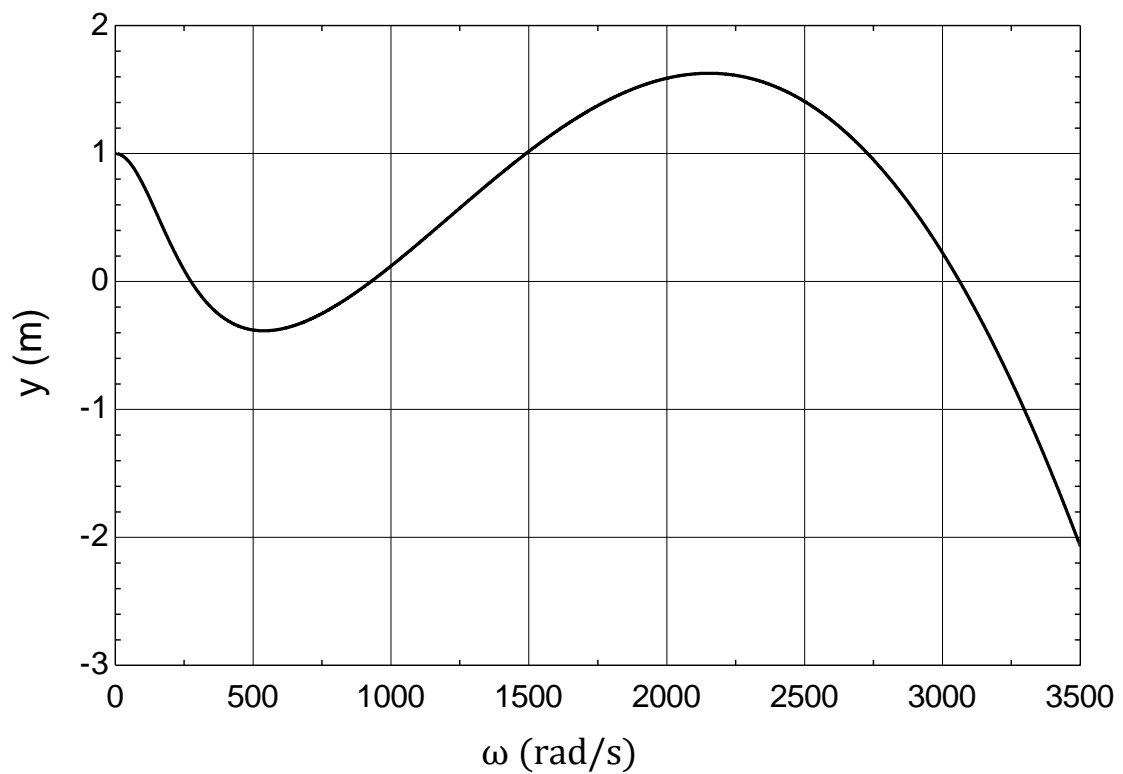

Figure A.1.4: Displacement vs. Natural frequency in coupled bending-twisting vibration for 2 DOFS [c_1=0.2 mm and c_2=0.1 mm].

Natural frequency (rad/s):

$$\omega_1 = 195$$

$$\omega_2 = 717$$
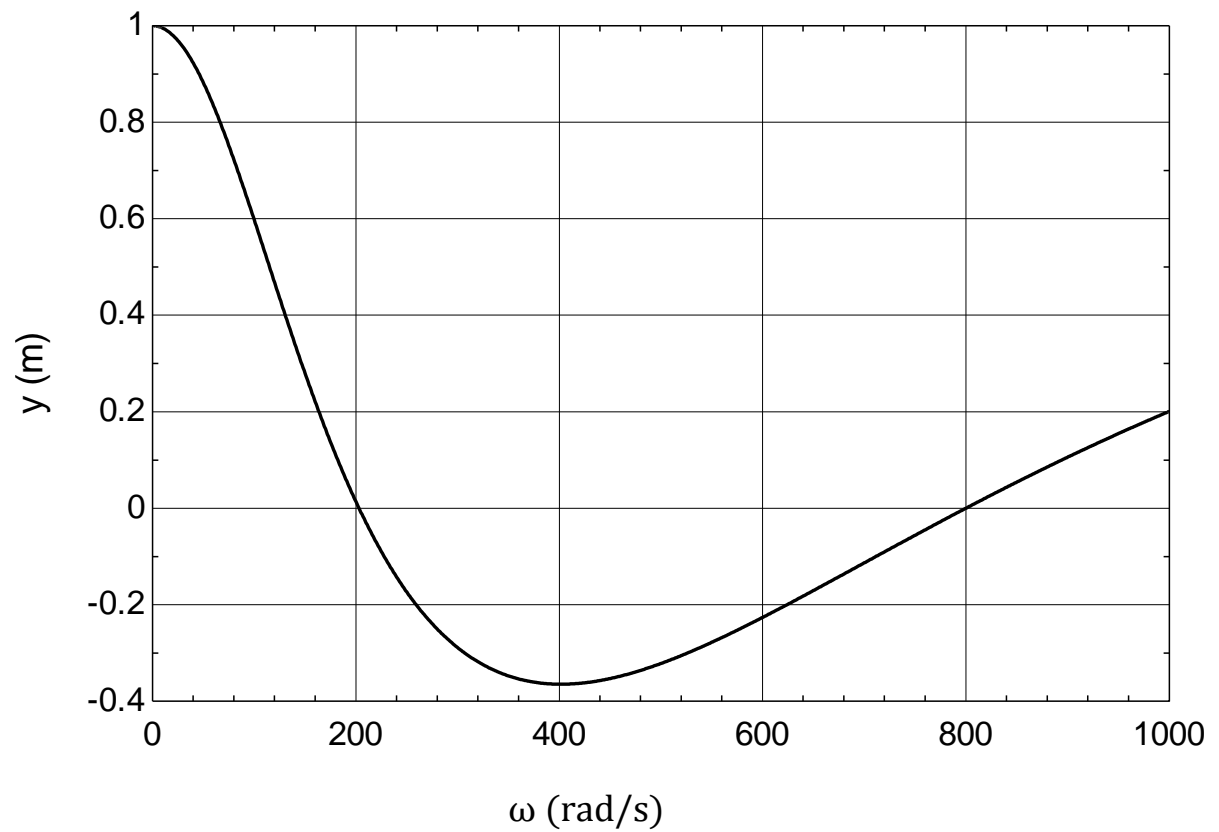
Figure A.1.5: Displacement vs. Natural frequency in coupled bending-twisting vibration for 2 DOFS [c_1=0.4 mm and c_2=0.08 mm].

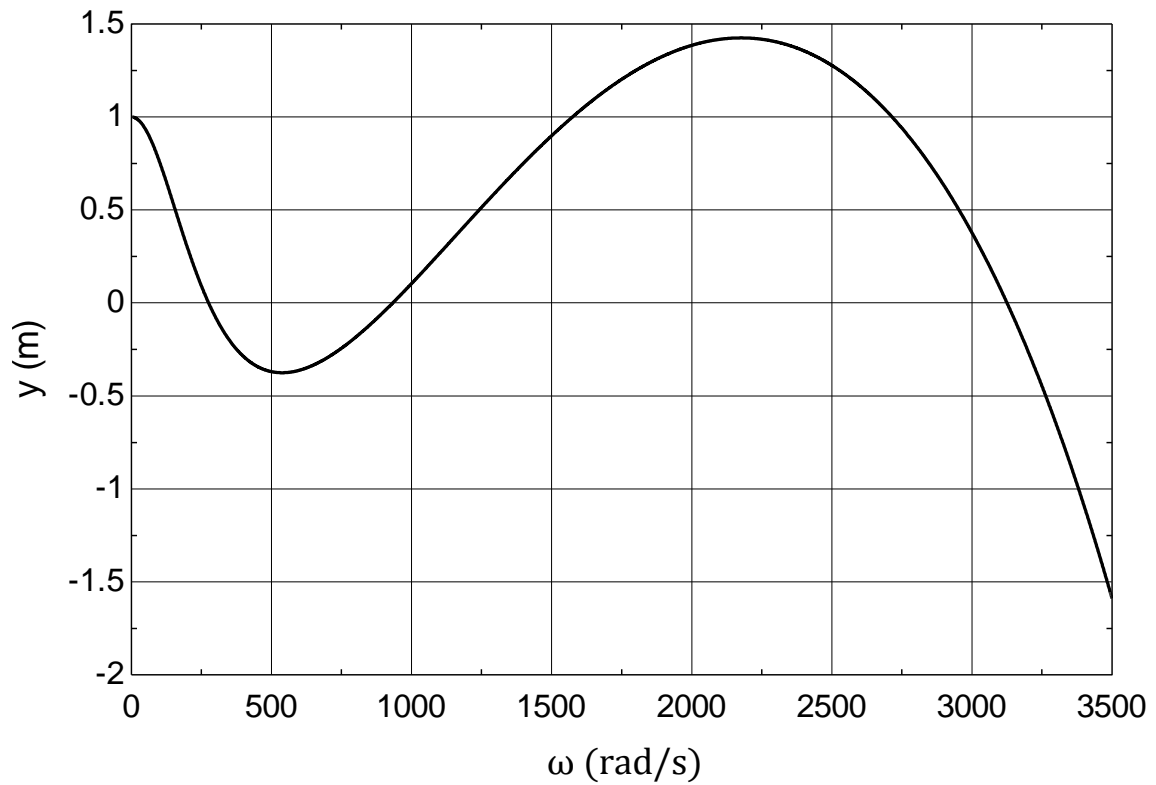Natural frequency (rad/s):

$$\omega_1 = 203$$

$$\omega_2 = 800$$
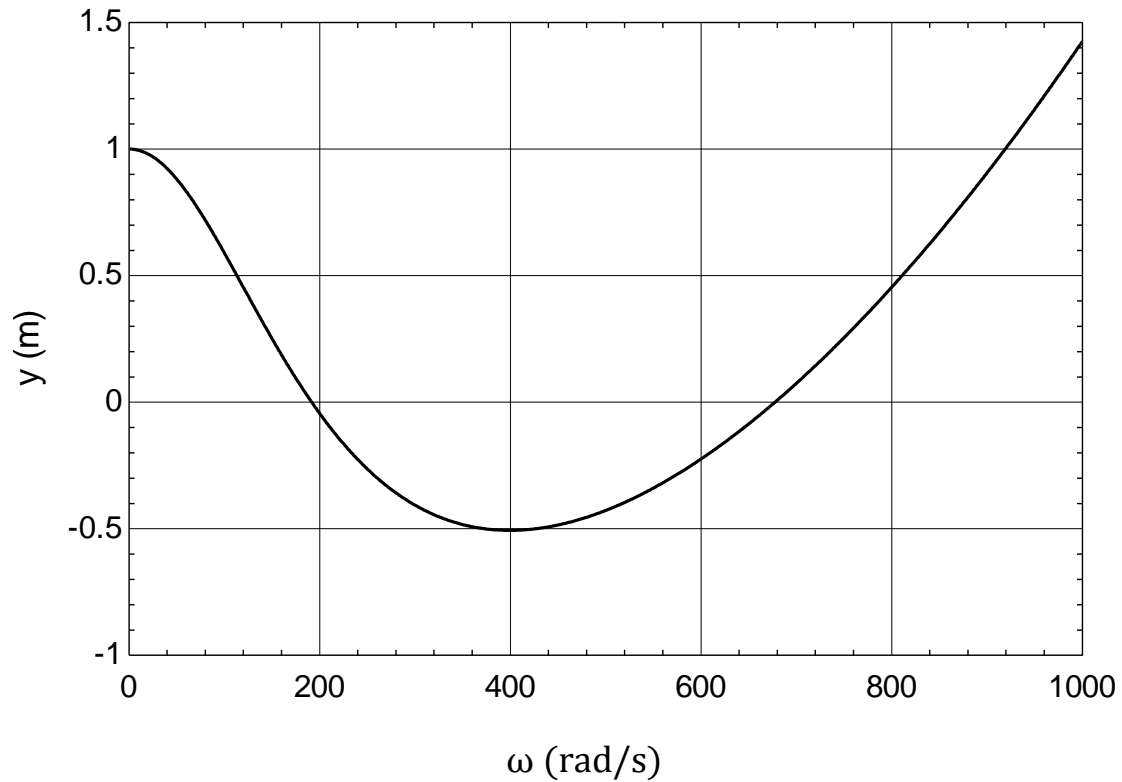
Figure A.1.6: Displacement vs. Natural frequency in coupled bending-twisting vibration for 2 DOFS [c_1=0.05 mm and c_2=0.025 mm].

Natural frequency (rad/s):

$$\omega_1 = 191$$

$$\omega_2 = 678$$

A.2: LUMPED MASSES ARE AT UNEQUAL DISTANCE (SHORT SIDE)
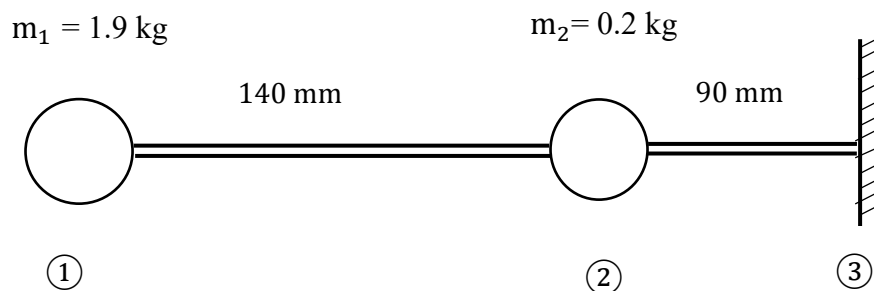
Figure A.2: Lumped parameter system in stockbridge damper [Short side & lumped masses are at unequal distance for 2DOFS].
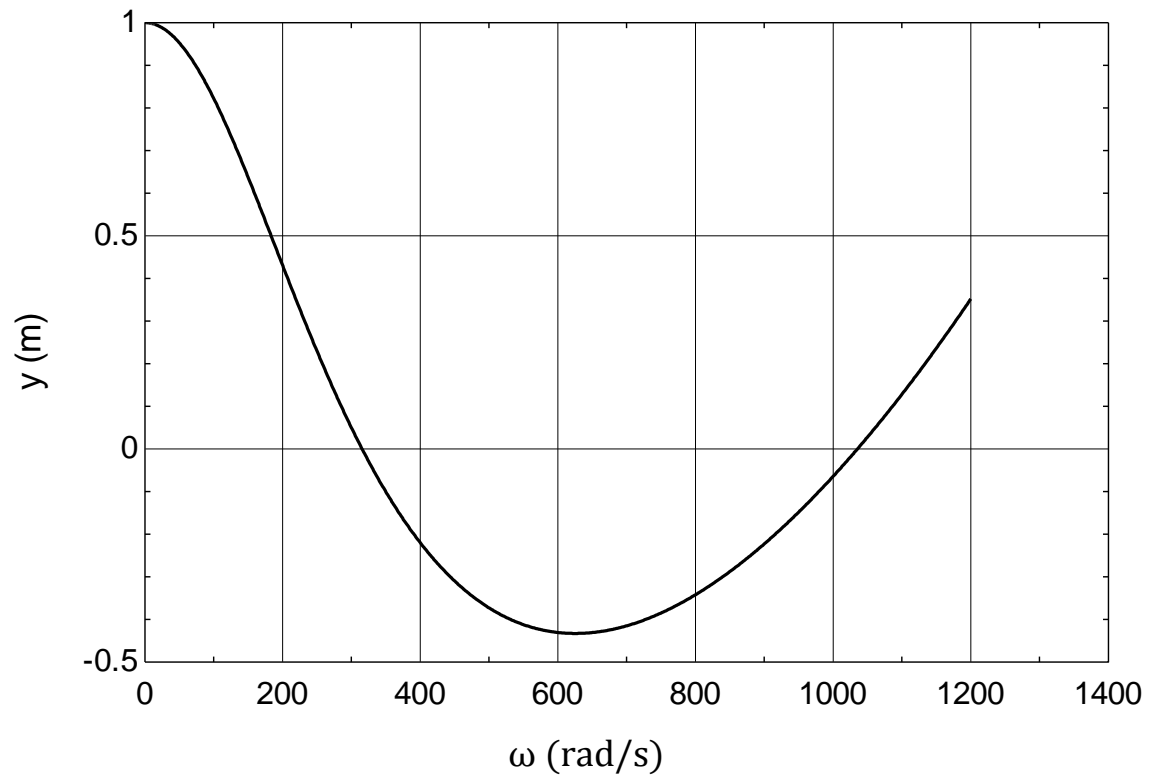
Figure A.2.1: Displacement vs. Natural frequency in uncoupled bending vibration for 2 DOFS [c_1=0 mm, c_2=0 mm].

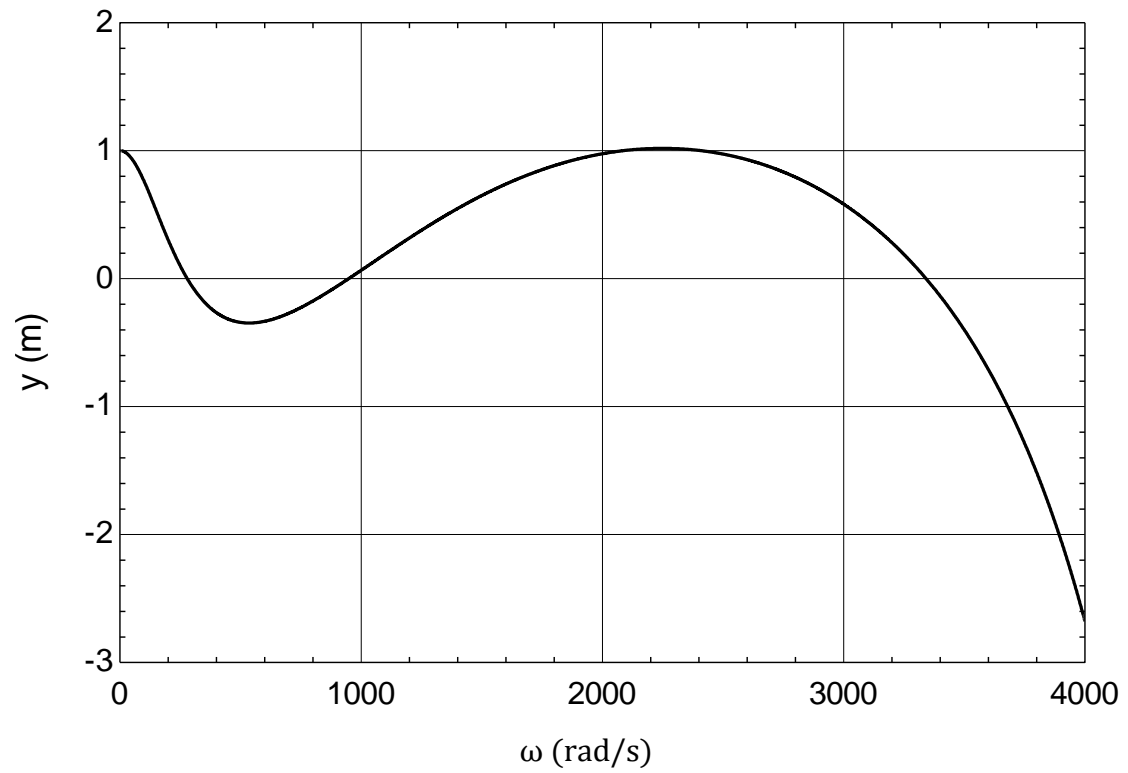Natural frequency (rad/s):

$$\omega_1 = 315$$
$$\omega_2 = 1035$$
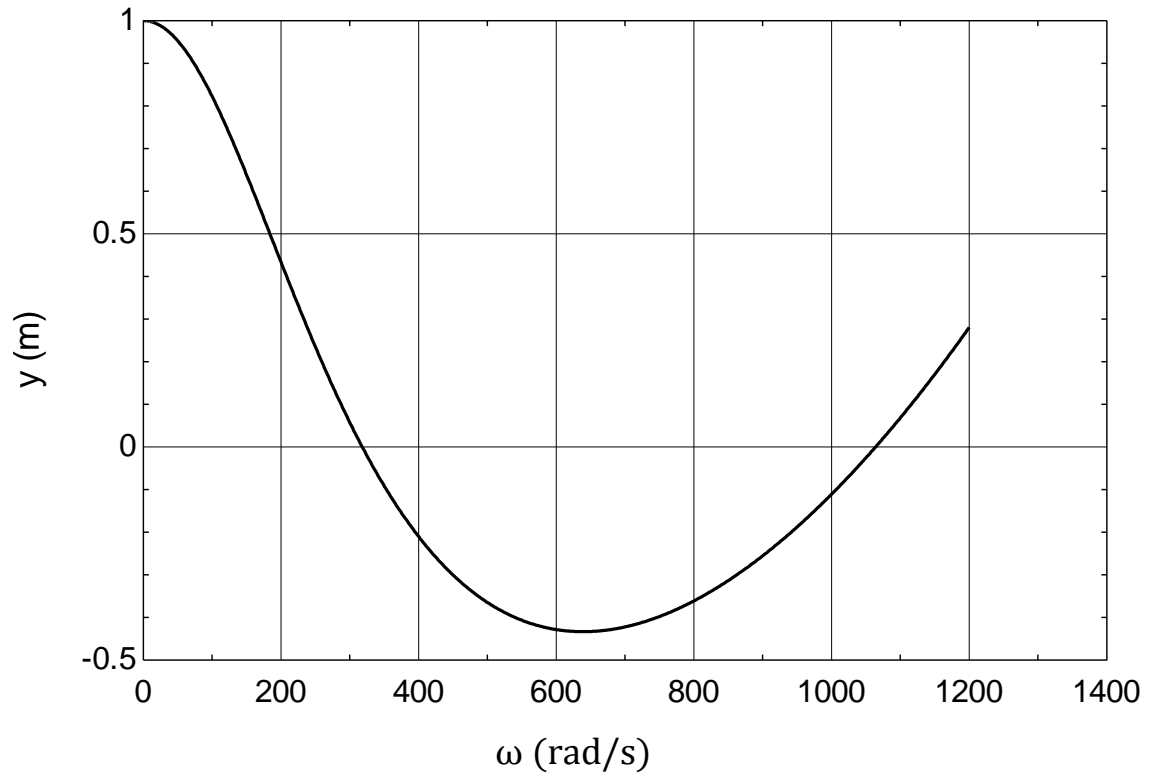
Figure A.2.2: Displacement vs. Natural frequency in coupled bending-twisting vibration for 2 DOFS [c_1=0.1 mm, c_2=0.05 mm].

Natural frequency (rad/s):

$$\omega_1 = 318$$
$$\omega_2 = 1063$$

Uncoupled bending and Coupled bending-twisting vibration comparison

The graph A.2.3 compares the influence of mass eccentricity in vibration between uncoupled bending and coupled bending-twisting vibration modes, which were generated using graphs A.2.1 and A.2.2 respectively.
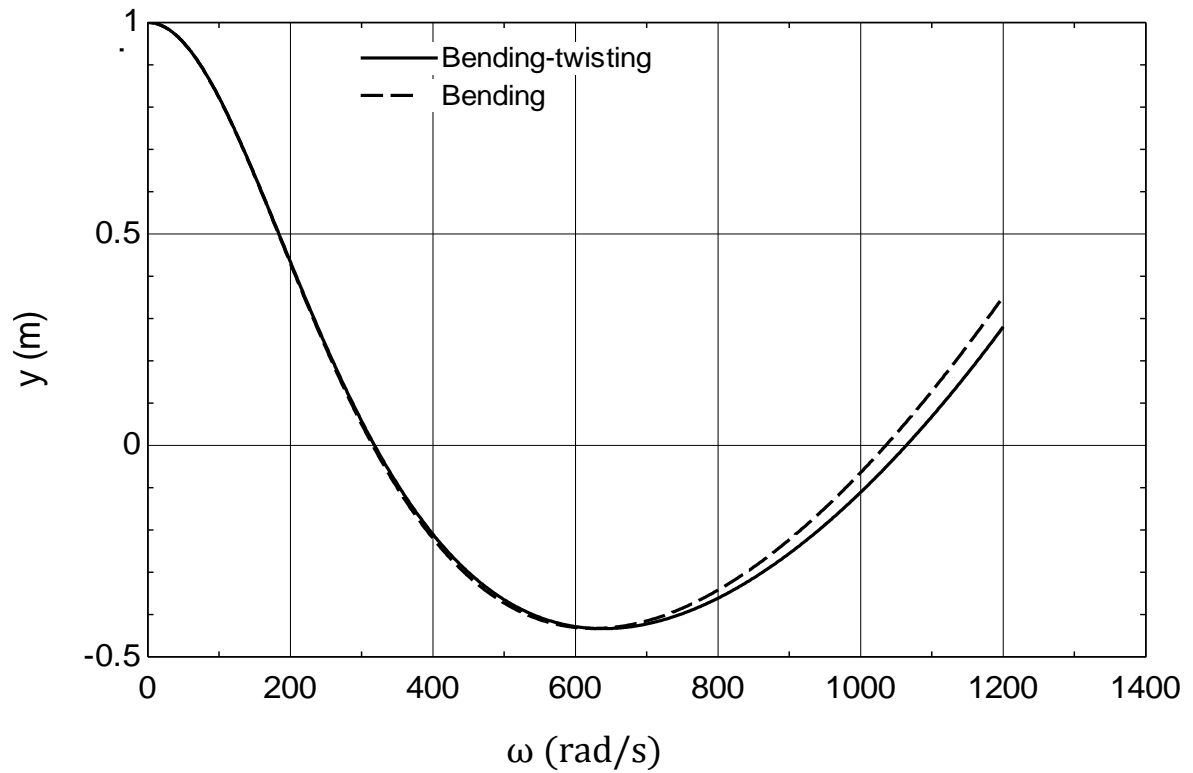
Figure A.2.3: Displacement vs. Natural frequency in uncoupled bending and coupled bending-twisting vibration for 2 DOFS (short side unequal distance).
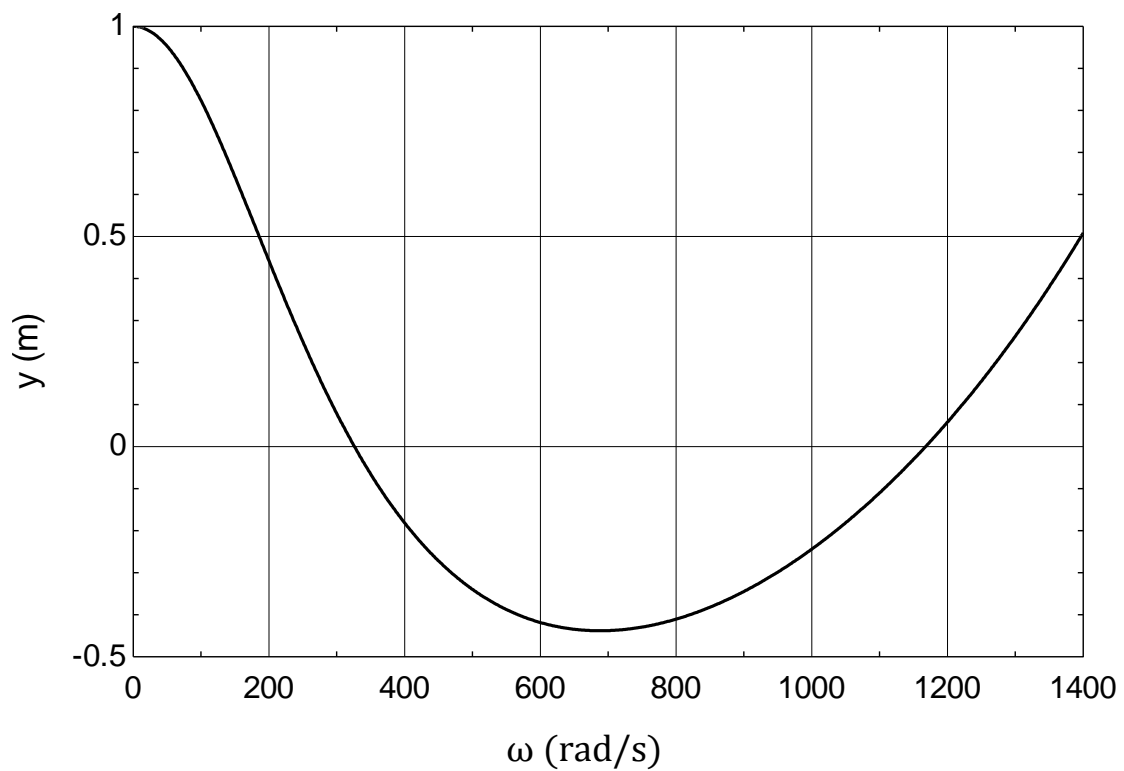
Figure A.2.4: Displacement vs. Natural frequency in coupled bending-twisting vibration for 2 DOFS [c_1=0.2 mm, c_2=0.1 mm].

Natural frequency (rad/s):

$$\omega_1 = 325$$

$$\omega_2 = 1168$$

Figure A.2.5: Displacement vs. Natural frequency in coupled bending-twisting vibration for 2 DOFS [c_1=0.4 mm, c_2=0.08 mm].

Natural frequency (rad/s):

$$\omega_1 = 348$$

$$\omega_2 = 1238$$

Figure A.2.6: Displacement vs. Natural frequency in coupled bending-twisting vibration for 2 DOFS [c_1=0.05 mm, c_2=0.025 mm].

Natural frequency (rad/s):

$$\omega_1 = 316$$
$$\omega_2 = 1043$$

Appendix-B

Stockbridge damper acting as a 3 DOFS

B.1. Lumped masses are at unequal distance (Long side)

Figure B.1: Lumped parameter system in stockbridge damper [Long side & lumped masses are at unequal distance for 3DOFS].
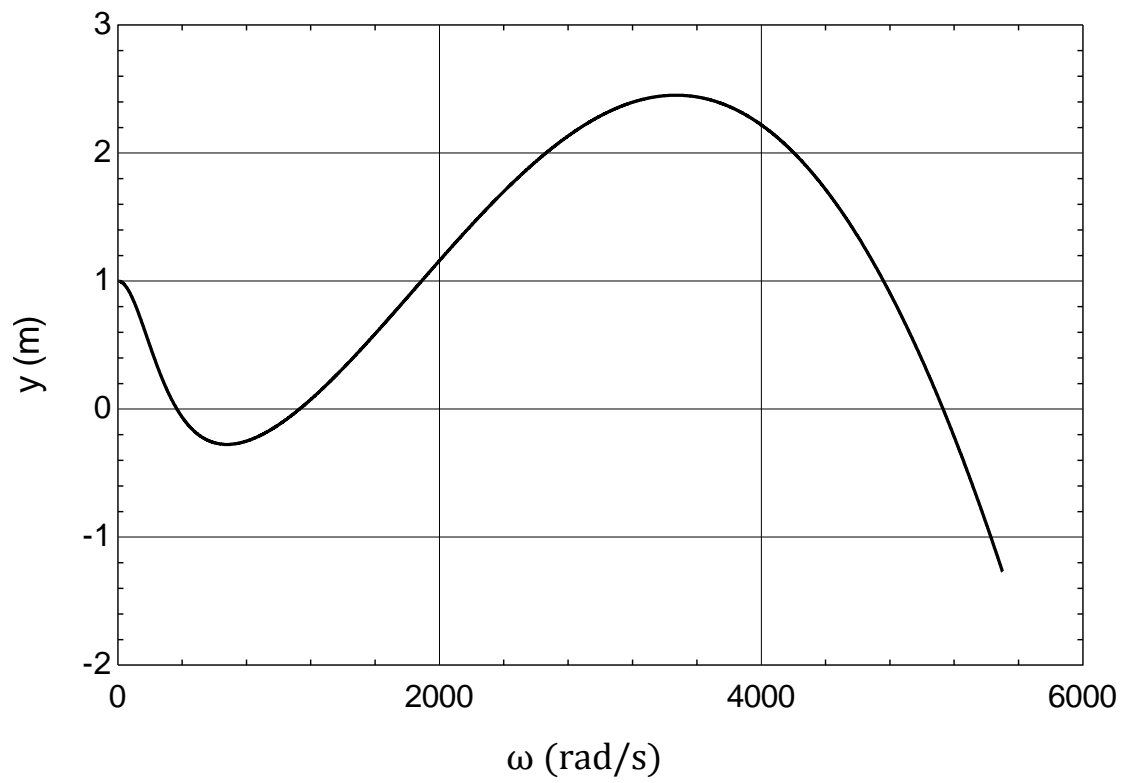

Figure B.1.1: Displacement vs. Natural frequency in uncoupled bending vibration for 3 DOFS [c_1=0 mm, c_2=0 mm and c_3=0 mm].

Natural frequency (rad/s):

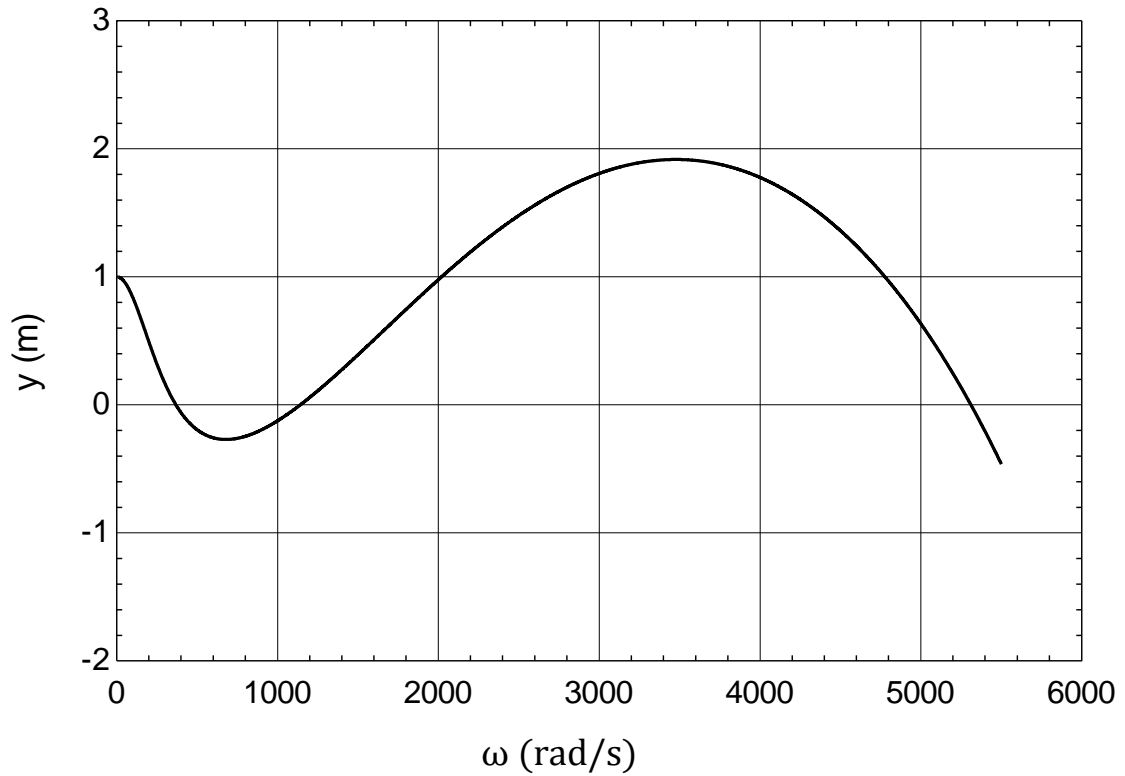$$\omega_1 = 274$$

$$\omega_2 = 928$$

$$\omega_3 = 3062$$

Figure B.1.2: Displacement vs. Natural frequency in coupled bending vibration for 3 DOFS [c_1=0.1 mm, c_2=0.05 mm and c_3=0.01 mm].

Natural frequency (rad/s):

$$\omega_1 = 275$$

$$\omega_2 = 932$$

$$\omega_3 = 3125$$

Uncoupled bending and Coupled bending-twisting vibration comparison

Graph B.1.3 compares the influence of mass eccentricity in vibration between uncoupled bending and coupled bending-twisting vibration modes, which were generated using graphs B.1.1 and B.1.2 respectively.
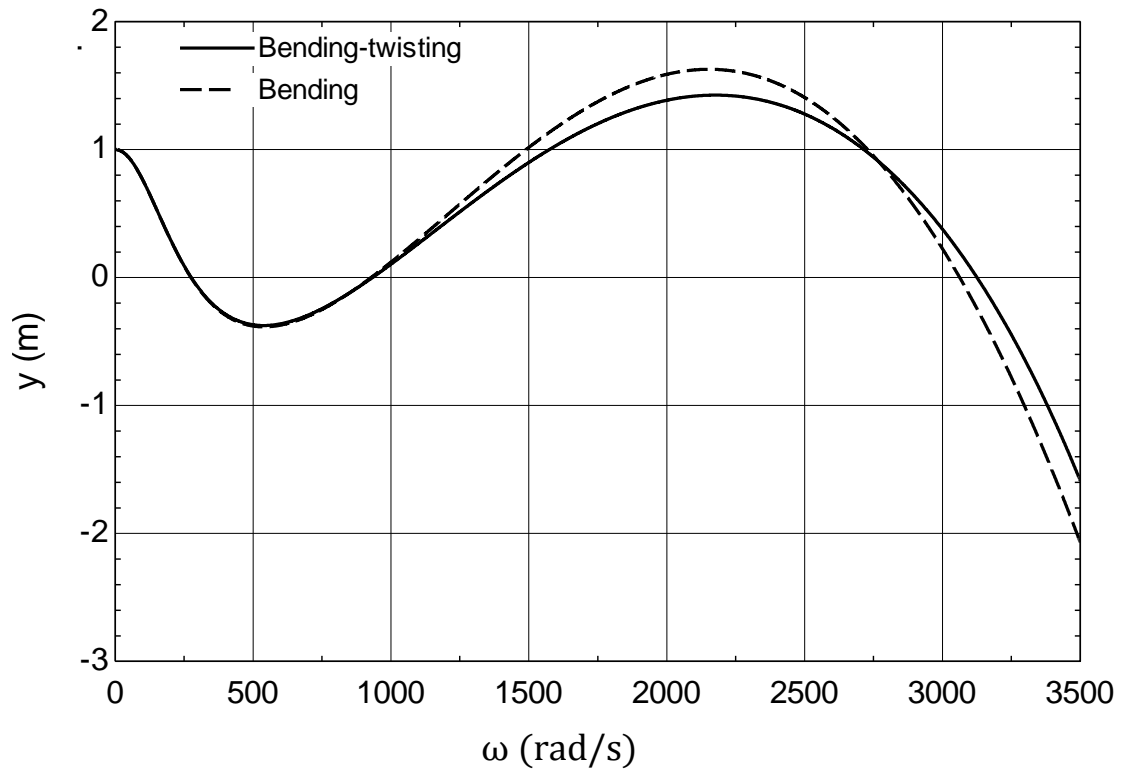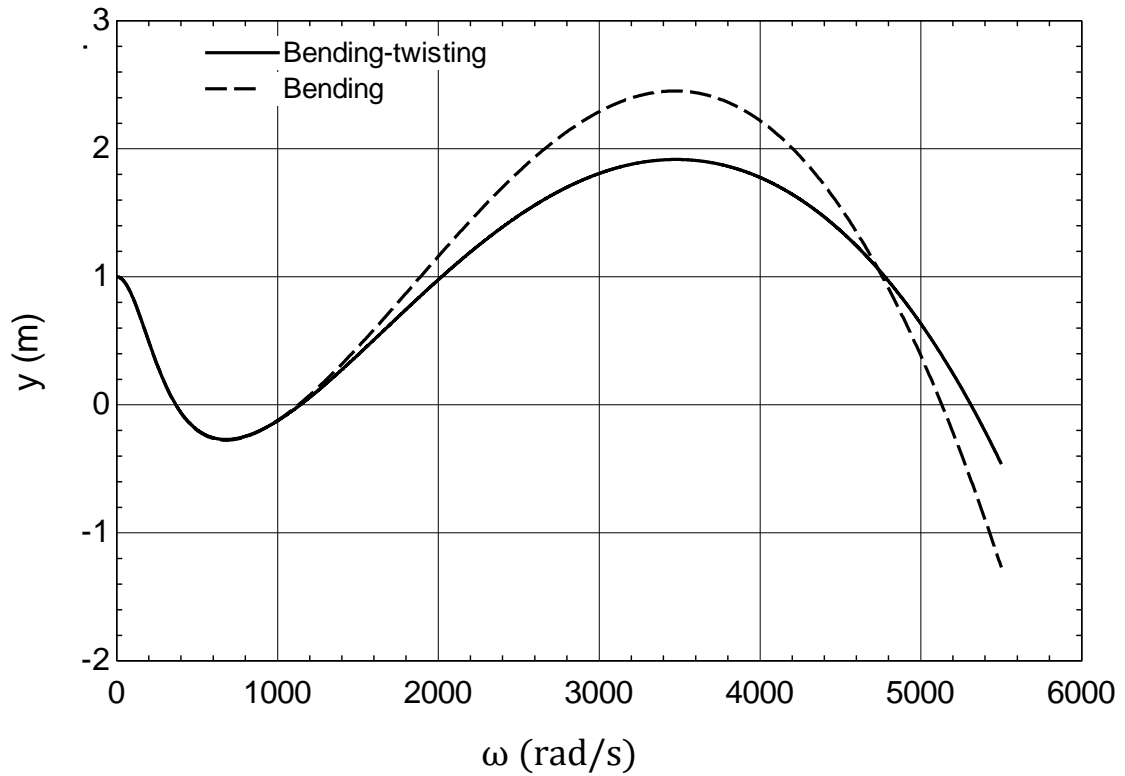
Figure B.1.3: Displacement vs. Natural frequency in uncoupled bending and coupled bending-twisting vibration for 3 DOFS
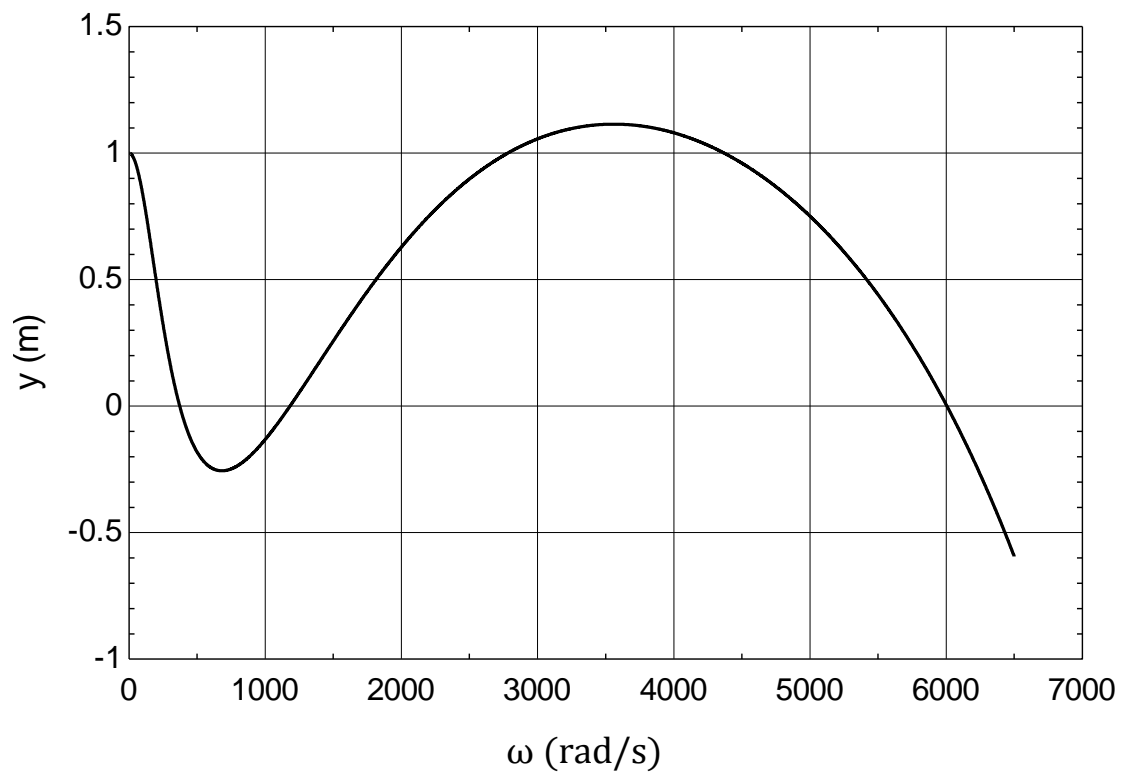
Figure B.1.4: Displacement vs. Natural frequency in coupled bending vibration for 3 DOFS [c_1=0.2 mm, c_2=0.1 mm, c_3=0.02 mm].

Natural frequency (rad/s):

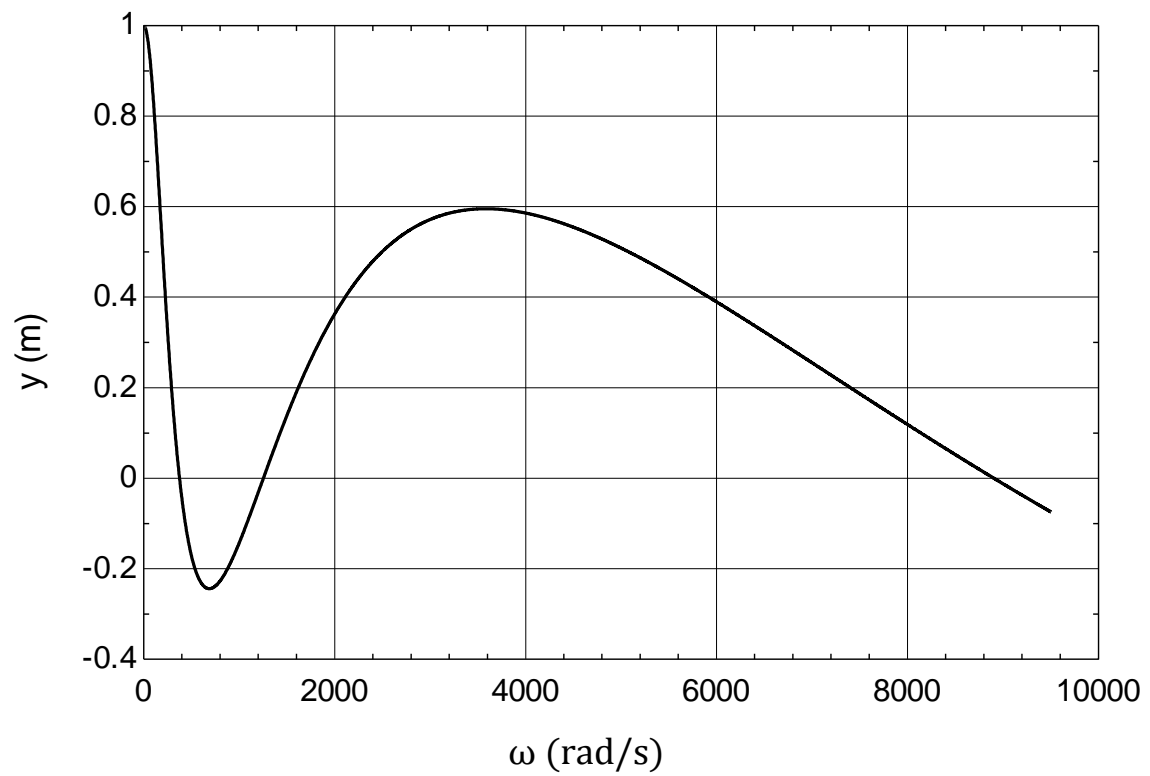$$\omega_1 = 278$$

$$\omega_2 = 948$$

$$\omega_3 = 3341$$
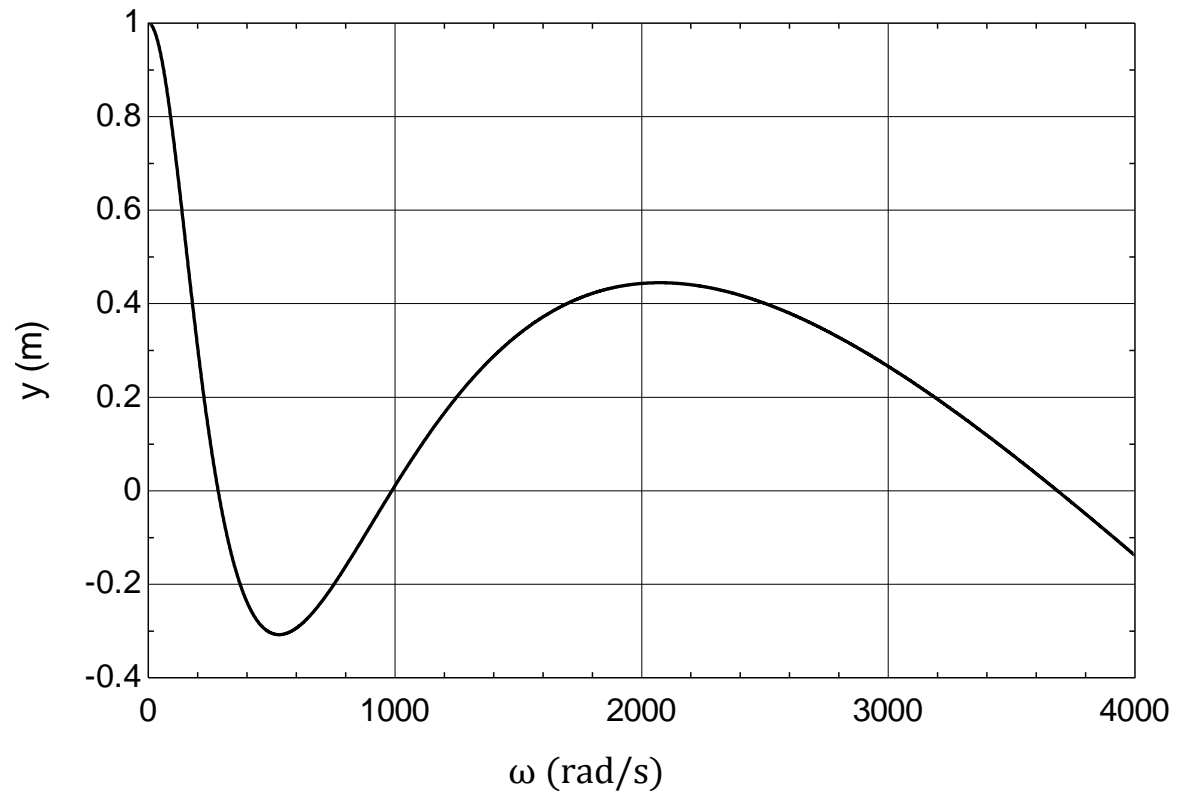
Figure B.1.5: Displacement vs. Natural frequency in coupled bending vibration for 3 DOFS [c_1=0.4 mm; c_2=0.08 mm and c_3=0.016 mm].

Natural frequency (rad/s):

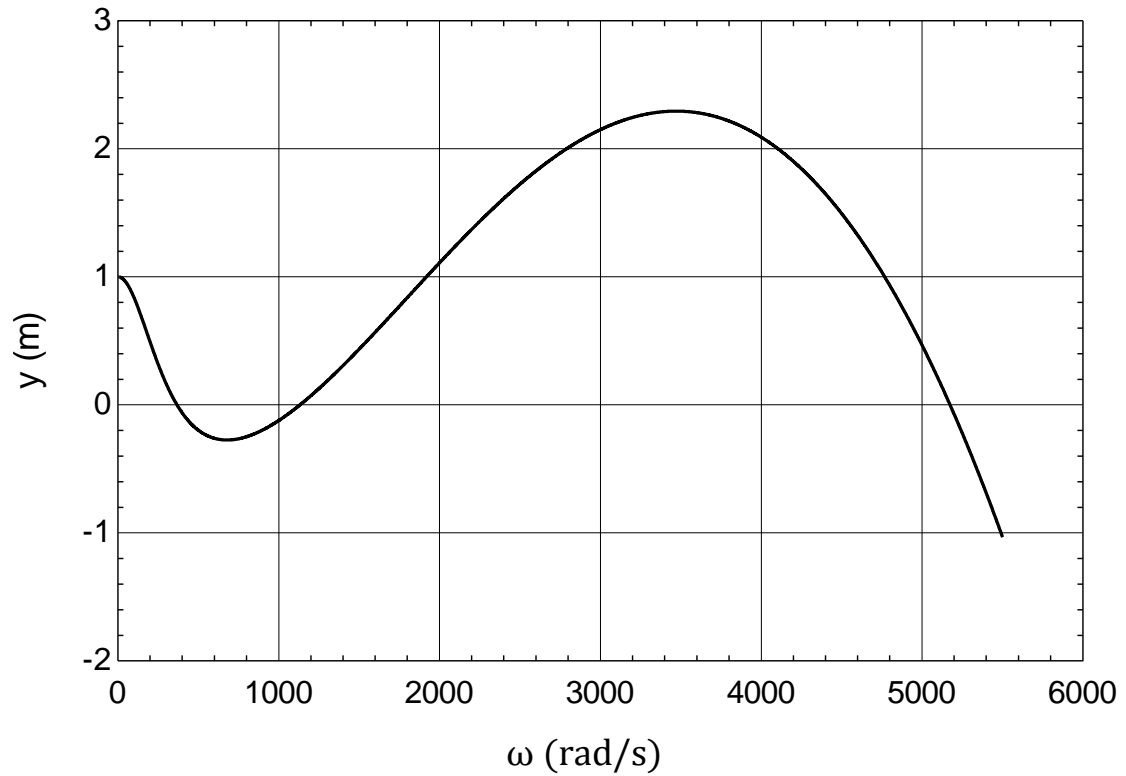$$\omega_1 = 283$$

$$\omega_2 = 987$$

$$\omega_3 = 3685$$
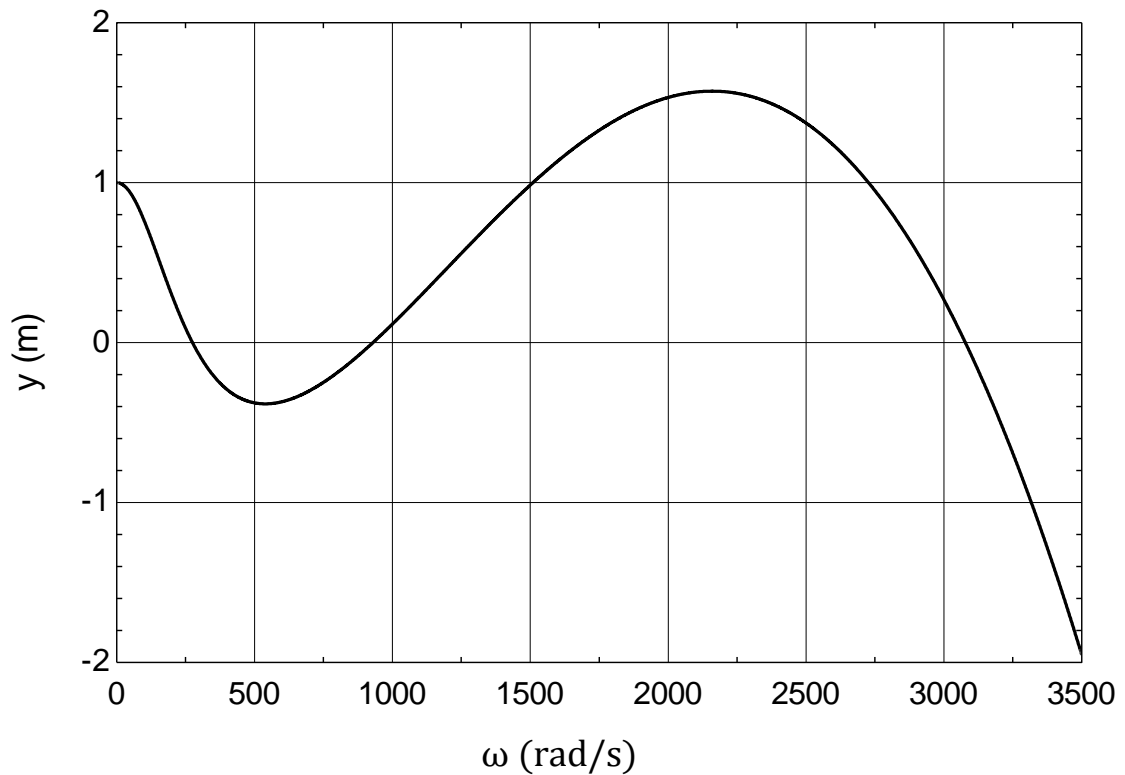
Figure B.1.6: Displacement vs. Natural frequency in coupled bending vibration for 3 DOFS [c_1=0.05 mm; c_2=0.025 mm and c_3=0.005 mm].

Natural frequency (rad/s):

$$\omega_1 = 274$$

$$\omega_2 = 929$$

$$\omega_3 = 3077$$

B.2: Lumped masses are at equal distance (short side)

$m_1 = 1.9$ kg $m_2 = 0.1$ kg $m_3 = 0.1$ kg
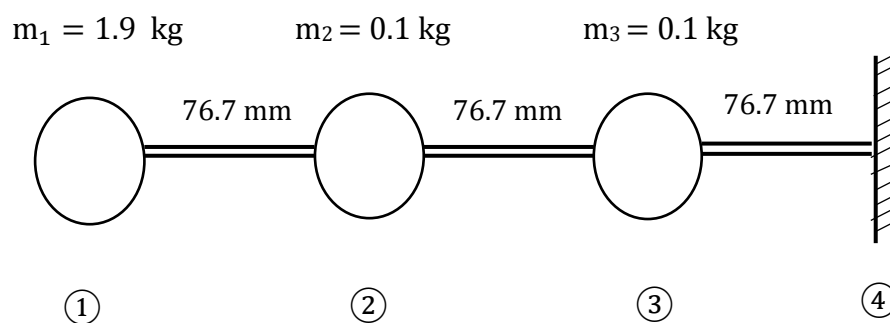
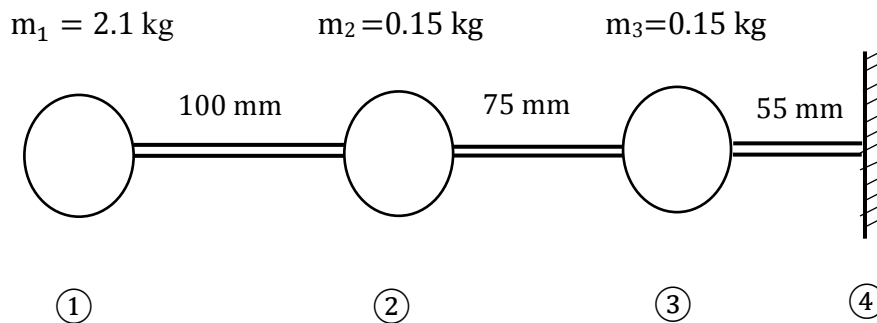
Figure B.2: Lumped parameter system in stockbridge damper [short side equal distance for 3DOFS].

Figure B.2.1: Displacement vs. Natural frequency in uncoupled bending vibration for 3
DOFS [c_1=0 mm, c_2=0 mm and c_3=0 mm].

Natural frequency (rad/s):

$$\omega_1 = 336$$

$$\omega_2 = 1129$$

$$\omega_3 = 5129$$

Figure B.2.2: Displacement vs. Natural frequency in coupled bending vibration for 3
DOFS [c_1=0.1 mm, c_2=0.05 mm and c_3=0.01 mm].

Natural frequency (rad/s):

$$\omega_1 = 368$$
$$\omega_2 = 1141$$
$$\omega_3 = 5310$$

Uncoupled bending and Coupled bending-twisting vibration comparison

The graph B.2.3 compares the influence of mass eccentricity in vibration between
uncoupled bending and coupled bending-twisting vibration modes, which were generated
using graphs B.2.1 and B.2.2 respectively.

Figure B.2.3: Displacement vs. Natural frequency in uncoupled bending and coupled bending-twisting vibration for 3 DOFS.
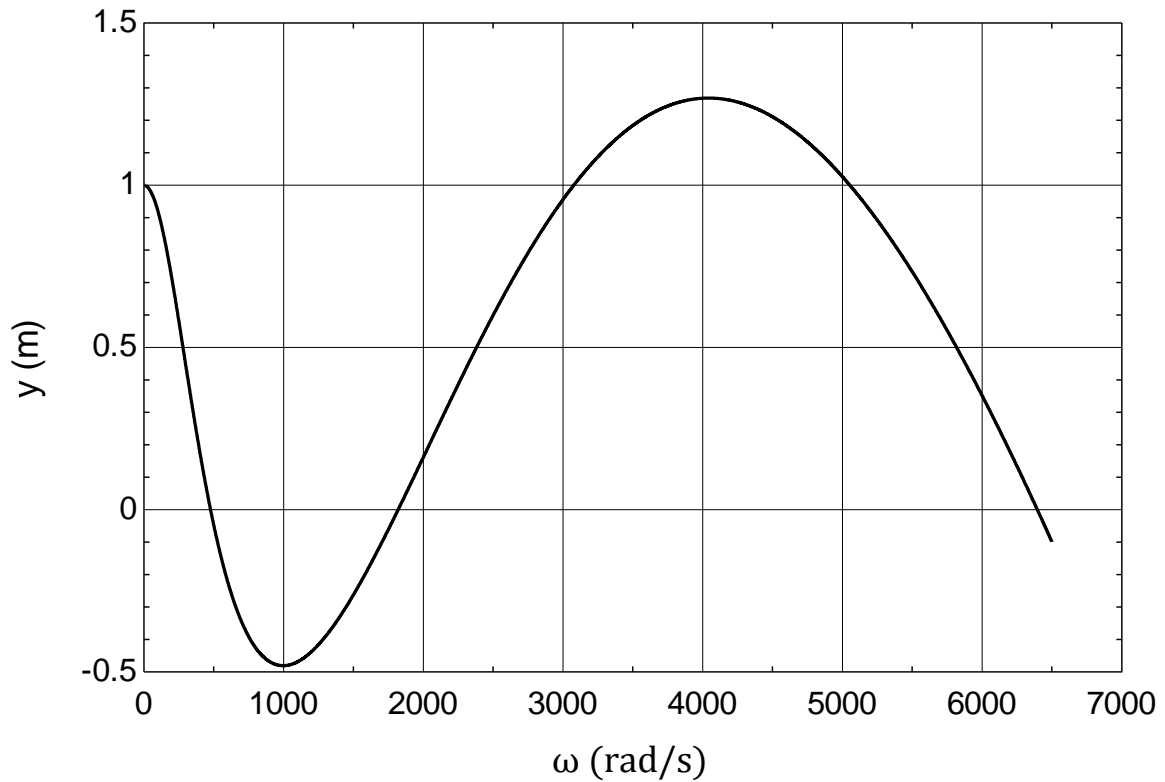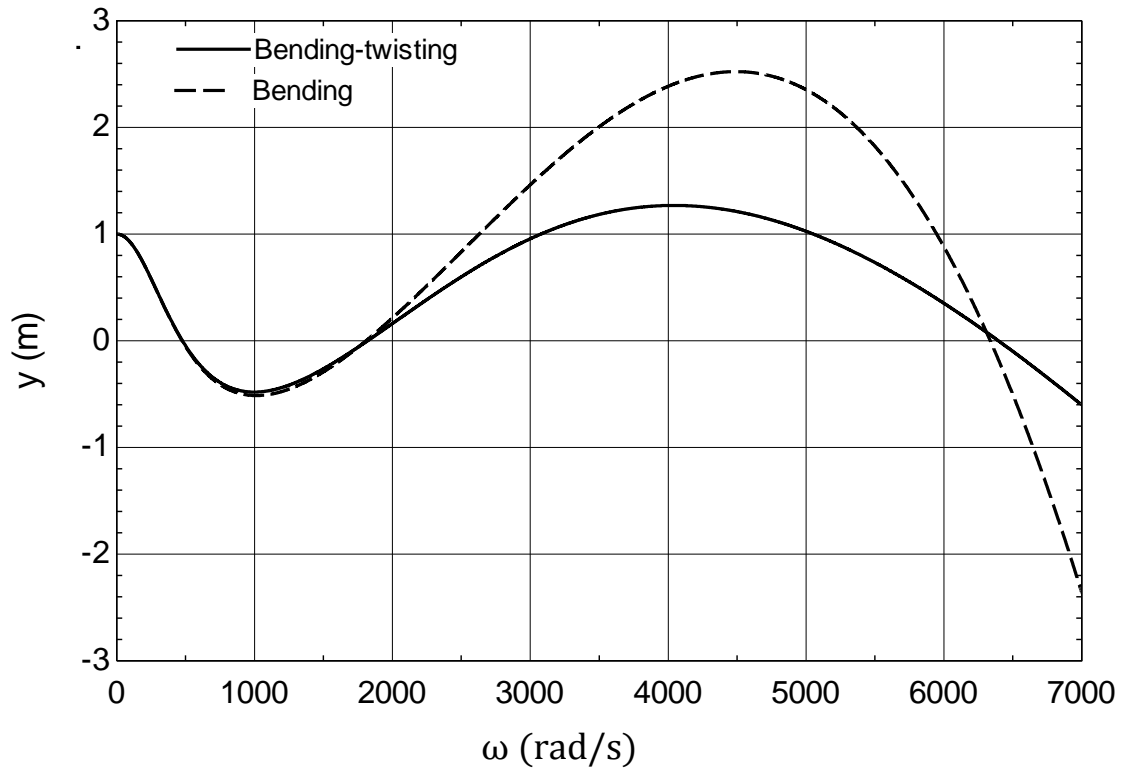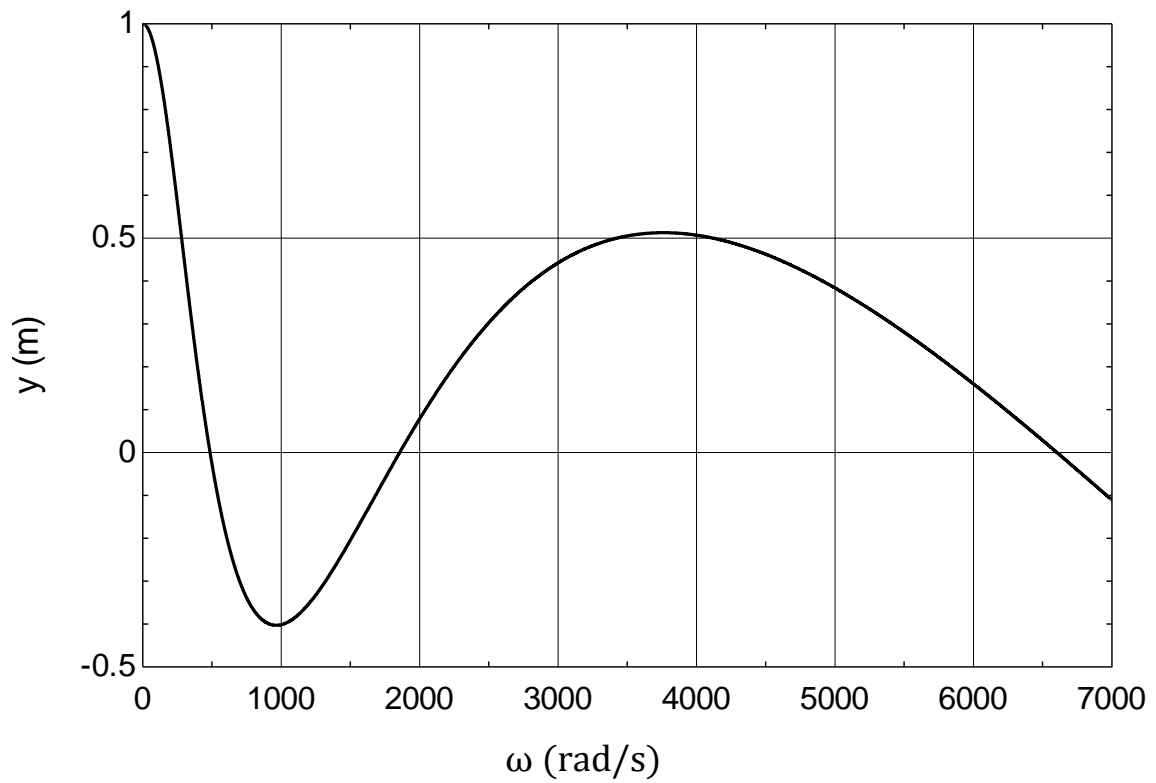

Figure B.2.4: Displacement vs. Natural frequency in coupled bending vibration for 3 DOFS [c_1=0.2 mm, c_2=0.1 mm and c_3=0.02 mm].

Natural frequency (rad/s):

$$\omega_1 = 371$$

$$\omega_2 = 1182$$

$$\omega_3 = 6005$$

Figure B.2.5: Displacement vs. Natural frequency in coupled bending vibration for 3 DOFS [c_1=0.4 mm; c_2=0.08 mm. and c_3=0.016 mm].

Natural frequency (rad/s):

$$\omega_1 = 374$$

$$\omega_2 = 1253$$

$$\omega_3 = 8901$$

Figure B.2.6: Displacement vs. Natural frequency in coupled bending vibration for 3 DOFS [c_1=0.05 mm; c_2=0.025 mm and c_3=0.005 mm].

Natural frequency (rad/s):

$$\omega_1 = 366$$
$$\omega_2 = 1133$$
$$\omega_3 = 5173$$

B.3: Lumped masses are at unequal distance (short side)

Figure B.3: Lumped parameter system in stockbridge damper [Short side unequal distance for 3DOFS].
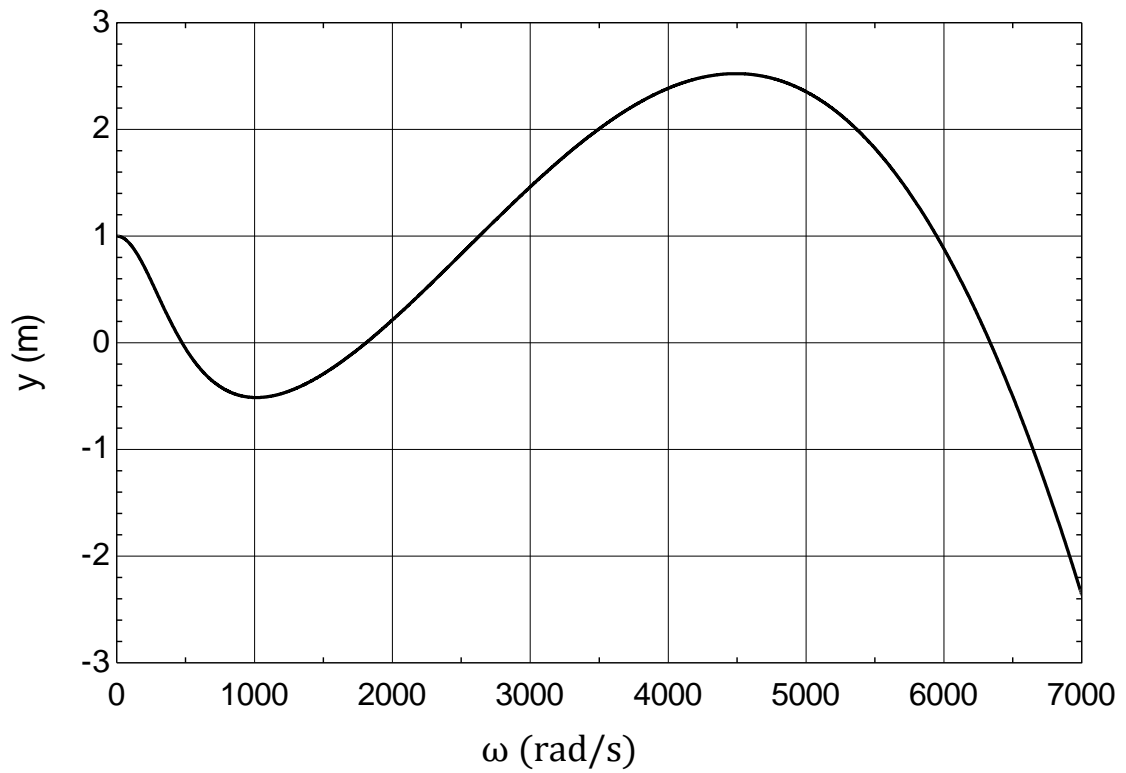
Figure B.3.1: Displacement vs. Natural frequency in uncoupled bending vibration for 3 DOFS [c_1=0 mm, c_2=0 mm and c_3=0 mm].

Natural frequency (rad/s):

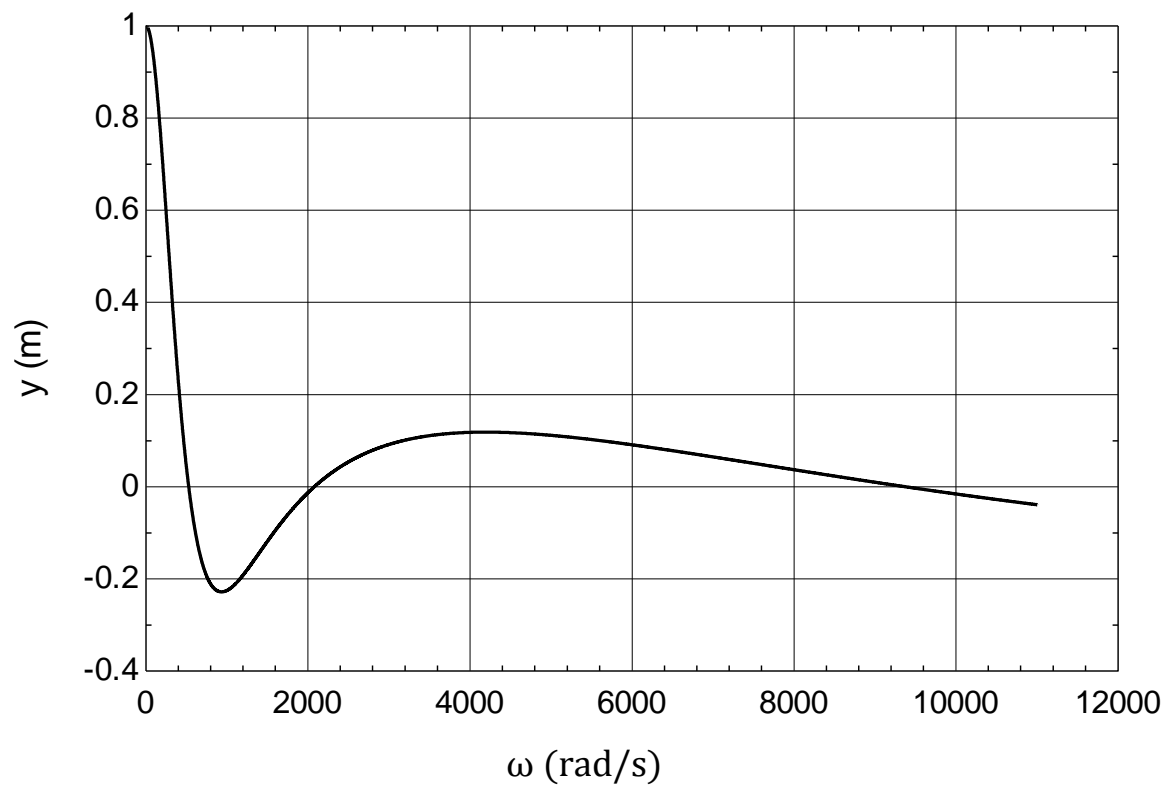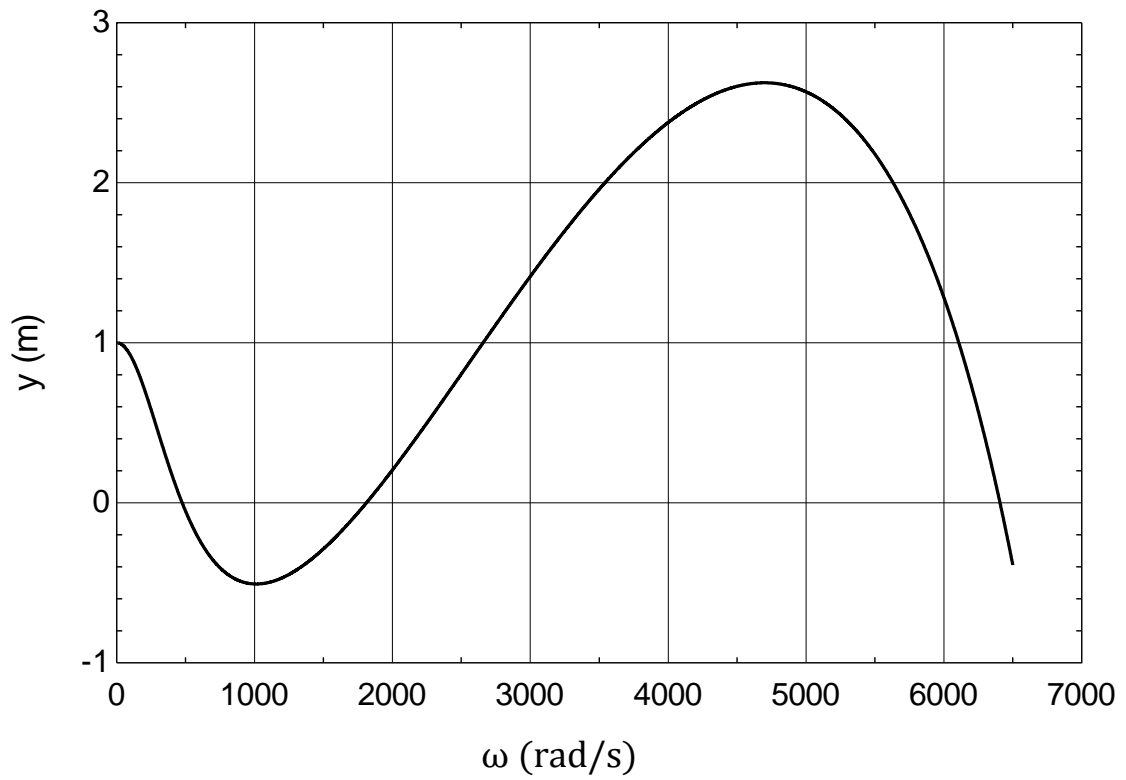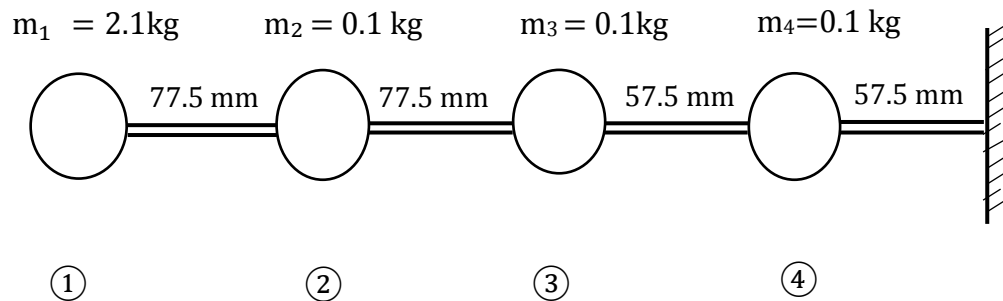$$\omega_1 = 472$$

$$\omega_2 = 1808$$

$$\omega_3 = 6335$$

Figure B.3.2: Displacement vs. Natural frequency in coupled bending vibration for 3 DOFS [c_1=0.1 mm, c_2=0.05 mm and c_3=0.01 mm].

Natural frequency (rad/s):

$$\omega_1 = 476$$
$$\omega_2 = 1820$$
$$\omega_3 = 6395$$

<u>Uncoupled bending and Coupled bending-twisting vibration comparison</u>

The graph B.3.3 compares the influence of mass eccentricity in vibration between uncoupled bending and coupled bending-twisting vibration modes, which were generated using graphs B.3.1 and B.3.2 respectively.

Figure B.3.3: Displacement vs. Natural frequency in uncoupled bending and coupled bending-twisting vibration for 3 DOFS.

Figure B.3.4: Displacement vs. Natural frequency in coupled bending vibration for 3 DOFS [c_1=0.2 mm; c_2=0.1 mm and c_3=0.02 mm].

Natural frequency (rad/s):

$$\omega_1 = 485$$

$$\omega_2 = 1855$$

$$\omega_3 = 6602$$

Figure B.3.5: Displacement vs. Natural frequency in coupled bending vibration for 3 DOFS [c_1=0.4 mm; c_2=0.08 mm. and c_3=0.016 mm].

Natural frequency (rad/s):

$$\omega_1 = 526$$

$$\omega_2 = 2078$$

$$\omega_3 = 9369$$
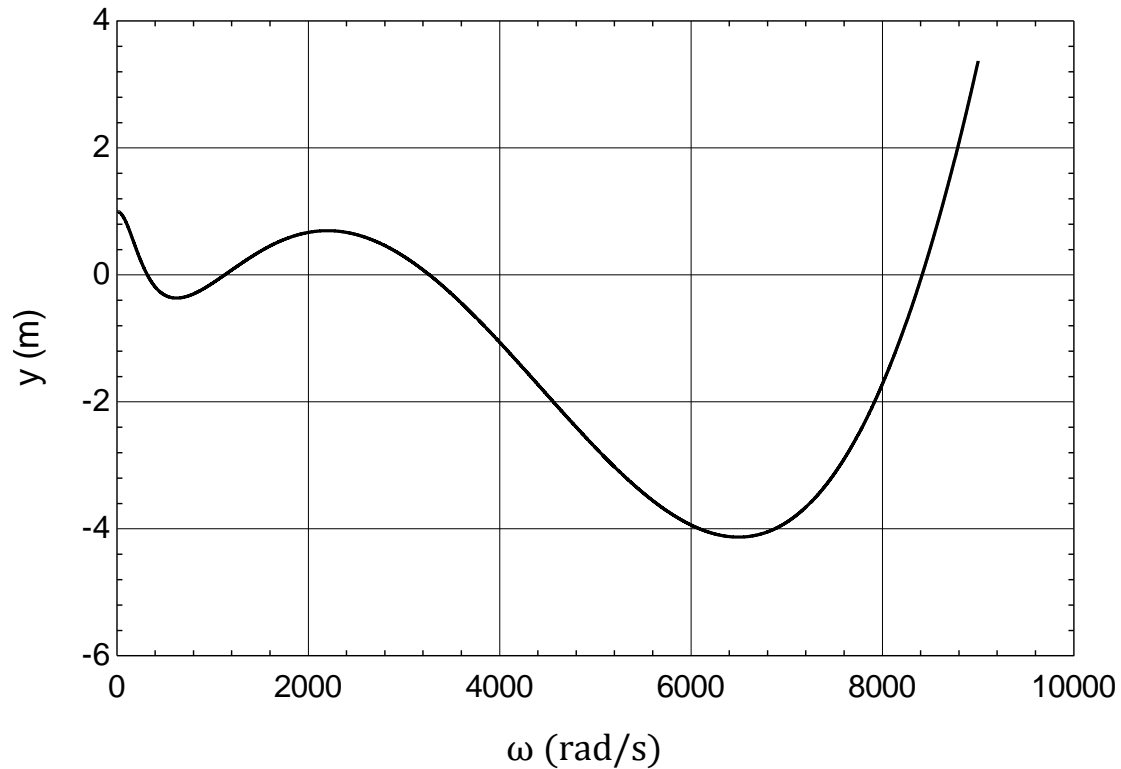
Figure B.3.6: Displacement vs. Natural frequency in coupled bending vibration for 3 DOFS [c_1=0.05 mm; c_2=0.025 mm and c_3=0.005 mm].

Natural frequency (rad/s):

$$\omega_1 = 474$$

$$\omega_2 = 1811$$

$$\omega_3 = 6355$$

Appendix-C

Stockbridge damper acting as a 4 DOFS (Long side)

C.1: Lumped masses are at unequal distance

Figure C.1: Lumped parameter system in stockbridge damper [Long side unequal distance for 4DOFS].
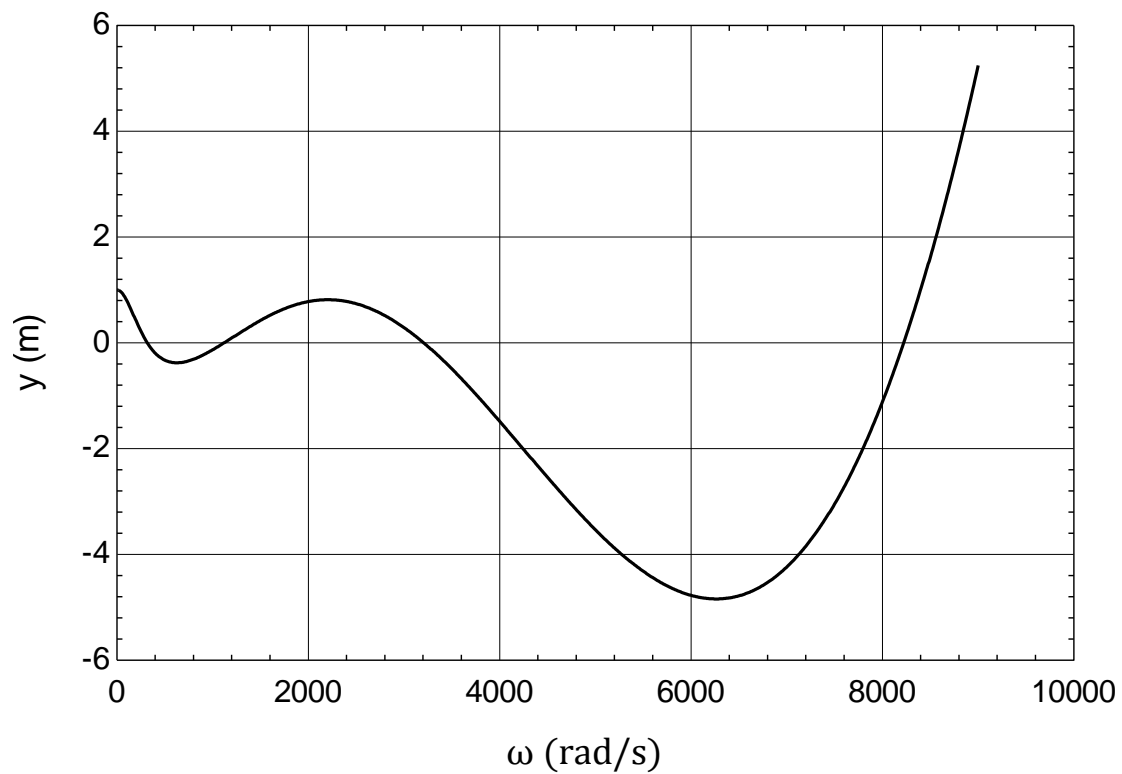
Figure C.1.1: Displacement vs. Natural frequency in uncoupled bending vibration for 4 DOFS [c_1=0 mm, c_2=0 mm, c_3=0 mm and c_4=0 mm].

Natural frequency (rad/s):

$$\omega_1 = 315$$
$$\omega_2 = 1120$$
$$\omega_3 = 3205$$
$$\omega_4 = 8223$$

Figure C.1.2: Displacement vs. Natural frequency in coupled bending vibration for 4 DOFS [c_1=0.1 mm, c_2=0.05 mm, c_3=0.01 mm and c_4=0.001 mm].

Natural frequency (rad/s):

$$\omega_1 = 316$$
$$\omega_2 = 1127$$
$$\omega_3 = 3264$$
$$\omega_4 = 8414$$

Uncoupled bending and Coupled bending-twisting vibration comparison

The graph C.1.3 compares the influence of mass eccentricity in vibration between uncoupled bending and coupled bending-twisting vibration modes, which were generated using graphs C.1.1 and C.1.2 respectively.
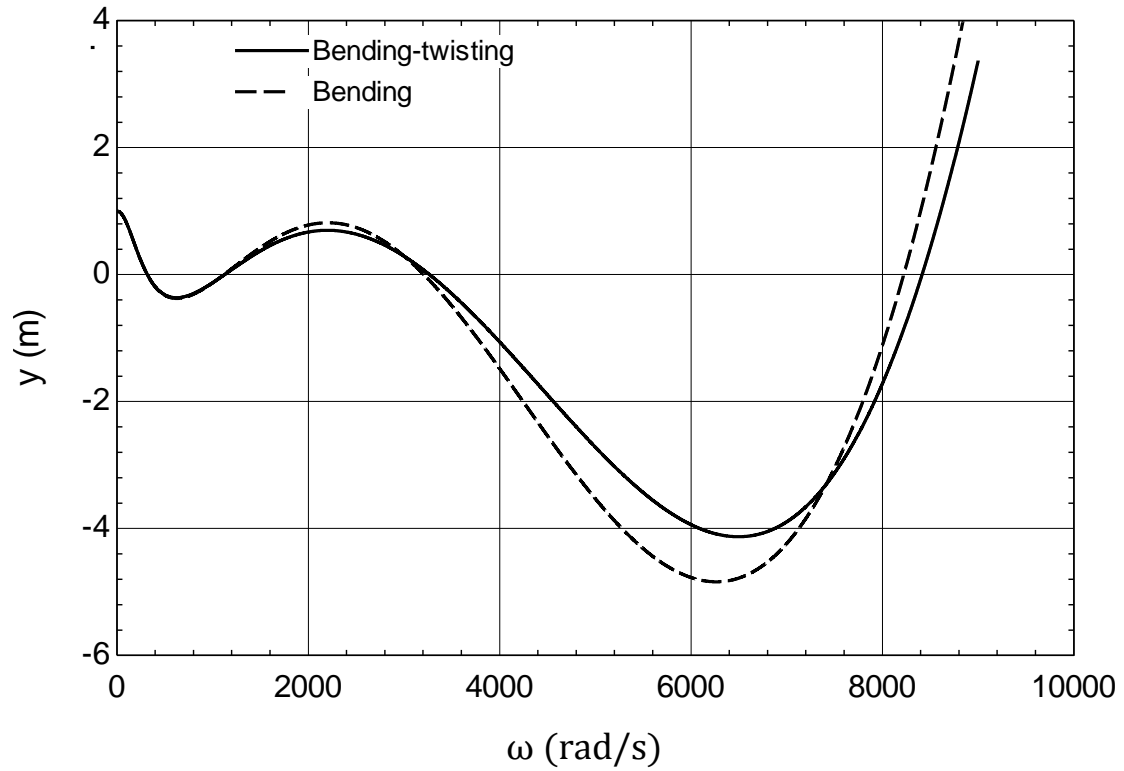
Figure C.1.3: Displacement vs. Natural frequency in uncoupled bending and coupled bending-twisting vibration for 4 DOFS.
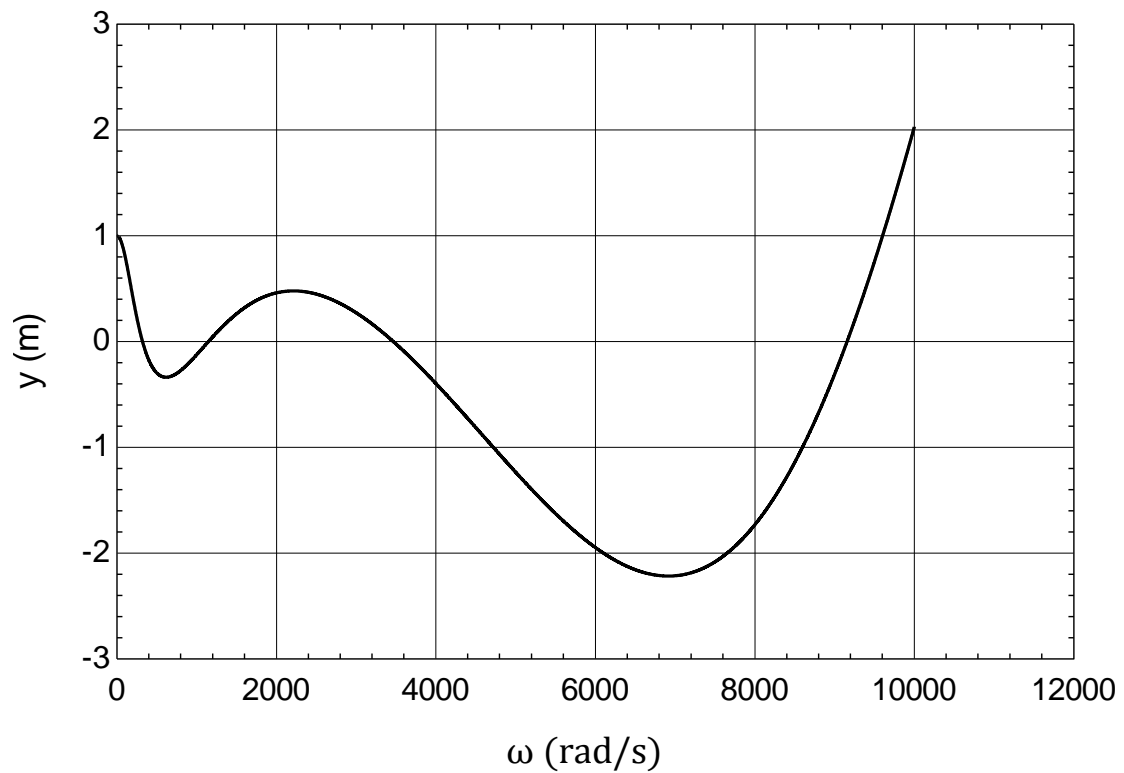

Figure C.1.4: Displacement vs. Natural frequency in coupled bending vibration for 4 DOFS [c_1=0.2 mm; c_2=0.1 mm; c_3=0.02 mm and c_4=0.002 mm.].

Natural frequency (rad/s):

$$\omega_1 = 318$$
$$\omega_2 = 1147$$
$$\omega_3 = 3464$$
$$\omega_4 = 9156$$
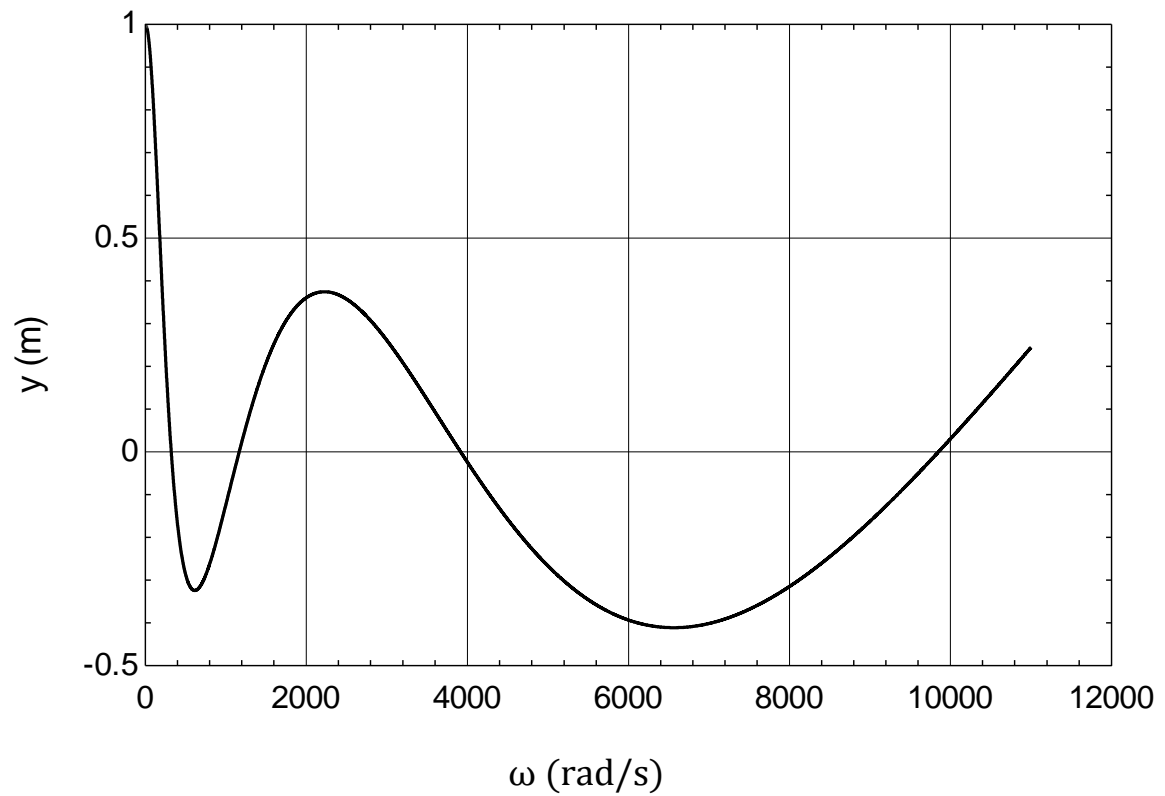

Figure C.1.5: Displacement vs. Natural frequency in coupled bending vibration for 4 DOFS [c_1=0.3 mm; c_2=0.08 mm; c_3=0.016 mm and c_4=0.002 mm].

Natural frequency (rad/s):

$$\omega_1 = 321$$
$$\omega_2 = 1164$$
$$\omega_3 = 3905$$
$$\omega_4 = 9850$$
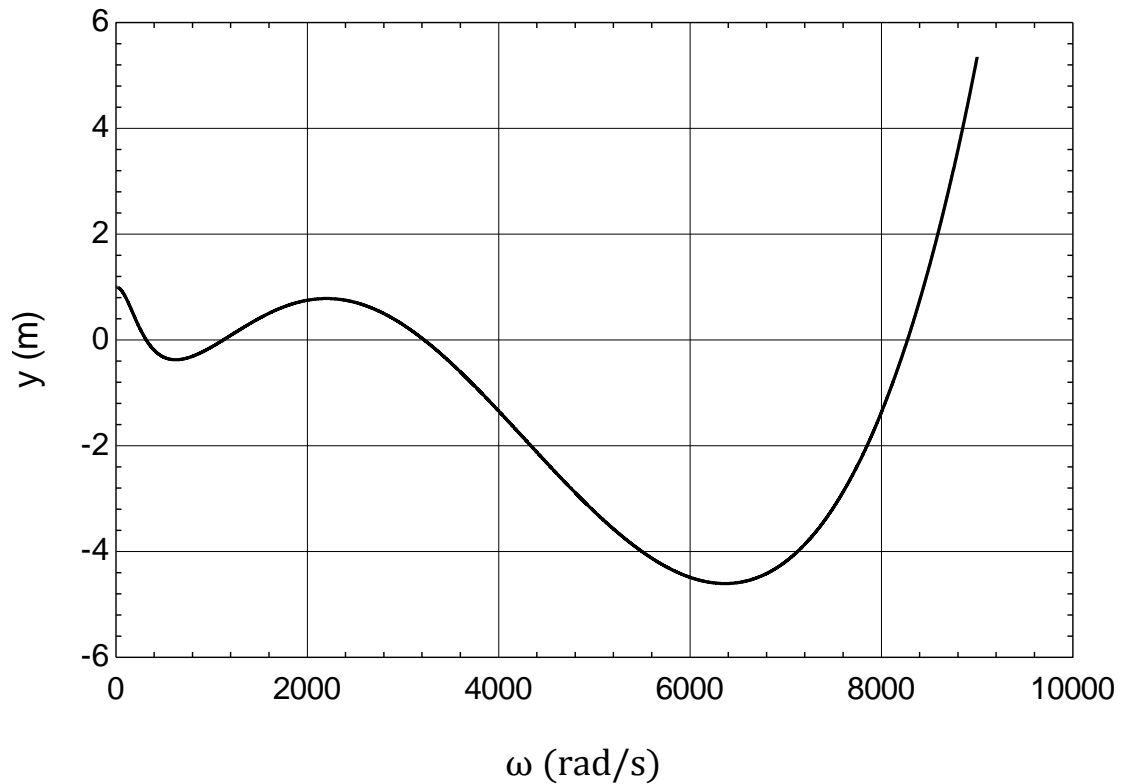
Figure C.1.6: Displacement vs. Natural frequency in coupled bending vibration for 4 DOFS [c_1=0.05 mm, c_2=0.025 mm, c_3=0.005 mm and c_4=0.0025 mm].

Natural frequency (rad/s):

$$\omega_1 = 315$$
$$\omega_2 = 1122$$
$$\omega_3 = 3220$$
$$\omega_4 = 8272$$

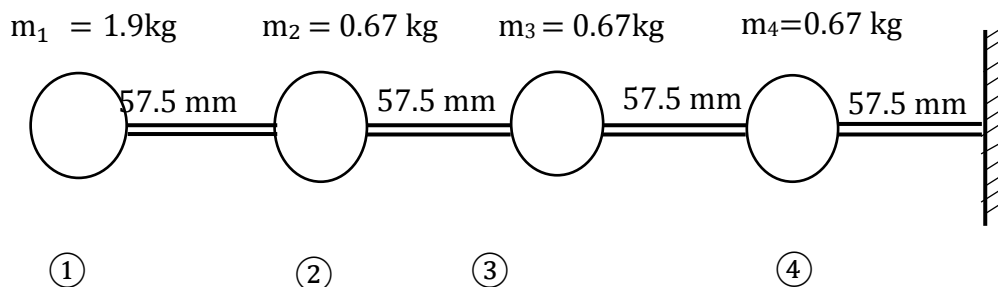## C.2: Lumped masses are at equal distance (Short side)

Figure 3.2: Lumped parameter system in stockbridge damper [Short side equal distance for 4DOFS].
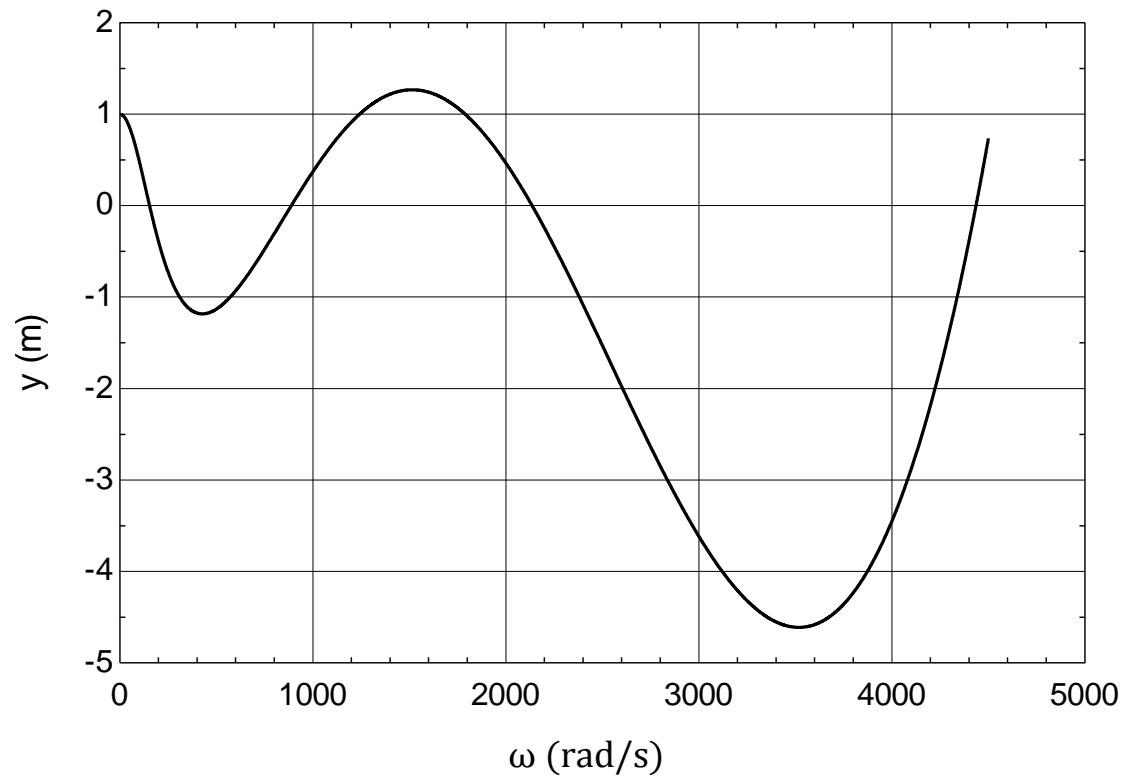
Figure C. 2.1: Displacement vs. Natural frequency in uncoupled bending vibration for 4 DOFS [c_1=0 mm, c_2=0 mm, c_3=0 mm and c_4=0 mm].

Natural frequency (rad/s):

$$\omega_1 = 153$$
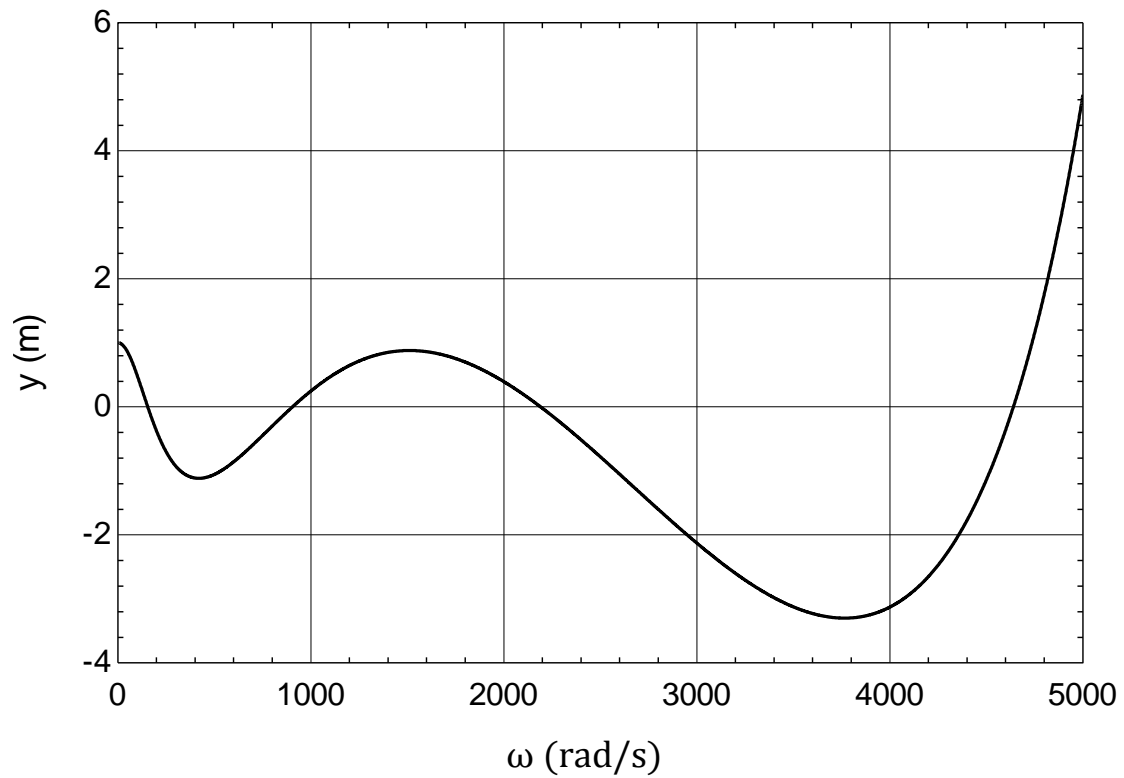$$\omega_2 = 887$$
$$\omega_3 = 2135$$
$$\omega_4 = 4437$$

Figure C.2.2: Displacement vs. Natural frequency in coupled bending vibration for 4 DOFS [c_1=0.1 mm, c_2=0.05 mm, c_3=0.01 mm and c_4=0.001 mm].

Natural frequency (rad/s):

$$\omega_1 = 154$$
$$\omega_2 = 905$$
$$\omega_3 = 2189$$
$$\omega_4 = 4640$$

Uncoupled bending and Coupled bending-twisting vibration comparison

The graph C.2.3 compares the influence of mass eccentricity in vibration between uncoupled bending and coupled bending-twisting vibration modes, which were generated using graphs C.2.1 and C. 2.2 respectively.
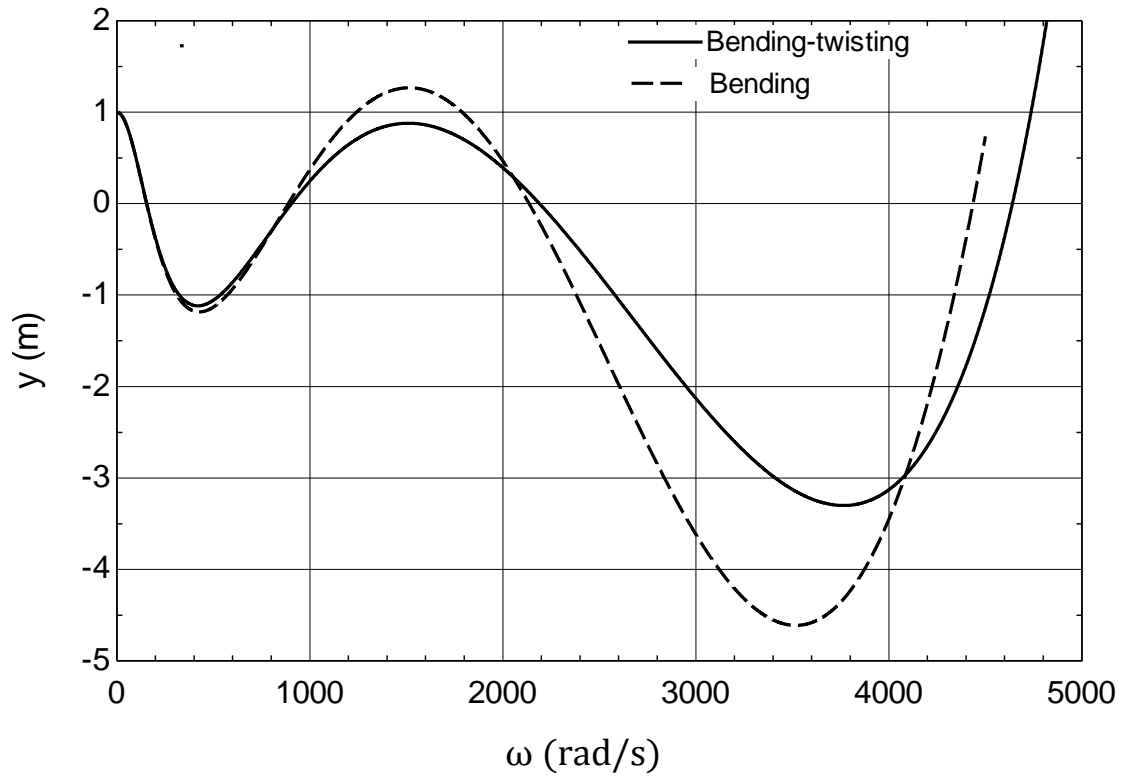
Figure C.2.3: Displacement vs. Natural frequency in uncoupled bending and coupled bending-twisting vibration for 4 DOFS.
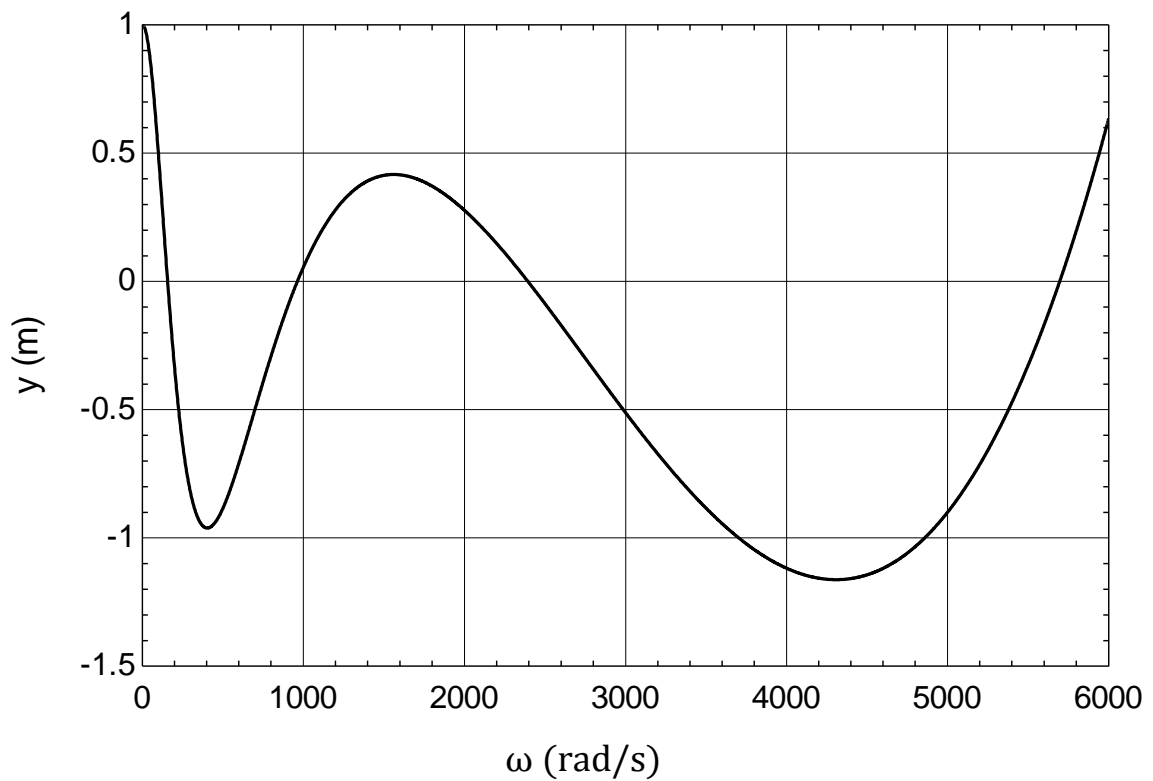

Figure C.2.4: Displacement vs. Natural frequency in coupled bending vibration for 4 DOFS [c_1=0.2 mm; c_2=0.1 mm; c_3=0.02 mm and o c_4=0.002 mm].

Natural frequency (rad/s):

$$\omega_1 = 156$$
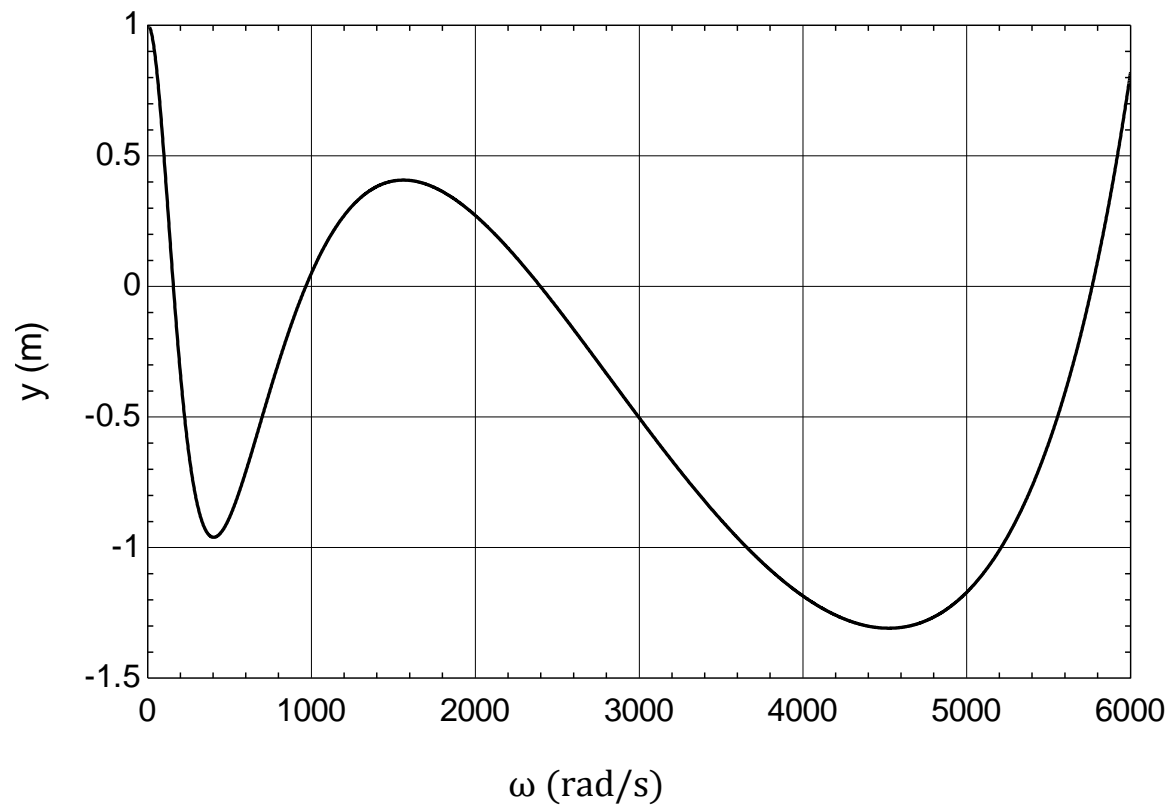$$\omega_2 = 962$$
$$\omega_3 = 2393$$
$$\omega_4 = 5696$$

Figure C.2.5: Displacement vs. Natural frequency in coupled bending vibration for 4 DOFS [c_1=0.25 mm, c_2=0.08 mm, c_3=0.016 mm and c_4=0.002 mm].

Natural frequency (rad/s):

$$\omega_1 = 158$$
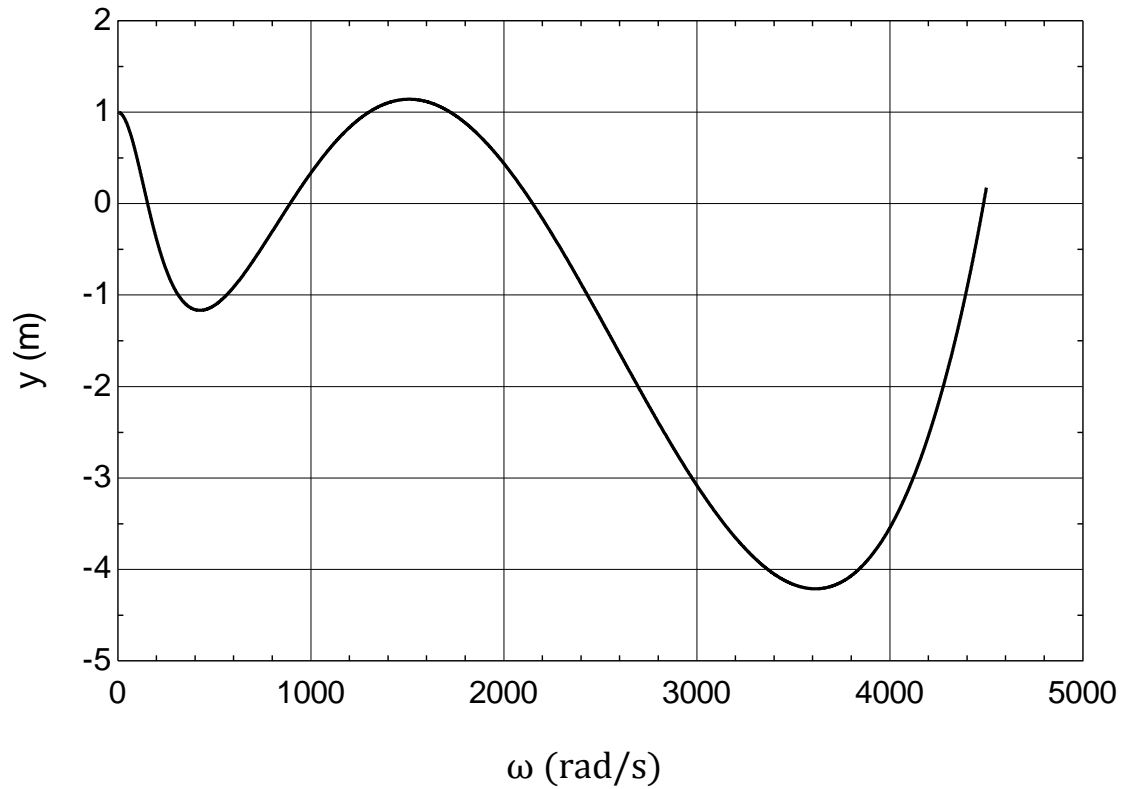$$\omega_2 = 966$$
$$\omega_3 = 2398$$
$$\omega_4 = 5764$$

Figure C.2.6: Displacement vs. Natural frequency in coupled bending vibration for 4 DOFS [c_1=0.05 mm; c_2=0.025 mm; c_3=0.005 mm and c_4=0.0025 mm].

Natural frequency (rad/s):

$$\omega_1 = 153$$
$$\omega_2 = 892$$
$$\omega_3 = 2149$$
$$\omega_4 = 4485$$

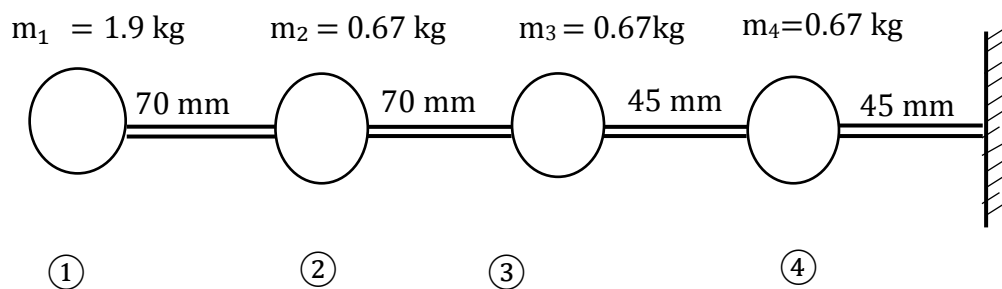## C.3: Lumped masses are at unequal distance (Short side)

Figure C.3: Lumped parameter system in stockbridge damper [Short side unequal distance for 4DOFS].
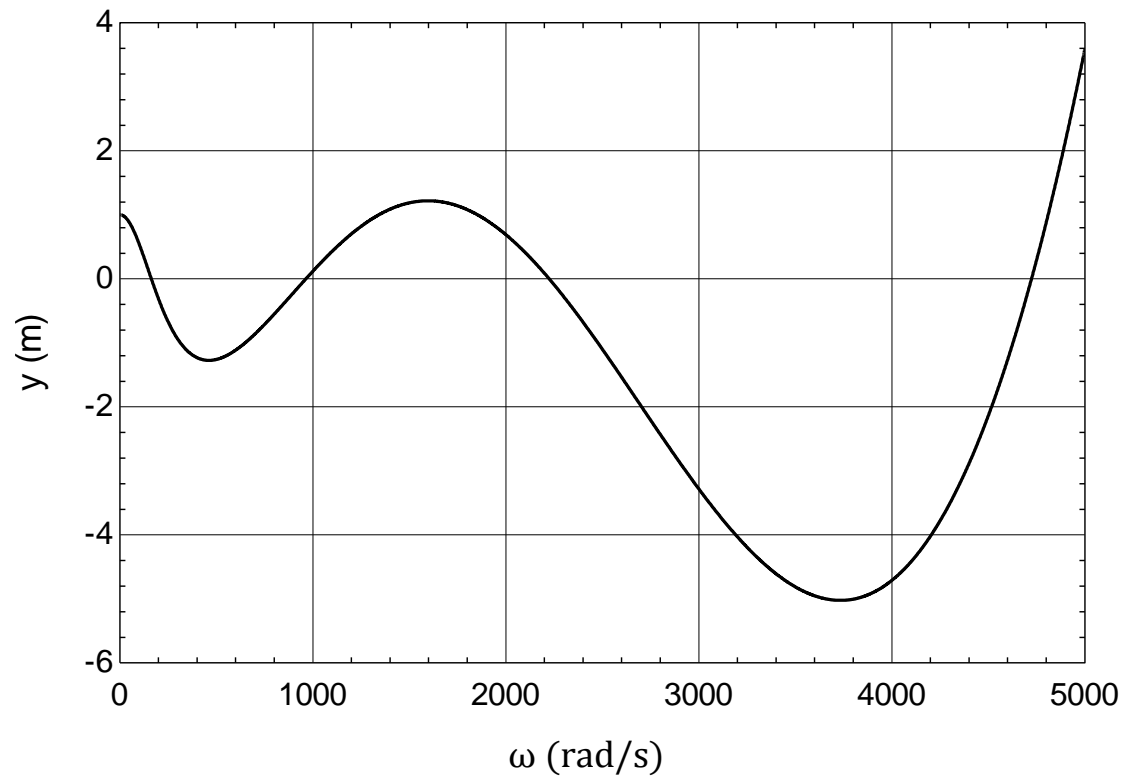
Figure C.3.1: Displacement vs. Natural frequency in uncoupled bending vibration for 4 DOFS [c_1=0 mm, c_2=0 mm, c_3=0 mm and c_4=0 mm].

Natural frequency (rad/s):

$$\omega_1 = 162$$
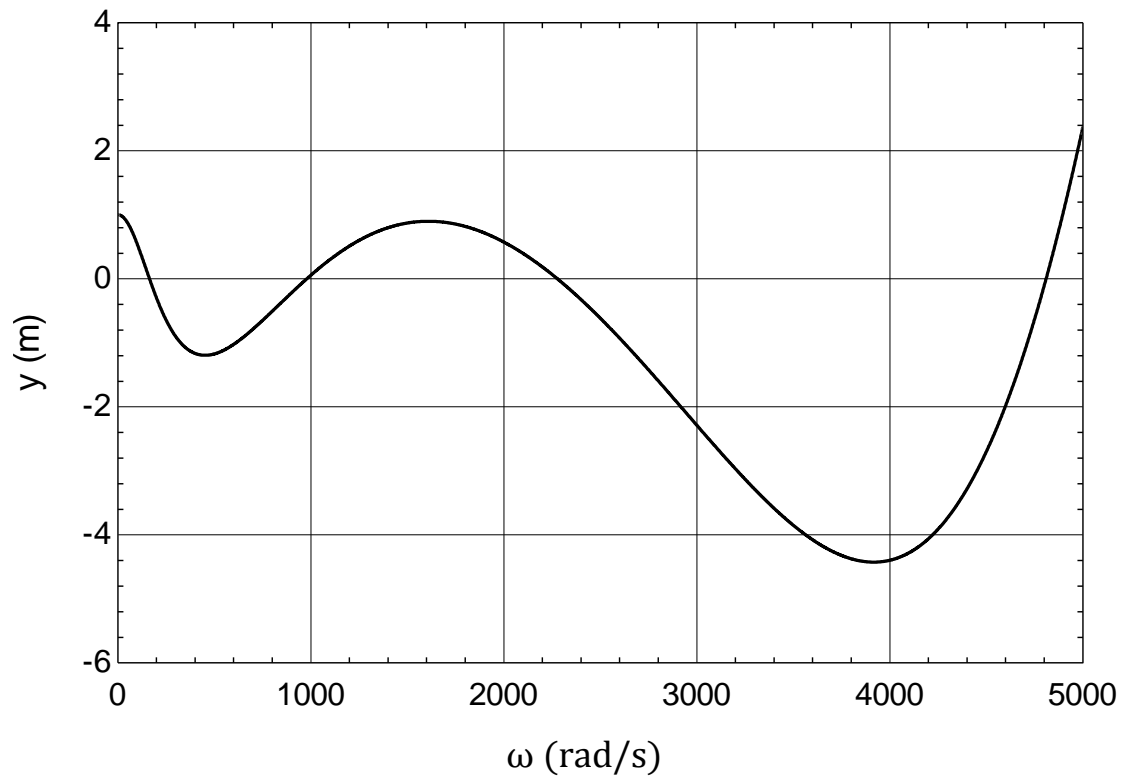$$\omega_2 = 963$$
$$\omega_3 = 2225$$
$$\omega_4 = 4724$$

Figure C.3.2: Displacement vs. Natural frequency in coupled bending vibration for 4 DOFS [c_1=0.1 mm, c_2=0.05 mm, c_3=0.01 mm and c_4=0.001 mm].

Natural frequency (rad/s):

$$\omega_1 = 163$$
$$\omega_2 = 978$$
$$\omega_3 = 2276$$
$$\omega_4 = 4810$$

<u>Uncoupled bending and Coupled bending-twisting vibration comparison</u>

The graph C.3.3 compares the influence of mass eccentricity in vibration between uncoupled bending and coupled bending-twisting vibration modes, which were generated using graphs C.3.1 and C.3.2 respectively.
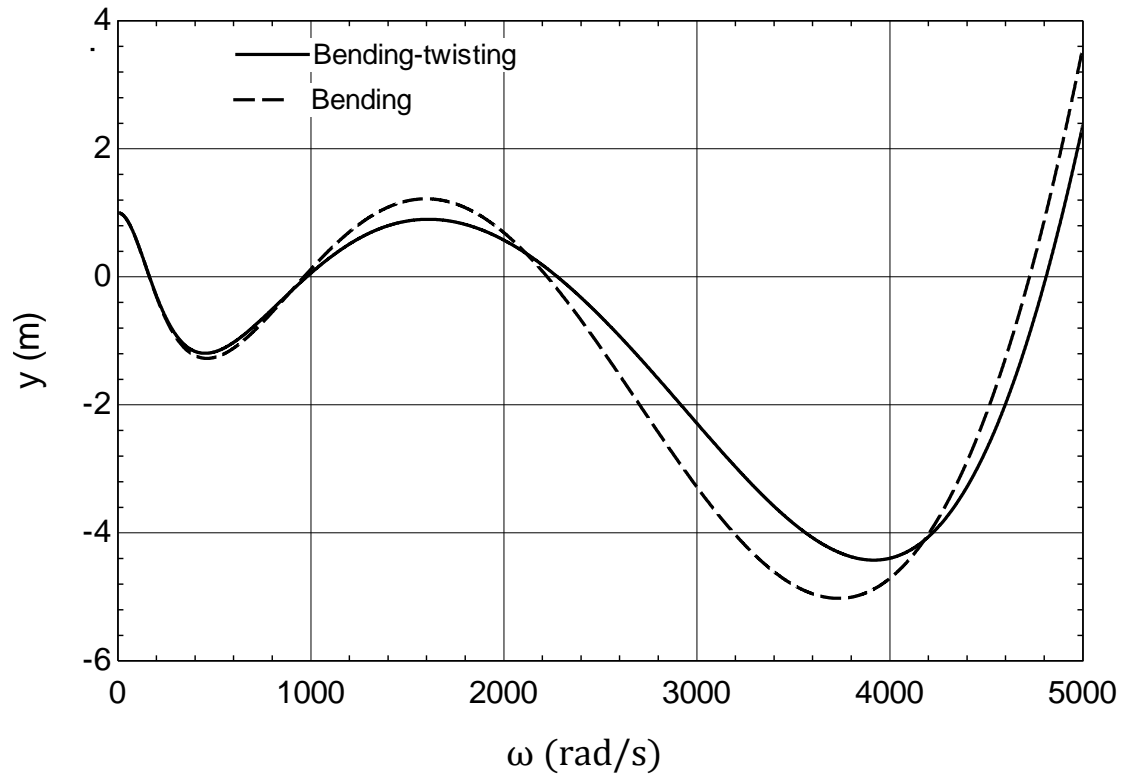
Figure C.3.3: Displacement vs. Natural frequency in uncoupled bending and coupled bending-twisting vibration for 4 DOFS.
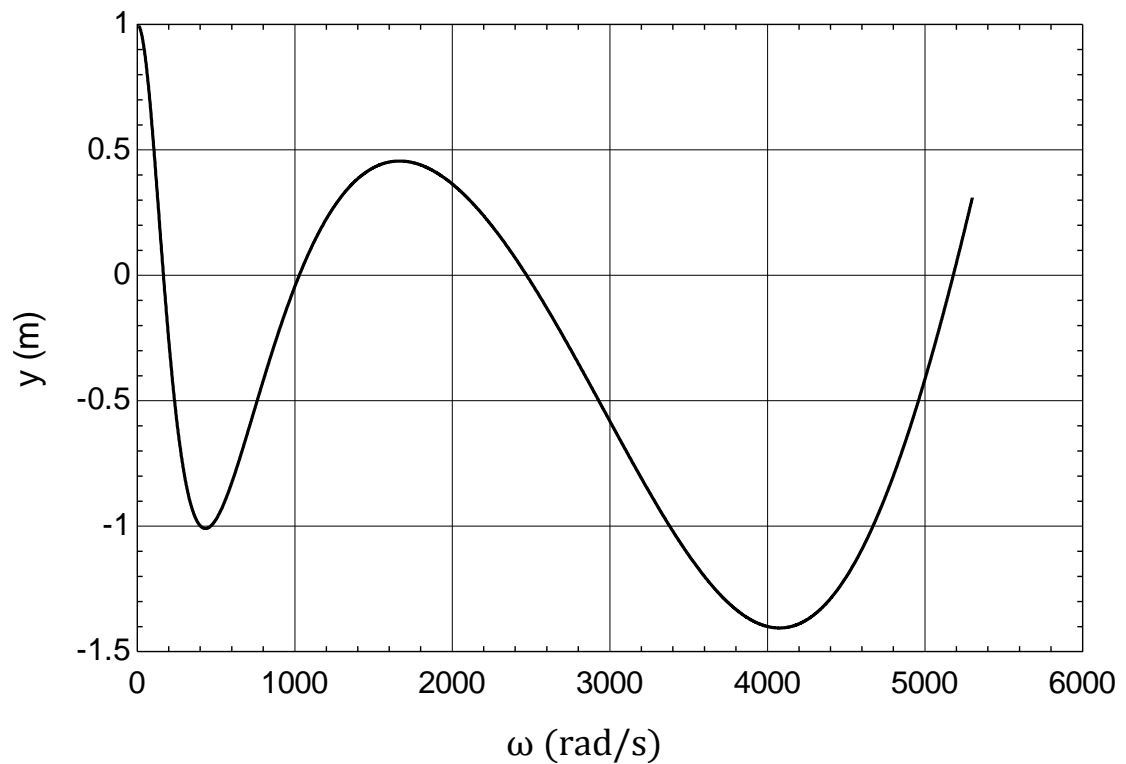

Figure C.3.4: Displacement vs. Natural frequency in coupled bending vibration for 4 DOFS [c_1=0.2 mm; c_2=0.1 mm; c_3=0.02 mm and c_4=0.002 mm].

Natural frequency (rad/s):

$$\omega_1 = 165$$
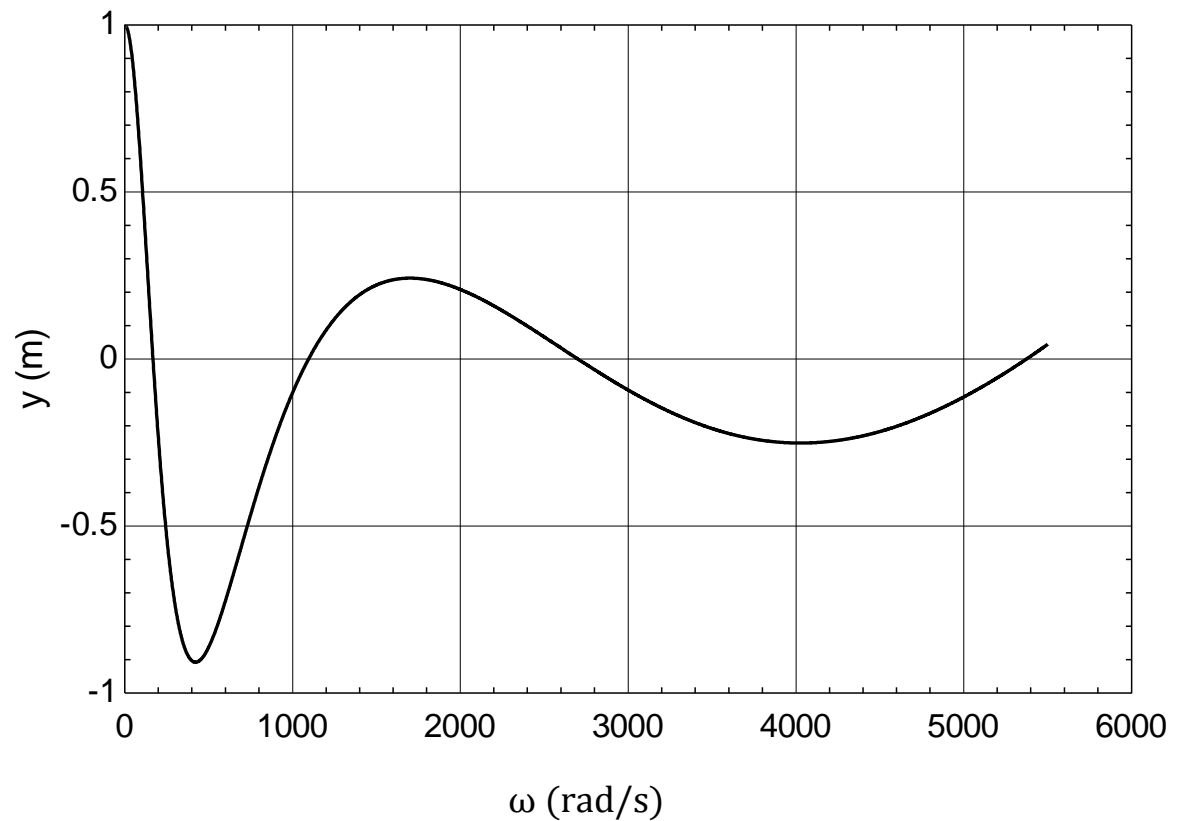$$\omega_2 = 1029$$
$$\omega_3 = 2470$$
$$\omega_4 = 5178$$

Figure C.3.5: Displacement vs. Natural frequency in coupled bending vibration for 4 DOFS [c_1=0.3 mm; c_2=0.08 mm; c_3=0.016 mm and c_4=0.002 mm].

Natural frequency (rad/s):

$$\omega_1 = 167$$
$$\omega_2 = 1094$$
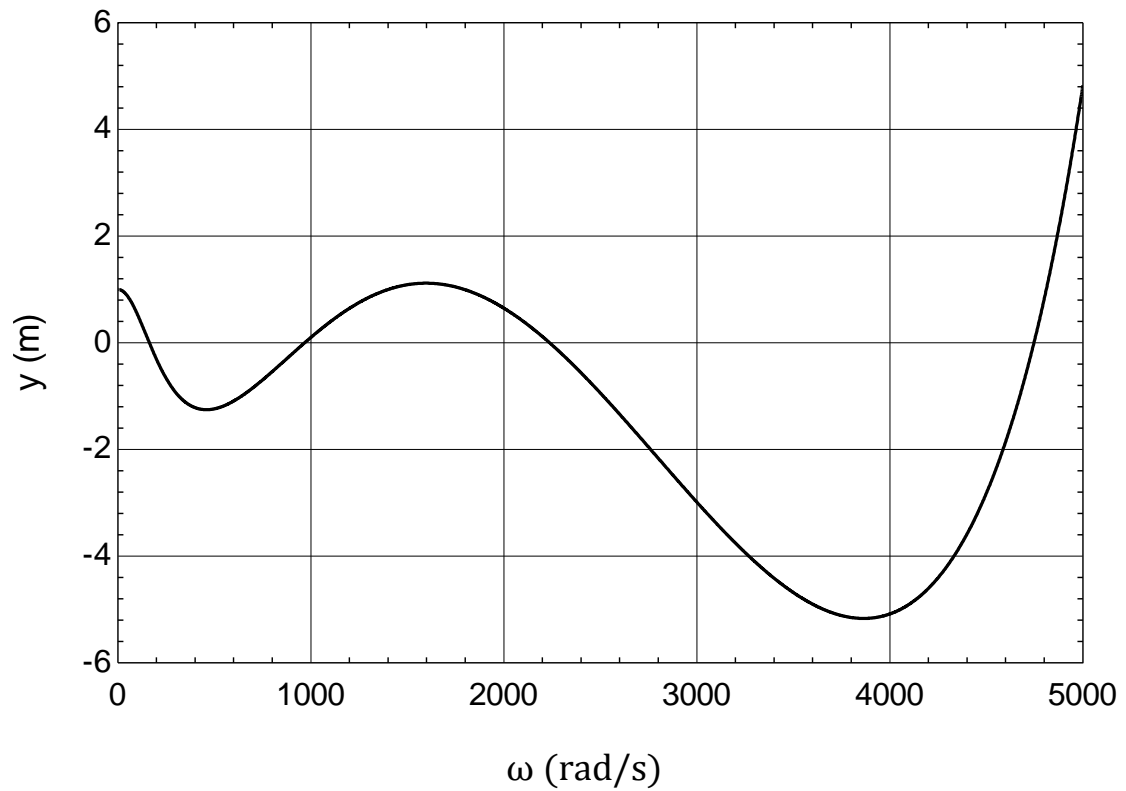$$\omega_3 = 2699$$
$$\omega_4 = 5373$$

Figure C.3.6: Displacement vs. Natural frequency in coupled bending vibration for 4 DOFS [c_1=0.05 mm; c_2=0.025 mm; c_3=0.005 mm and c_4=0.0025 mm].

Natural frequency (rad/s):

$$\omega_1 = 163$$
$$\omega_2 = 968$$
$$\omega_3 = 2236$$
$$\omega_4 = 4746$$

.

Appendix-D

Programming code

Program for finding natural frequency for 2DOFS

```
duplicate i=1,2
v[i+1]=v[i]-mass[i]* omega^2*(y[i]+c[i]*phi[i])
M[i+1]=M[i]-v[i+1]*L[i]
T[i+1]=T[i]+J[i]*omega^2 *phi[i]+mass[i]*c[i]*omega^2 *y[i]
theta[i+1]=theta[i]+m[i+1]*L[i]/(ei) +v[i+1]*L[i]^2/(2*ei)
y[i+1]=y[i]+theta[i]*L[i]+M[i+1]*L[i]^2/(2*ei) +v[i+1]*L[i]^3/(3*ei)
phi[i+1]=phi[i]+T[i+1]*h[i]
h[i]=L[i]/(G*ip)
J[i]=MASS[i]*c[i]^2
end
L[1]=
L[2]=
L[3]=
G=79.3*10^9
i=4.91*10^(-10)
c[1]=
c[2]=
ei=98.2
mass[1]=
mass[2]=
mass[3]=
v[1]=0 ;m[1]=0;T[1]=0;y[1]=1
theta[3]=0
phi[3]=0
{omega=10}
```

Program for finding natural frequency for 3DOFS
```
duplicate i=1,3
v[i+1]=v[i]-mass[i]* omega^2*(y[i]+c[i]*phi[i])
M[i+1]=M[i]-v[i+1]*L[i]
T[i+1]=T[i]+J[i]*omega^2 *phi[i]+mass[i]*c[i]*omega^2 *y[i]
```

theta[i+1]=theta[i]+m[i+1]*L[i]/(ei) +v[i+1]*L[i]^2/(2*ei)

y[i+1]=y[i]+theta[i]*L[i]+M[i+1]*L[i]^2/(2*ei) +v[i+1]*L[i]^3/(3*ei)

phi[i+1]=phi[i]+T[i+1]*h[i]

h[i]=L[i]/(G*ip)

J[i]=MASS[i]*c[i]^2

end

L[1]=

L[2]=

L[3]=

L[4]=

G=79.3*10^9

i=4.91*10^(-10)

c[1]=

c[2]=

c[3]=

ei=98.2

mass[1]=

mass[2]=

mass[3]=

mass[4]=

v[1]=0 ;m[1]=0;T[1]=0;y[1]=1

theta[4]=0

phi[4]=0

{omega=10}

Program for finding natural frequency for 4DOFS

duplicate i=1,4

v[i+1]=v[i]-mass[i]* omega^2*(y[i]+c[i]*phi[i])

M[i+1]=M[i]-v[i+1]*L[i]

T[i+1]=T[i]+J[i]*omega^2 *phi[i]+mass[i]*c[i]*omega^2 *y[i]

theta[i+1]=theta[i]+m[i+1]*L[i]/(ei) +v[i+1]*L[i]^2/(2*ei)

y[i+1]=y[i]+theta[i]*L[i]+M[i+1]*L[i]^2/(2*ei) +v[i+1]*L[i]^3/(3*ei)

phi[i+1]=phi[i]+T[i+1]*h[i]

h[i]=L[i]/(G*ip)

J[i]=MASS[i]*c[i]^2

end

L[1]=

L[2]=

L[3]=

L[4]=

L[5]=

G=79.3*10^9

i=4.91*10^(-10)

c[1]=

c[2]=

c[3]=

c[4]=

ei=98.2

mass[1]=

mass[2]=

mass[3]=

mass[4]=

v[1]=0 ;m[1]=0;T[1]=0;y[1]=1

theta[5]=0

phi[5]=0

{omega=10}

Appendix E

Alternating method for finding natural frequency

Stockbridge damper has been modeled as a cantilever beam with a concentrated damper mass at it's free end. The flexibility influence coefficients can be used to set up the equations with a force P and a moment M at the free end shown in figure E.1. The deflection and slope at the free end are

$$y = a_{11}P + a_{12}M$$
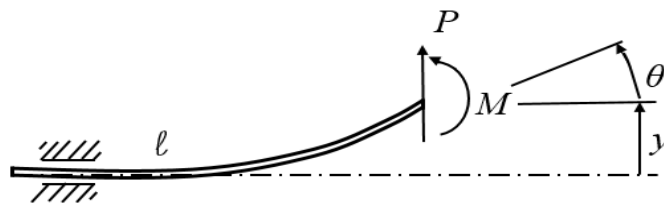
$$\theta = a_{21}P + a_{22}M$$

Figure E.1: Deflection of a cantilever beam.

This can be expressed by the matrix equation

$$\begin{Bmatrix} y \\ \theta \end{Bmatrix} = \begin{bmatrix} a_{11} & a_{12} \\ a_{21} & a_{22} \end{bmatrix}$$

The influence coefficients in this equation are $a_{11} = (\frac{l^3}{3EI})$, $a_{12}=a_{21}= (\frac{l^2}{2EI})$, $a_{22}=\frac{l}{EI}$.

Dunkerley's equation is useful for estimating the fundamental frequency of a system undergoing vibration testing.
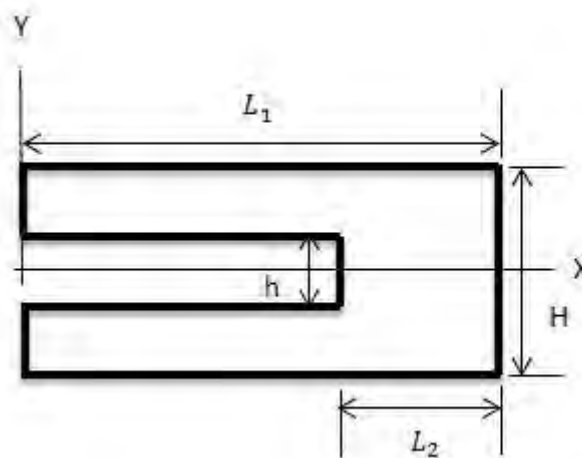

Figure E.2: Cross-sectional view of stockbridge damper mass.

For the basis of the Dunkerley's equation [9], we examine the characteristic equation formulated from the flexibility coefficients, which is

$$
\begin{vmatrix}
(a_{11}m_1 - \dfrac{1}{\omega^2}) & a_{12}m_2 \\[2ex]
a_{21}m_1 & (a_{22}m_2 - \dfrac{1}{\omega^2})
\end{vmatrix}
$$

$$
= \begin{vmatrix}
(\dfrac{l^3}{3EI}m_1 - \lambda^2) & \dfrac{l^2}{2EI}m_2 \\[2ex]
\dfrac{l^2}{2EI}m_1 & (\dfrac{l}{EI}m_2 - \lambda^2)
\end{vmatrix}
$$

Where, $\dfrac{1}{\omega^2} = \lambda^2$, $m_1 = 2.45 \text{kg}$, H=0.08m, h=0.35m, $m_2 = I_{xx} = \dfrac{1}{12}\{2.45*(0.08)^2 - 0.35*(0.35)^2\} = 1.25*10^{-3} \text{ kg}m^2$, $l = 0.27$ m, EI $= 98.2$ Nm^2, $L_1 = 0.13$ m, $L_2 = 0.04$ m.

Expanding this determinant, we obtain two degree equation in $\dfrac{1}{\omega^2}$.

$\Rightarrow \{(\dfrac{l^3}{3EI}m_1 - \lambda^2)(\dfrac{l}{EI}m_2 - \lambda^2)\} - \{(\dfrac{l^2}{2EI}m_1)(\dfrac{l^2}{2EI}m_2)\} = 0$

The natural frequencies of the system are determined as $\omega_1 = 122 \; rad/s$, $\omega_2 = 695 \; rad/s$. By substituting into Dunkerly's formula rearranged in the following form, the natural frequency of the system is determined as

$$
\dfrac{1}{\omega_1{}^2} = a_{11}m_1 + a_{22}m_2
$$

$$
\Rightarrow \omega_1 = 82 \; rad/s.
$$

Where, ω_1 is the fundamental natural frequency of the system.